The role of well testing in geothermal resource assessment

Uwera Rutagarama

Faculty of Earth Sciences
University of Iceland
2012

The role of well testing in geothermal resource assessment

Uwera Rutagarama

60 ECTS thesis submitted in partial fulfilment of a
Magister Scientiarum degree in Geophysics

Advisor(s)
Gylfi Páll Hersir
Páll Jónsson

Faculty Representative
Sigrún Hreinsdóttir

Examiner
Grímur Björnsson

Faculty of Earth Sciences
School of Engineering and Natural Sciences
University of Iceland
Reykjavik, March 2012

The role of well testing in geothermal resource assessment

60 ECTS thesis submitted in partial fulfillment of a *Magister Scientiarum* degree in Geophysics

Faculty of Earth Sciences
School of Engineering and Natural Sciences
University of Iceland
Askja, Sturlugata 7
101, Reykjavik
Iceland

Telephone: 525 4000

Bibliographic information:
Rutagarama, U., 2012, *The role of well testing in geothermal resource assessment*, Master's thesis, Faculty of Earth Sciences, University of Iceland, pp. 86.

Printing: Pixel Prentþjónusta
Reykjavik, Iceland, March 2012

Abstract

In this thesis, different approaches and methods for analysing well test data to estimate the capacity of a geothermal field are evaluated. The thesis lays emphasis on well completion and flow tests data, and uses the Reykjanes geothermal field in southwest Iceland as an example for the application of the selected methods. Analyses of data from step-rate injection tests, temperature and pressure profiles as well as discharge tests conducted in the Reykjanes geothermal field are presented. Six wells, RN-12, RN-13b, RN-17b, RN-18, RN-23 and RN-29 were selected for the study. The computer numerical software, Well Tester, is used for the step-rate injection test analysis. Temperature and pressure profiles are analysed to estimate the formation temperature and the initial reservoir pressure. Flow characteristics are evaluated from the lip pressure method and the steam-water separator method, respectively. The wellbore simulator, HOLA, is used to evaluate the generating capacity and productivity indices of individual wells. The injectivity and productivity indices are compared with results from other similar high temperature geothermal fields. The volumetric method based on well test data is applied to predict the electrical generation capacity of the Reykjanes geothermal system. The estimated values of permeability-thickness from the injection tests range from 1 Dm to 30 Dm, whereas the storativity ranges from $5 \cdot 10^{-8}$ m/Pa to $2 \cdot 10^{-7}$ m/Pa. The reservoir temperature estimate is between 280 ^{o}C and 340 ^{o}C. The average capacity for producing electricity is estimated around 10 MW_e per well. The resource assessment is performed for two cases. Case I considers the surface alteration area of the Reykjanes field of 2 km^2 while case II considers the low resistivity sheet at 1000 m depth b.s.l. of an area of 11 km^2. The Monte Carlo simulation for case I predicts with 90% confidence interval a generating capacity between 34 MW_e and 102 MW_e for a recoverable heat, with a most likely value of 65 MW_e and between 20 MW_e and 61 MW_e with a most likely value of 39 MW_e for 30 years and 50 years, respectively. For case II, the simulation predicts with 90 % confidence interval a generating capacity between 38 MW_e and 290 MW_e with a most likely value of 132 MW_e and between 23 MW_e and 174 MW_e with a most likely value of 79 MW_e for 30 years and 50 years, respectively.

To my wonderful mother,

The best and strongest woman in my life,
Thank you for making me who I am today.

To my beautiful children,

My precious gift,
Always keep in mind that you can achieve whatever you want in life.
Believe in yourselves, work hard and treasure true friendship.

Table of contents

List of Figures

List of Tables

Nomenclature

A = Cross-section area of the lip (cm^2);

C = Wellbore storage coefficient (m^3/Pa);

c= Compressibility (Pa^{-1});

E = Heat energy (kJ);

g = Gravity (m/s^2);

H = Fluid enthalpy (kJ/kg);

h = Thickness (m);

II = Injectivity index ((L/s)/bar);

k = Intrinsic permeability (m^2);

k_r = Relative permeability of the phases (m^2);

L = Power plant capacity factor (%);

m = Slope of semi logarithmic straight line;

p = Pressure (bar-g);

P= Power plant capacity (MW_e);

P_c = Lip pressure (bar-a);

p_D = Dimensionless Pressure;

p_e= Pressure at outer boundary(bar-a);

PI = Productivity index ((kg/s)/bar);

q = Volumetric flow rate (m^3/s);

q = Production or injection flow rate (kg/s)

Q_{feed} = Mass flow rate at feedzone (kg/s);

r = Radial distance (m);

r_D = Dimensionless radius (m);

r_e = external boundary radius (m);

R_f = Recovery factor;

r_w = Wellbore radius (m);

S= Steam saturation;

S = Storage coefficient or Storativity (m/Pa);

s = Skin factor;

T = Temperature (°C);

T = Transmissivity (m^3/Pa s);

t = Time (s);

t_D = Dimensionless time based on well bore radius;

V = Volume (m^3);

W= Water level (m);

X = Steam mass fraction ratio;

z = Vertical coordinate (m);

φ = Porosity;

μ = Dynamic viscosity (Pa s);

ρ = Fluid density (kg/m^3);

η = Conversion efficiency (%).

Subscripts

s = Steam

t = Total

w = Water

Acknowledgements

This thesis would not have been possible without the support and the help of the institutions and resource persons who contributed in the preparation and completion of this study.

First and foremost, my utmost gratitude goes to the Government of Rwanda and the Government of Iceland through the University of Iceland (UI) and the United Nations University Geothermal Training Programme (UNU-GTP) for the opportunity and the financial support.

My absolute appreciation goes to the UNU-GTP Director, Dr. Ingvar B. Friðleifsson and the Deputy Director, Lúðvík S. Georgsson for the opportunity to complete this MSc programme. To the UNU-GTP staff: Thórhildur Ísberg, Markús A.G. Wilde, Ingimar Guðni Haraldsson and Málfríður Ómarsdóttir for their kind assistance.

I am grateful to my advisors, Gylfi Páll Hersir and Páll Jónsson for their overall supervision and for sharing their valuable knowledge throughout this project. My thanks are extended to Sigrún Hreinsdóttir, the representative of the Faculty of Earth Sciences at UI, for the help and support, to Grímur Björnsson for reviewing this thesis with valuable comments and to all the lecturers for the high-quality courses provided.

I am thankful to Dr. Guðni Axelsson for the valuable discussions and his helpful suggestions during this study.

I am indebted to Ómar Sigurðsson from HS Orka for providing the Reykjanes geothermal field data for the thesis. The data are the property of HS Orka and are used in the thesis with their permission which is acknowledged.

My appreciation is extended to Rósa Jónsdóttir, Gunnlaugur Einarsson and Sæunn Halldórsdóttir for their valuable assistance.

Last but not least, to my family and friends for their endless patience and continuous encouragement. I am blessed to have you in my life.

And above all to the Almighty God, who made everything possible and gave me the strength to complete this journey.

1 Introduction

The exploration and development of a geothermal resource is divided into several phases starting with preliminary studies or surface exploration, drilling, reservoir evaluation and finally the resource utilisation involving the extraction of mass and heat from the geothermal reservoir. Reliable information about a given geothermal reservoir is important when deciding whether and how to exploit it in the best and most economical manner. To reach this decision, the deliverability (ability to produce) and the properties of the reservoir must be known.

Understanding the status and properties of a geothermal reservoir is of major importance for its development and management. This is achieved by combining well testing results with information from different disciplines (geology, geochemistry geophysics and drilling) through a comprehensive conceptual model. In Rwanda, the author's home country, the development of geothermal resources is in its early stages and it has reached a point where drilling needs to be carried out to prove the existence of a geothermal potential. For the Government of Rwanda, the exploitation of geothermal resources is currently a high priority. Drilling of the first three exploration wells is planned for the year 2012. The future plan is to use well head generating units to immediately generate power if exploration wells are successful. This requires having a clear picture of the reservoir characteristics and properties. Testing of the wells will provide key reservoir parameters for field development decisions.

Well testing is the first step in evaluating the energy that can be extracted from a given reservoir. Well tests or pressure transient tests after well completion and during discharge are performed in order to estimate wellbore and reservoir properties such as permeability, the initial reservoir pressure, the reservoir limits, the well productivity, etc. These estimates are important for field development decisions. During a well test, the temperature and the pressure response of a reservoir to changing production (or injection) conditions are monitored. The pressure can be measured in the well where the flow rate has been changed or in neighbouring wells (Horne, 1995). Downhole tools allow measurements of temperature and pressure in the wells at different depths to estimate the formation temperature and the initial reservoir pressure. Discharge tests after warm up of the well is key to estimate the deliverability of the well which determines the success of the well. During the energy production from a geothermal reservoir, monitoring data are collected to continuously upgrade the picture of the reservoir. All this information is essential for a successful reservoir assessment.

Through the history of geothermal exploration and development, several techniques have been applied to assess and manage geothermal resources all over the world ranging from simple correlation to detailed modeling. The capacity of a geothermal field can be determined by its size, heat content or production response. The first assessment of a geothermal field capacity is usually done by a volumetric method (Muffler and Cataldi, 1978) which involves estimating the energy production potential of a geothermal system based on size and temperature conditions. Other methods like the lumped parameter modeling (Axelsson, 1989) can simulate the pressure response to production of a reservoir

and give a better estimate based on available data during production. More complicated assessment such as numerical modeling requires large amounts of field data to understand the nature of the system.

In this study, the following research questions were asked: What are the current approaches and methods used in well testing? What kind of information is expected at different stages of well testing and how can this information contribute to the development of a new geothermal field? How can the results of well testing be used to estimate the production capacity of a geothermal field? How can the results be used in guiding decision making for the development of a field? The purpose of this thesis is to answer some of these questions using data from wells in the Reykjanes geothermal field as an example.

Chapter 2 of this thesis outlines the theoretical background of basics aspects of well testing. The main interpretation methods for well testing are presented in Chapter 3. Well data from step-rate injection tests are modelled using a numerical software Well Tester (Júlíusson et al., 2008) to estimate reservoir and well properties as well as the injectivity indices (Chapter 4). Pressure and temperature profiles are analysed and interpreted to estimate the formation temperature and the initial reservoir pressure as well as to locate the feed zones (Chapter 5). Lip pressure and steam separator discharge tests are used to estimate the flow characteristics and the productivity indices of selected wells. The results from the discharge tests are simulated using the wellbore simulator HOLA (Björnsson et al., 1993) to evaluate the generating capacity and productivity indices of the feed zones of individual wells. Injectivity and productivity indices are then compared to estimate a relationship between the two (Chapter 6). A resource assessment is carried out to estimate the reserves of the Reykjanes geothermal field from well test data (Chapter 7). Chapter 8 presents the conclusion of the thesis. Appendix A presents detailed results and graphs for Chapters 4 to 7.

2 Resource characterisation by well testing

The goal of the first chapter is to introduce various terminologies and give a theoretical background on aspects of well testing. In Section 2.1 and 2.2, a general introduction to geothermal resources and reservoirs is given. Definition and different aspects of well testing are introduced in Section 2.3. Overview information of the data source, the Reykjanes geothermal field, used for the methodology in the thesis is given in Section 2.4.

2.1 Generalities

Geothermal energy is the natural heat contained within the Earth that can, or could, be recovered and exploited. Heat flows from the interior of the earth to the surface either by convection through hot water mass transfer or by heat conduction. The most obvious manifestations of the Earth‘s thermal energy are in areas of recent volcanism and tectonic activity. Therefore, the temperature increase with depth, the volcanoes, geysers, hot springs, etc., are in a sense the visible or tangible expression of the heat in the interior of the Earth, but this heat also engenders other phenomena that are less discernible by man. Geothermal resources are distributed throughout the world and the greatest concentration of geothermal energy is in volcanic regions but may also be found as warm ground water in sedimentary rocks.

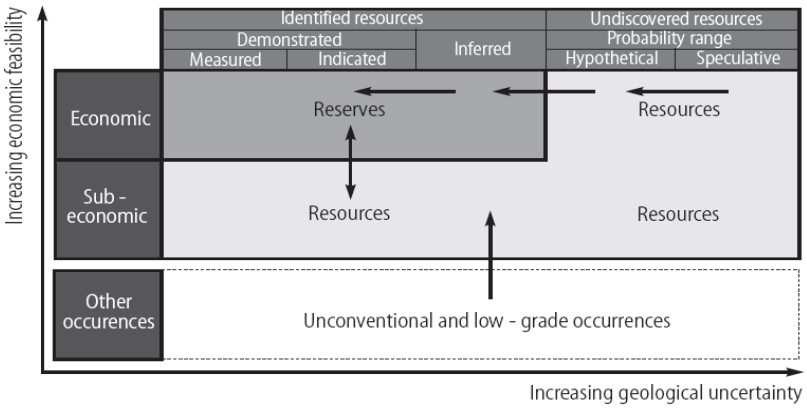

Figure 2.1: McKelvey diagram (modified from Goldemberg et al., 2000).

According to Muffler and Cataldi (1978), a geothermal resource is what should more precisely be called the accessible resource base; that is, all of the thermal energy stored between the Earth's surface and a specified depth in the crust, beneath a specified area and measured from local mean annual temperature. The accessible resource base includes the useful part (Resources) which could be produced at a price which will become competitive with other types of energy within a reasonable period of time. This category includes the identified economic resource (Reserves), part of the resources of a given area that can be extracted legally at a cost competitive with other commercial energy sources and that are known and characterised mostly by drilling. Those terminologies are easily illustrated through a modified McKelvey diagram (Figure 2.1) in which the degree of geological

assurance regarding resources is set along the horizontal axis and the economic feasibility (effectively equivalent to depth) is set along the vertical axis (Muffler and Cataldi, 1978).

2.2 Geothermal reservoir

A geothermal reservoir or reserves is usually defined as the section of an area of geothermal activity that is hot and permeable so that it can be exploited economically for the production of fluid and heat (Grant and Bixley, 2011). In other words, a geothermal reservoir needs a heat source, magma or geopressure; it needs to be confined in an aquifer and usually a caprock to hold the hot fluid in place. A schematic figure of a composite model of a geothermal reservoir is represented in Figure 2.2.

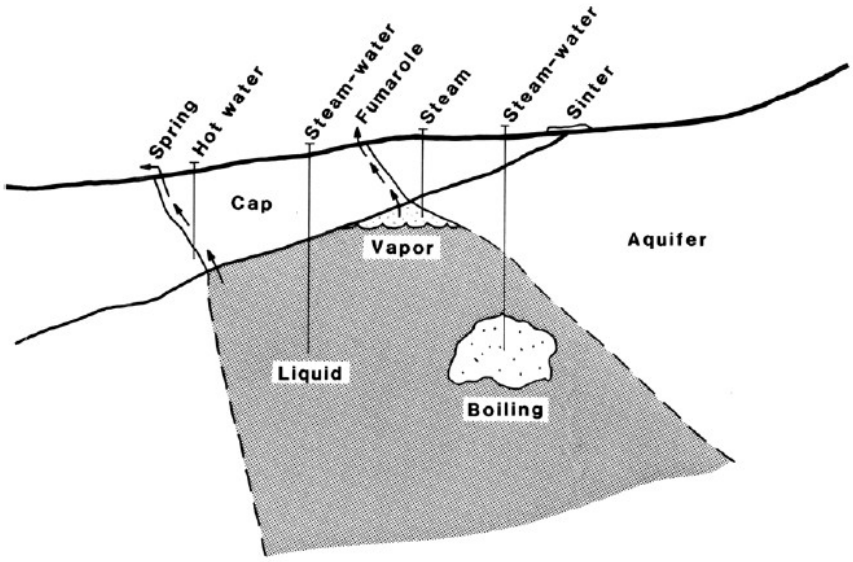

Figure 2.2: Schematic representation of a composite model of a geothermal reservoir (Gudmundsson, 1986).

Geothermal reservoirs have been classified in different ways (Bödvarsson, 1964; Axelsson and Gunnlaugsson, 2000). It is therefore of importance to define here the terminology that is in use to classify reservoirs:

- **Low temperature and high temperature reservoirs:** Low temperature geothermal systems have a base reservoir temperature below 150 ^{o}C, and high temperature systems have reservoir base temperatures above 200 ^{o}C. The intermediate system between these two systems has a base temperature between 150 ^{o}C and 200 ^{o}C. It is a medium temperature geothermal system.

- **Liquid-dominated and vapour-dominated reservoirs:** Geothermal reservoirs are conveniently categorised as either vapour dominated or liquid dominated. In each case the name refers to the phase which controls the pressure in the reservoir in its undisturbed state. When one phase is dominant, the other phase may also be present and partly mobile. A reservoir where steam and water co-exist is called a two-phase geothermal reservoir. It has to be pointed out that in high temperature geothermal

reservoirs, a decline in pressure caused by exploitation may initiate boiling in parts of the entire reservoir making a liquid dominated reservoir become a two-phase reservoir.

Geothermal reservoirs are in general more complex than petroleum and groundwater reservoirs, often requiring complicated approach. Geothermal reservoir engineering or physics is the scientific discipline that deals with fluid flow and energy transfer in geothermal systems (Axelsson, 2010). The main aim of geothermal reservoir physics is to evaluate the magnitude of the resource and the size of electric or thermal power plant that can be supported by a field over a designated project life usually in the range of 20 to 30 years. In order to address this, the reservoir engineer must undertake different field tests and analyses including (Bödvarsson and Witherspoon, 1989):

- Conducting temperature and pressure surveys to obtain information on the reservoir rocks and the feed zones properties,
- Interpreting well tests to evaluate the reservoir characteristics,
- Evaluating flow rates and enthalpies of producing wells to determine the deliverability of the wells,
- Evaluating performance of injection tests,
- Estimating reserves.

These steps are reviewed in Chapter 4 to Chapter 7.

2.3 Basics of well testing

The first step for a reservoir engineer is to estimate the relevant reservoir and wellbore parameters by a transient pressure test. This information is needed to confirm whether a well is satisfactorily drilled and to decide how to exploit the reservoir. The important reservoir and wellbore parameters are the permeability, the formation storage (or the storativity), the skin factor and the wellbore storage. The type of reservoir (porous or fractured) and the type and location of the reservoir boundaries are also important. Based on the well test objectives, several kinds of tests may be designed to determine these parameters and reservoir properties.

The following sub-sections describe the procedure of well testing (2.3.1), the reservoir and well properties (2.3.2) and the type of tests (2.3.3).

2.3.1 Well testing description

A well test is a fluid flow test conducted in wells to obtain data and information on the properties of the reservoir and the well. Well tests are done before exploiting the reservoir, but also after a period of production, to see whether and how much the reservoir properties have changed.

During a well test, the temperature and the pressure response of a reservoir to changing production (or injection) conditions are monitored. The pressure can be measured in the well where the flow rate has been changed or in neighbouring wells (Horne, 1995). Since the pressure response depends on the properties of the reservoir, it is possible to deduce various reservoir properties from the pressure response.

In practice, well testing (or pressure transient tests) consists essentially of changing the well's flow rate by fluid production from or injection into the well and measuring the well's response as a function of time. The shape of the reservoir response can then be matched against a library of type curves to identify a suitable reservoir model. Finally the model is fitted to the data and the reservoir and well parameters deduced from the model. To do so a mathematical model is built to describe the fluid flow in the reservoir/well system (Horne, 1995; Bourdarot, 1998). The procedure is illustrated in Figure 2.3. The foundation of this mathematical model is the pressure diffusion equation which describes isothermal single phase flow of a fluid through a homogeneous porous medium. To date, many methods have been proposed for the interpretation of transient tests and Chapter 3 is dedicated to the description of these methods.

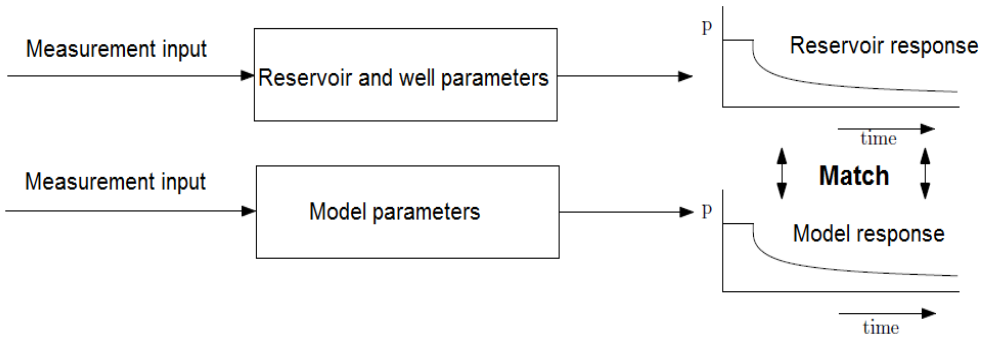

Figure 2.3: Well testing procedure (Horne, 1995).

2.3.2 Relevant reservoir and well properties

As already mentioned, the purpose of well tests is to determine reservoir and well properties. In this sub-section, the important reservoir and well properties are briefly defined and described.

Permeability of reservoir rocks

The permeability, k, controls the ability of the reservoir to transmit fluid. The higher the permeability, the easier it is for the fluid to flow through the rock matrix. In a geothermal reservoir, the fluid has to flow through the reservoir and for that reason the permeability of the rock is an important characteristic. The pressure response of the reservoir is very sensitive to the permeability. The permeability is measured in the unit Darcy, D, or milliDarcy, mD, where 1Darcy is equivalent to $0.987 \cdot 10^{-12} m^2 \sim 10^{-12}\ m^2$.

In case of a two phase geothermal reservoir, steam/water, each phase has its own relative permeability, k_{rs} and k_{rw}. These permeabilities are dependent on the fluid saturation. It is conventional to plot both permeabilities as a function of the water saturation, S_w, alone since the steam saturation, S_s, is related to the former through the simple relationship, $S_s = 1 - S_w$ (Dake, 1978). For fractured geothermal rock it is often assumed that the phases impede that $k_{rs}+k_{rw} = 1$ (Grant and Bixley, 2011).

In most geothermal systems, well tests are influenced by fractures. Fracture permeability is much higher than the permeability of the rock matrix and it has to be encountered for during well testing. It is the transmissivity, T, which is the ability of an aquifer to transmit

fluid, or the permeability-thickness, *kh*, that is determined during a test. It is therefore necessary to know the thickness of the reservoir to determine the reservoir permeability (Bourdarot, 1998).

According to Björnsson and Bödvarsson (1990), the permeability of most geothermal reservoirs ranges from 1 mD to 100 mD and the permeability- thickness, *kh,* from 1 Dm to 100 Dm (Darcy meter). Productive geothermal reservoirs have permeability-thickness, *kh* values of the order of 10 Dm or higher (Singhal & Gupta, 2010).

Reservoir storage capacity

The reservoir storage capacity or storativity, *S*, is another important characteristic of a reservoir since it is an indication of the fluid reserves in the geothermal reservoir. The reservoir storage capacity is defined as the volume of water released by unit volume of reservoir for unit drop in pressure (Kjaran and Elíasson, 1983). It controls the aquifer's capacity to store fluid. The reservoir storage capacity depends on the porosity and compressibility of both the rock matrix and the fluid.

In high temperature geothermal reservoirs, the fluid is often in two phases, liquid and vapour (Singhal & Gupta, 2010). Therefore, the storativity value of the reservoir will also depend on the relative proportions of these two phases. Since the compressibility of vapor is very large compared to that of the liquid, the value of the storativity will be large in a high temperature reservoir. Therefore, this does not necessarily mean a high porosity reservoir (Singhal & Gupta, 2010). However, the largest compressibilities occur in two phase reservoirs where the steam can be condensed into liquid water.

Wellbore Storage

Well testing measurements are commonly done at two locations: downhole and at the wellhead. In the latter case, an additional parameter, the wellbore storage, has to be considered when evaluating the reservoir system. When the well is opened to flow, the fluid at the surface is initially dominated by the expansion of the fluid stored in the wellbore and the reservoir contribution is initially negligible. Similarly, when a well is shut in, the flow rate will be zero at the top of the well, but not instantaneously at the bottom of the well, due to the compressibility of the fluid in the wellbore. In this case the wellbore storage effect is called after flow (Bourdet, 2002).

It has to be emphasised that the wellbore storage cannot be interpreted literally to give a wellbore volume. It should be considered as a nuisance effect that affects the form of the pressure transient curves. The wellbore storage is quantified in terms of a coefficient, *C*, which represents the volume of fluid that the wellbore itself will produce due to a unit drop of pressure (Grant and Bixley, 2011).

Skin effect and turbulence

Drilling of a well and well treatment operations cause changes of the reservoir characteristics in the vicinity of the well as compared to those further away in the reservoir. This effect is known as the skin effect. Mathematically, in a reservoir model, skin is represented as a region of increased or decreased permeability surrounding the wellbore (Figure 2.4). The skin factor, *s*, can be positive or negative. Positive skin

(damaged well) means an increase in pressure drop and negative skin (stimulated well) means a decrease in pressure drop at the interface between the reservoir and the wellbore (Agarwal et al., 1970, Ramey, 1970). Productive geothermal wells usually display a negative skin factor. According to Horne (1995), the skin effect can be described in terms of an effective wellbore radius which is the radius that the well appears to have due to the reduction or increase in flow caused by the skin effect.

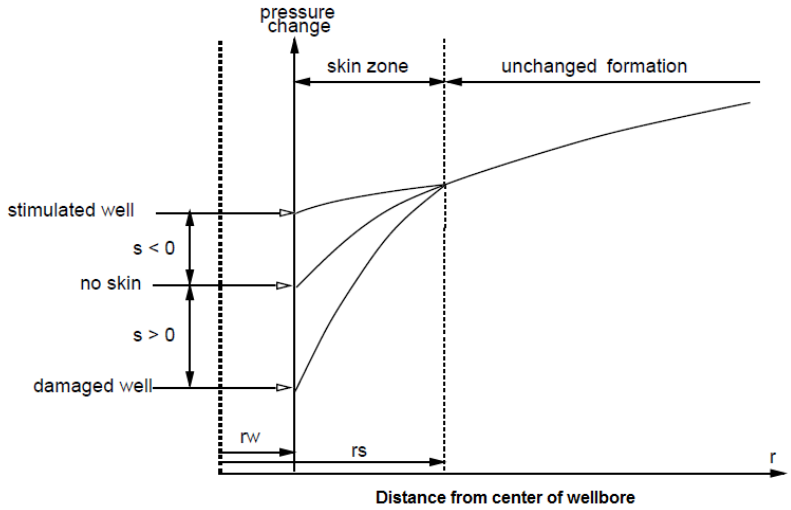

Figure 2.4: Pressure changes around a wellbore due to the skin effect (modified from Horne, 1995.

At high flow rates, or in fractured reservoirs, fluid flow tends to be turbulent, and Darcy's law (more details about Darcy's law can be found in Chapter 3) is no longer applicable. Skin due to turbulent flow or non Darcy flow is the additional pressure drop caused by high fluid velocity near the wellbore. Depending on the rate this effect can be significant and must be accounted for. It has to be noted that skin due to turbulence is always positive and is a part of the total skin. Thus, a production test on a stimulated well can still yield a positive total skin, *s,* value due to the turbulent component even if no skin damage is present.

Reservoir Boundaries

The size of the reservoir is important when estimating the amount of fluid recoverable from the reservoir. Therefore, the location and type of boundaries must be known. Two types of boundaries are most common, the closed and open boundaries.

According to Dake (1978) and Horne (1995), the closed or no-flow boundaries imply that there is no flow through the reservoir boundaries, the pressure perturbation associated with production from a well will be transmitted outward until it reaches all sides of the boundary and enters a state known as *pseudo-steady state*. The open boundaries mean that a constant pressure exists at the boundaries, that is, the reservoir is pressure supported by either an aquifer or by fluid injection. The effect of the constant pressure is known as *steady state*. Another intermediate state, *transient state* is usually observed before constant pressure or closed boundary effects are reached. In this case the reservoir behaves as if it was infinite for testing purposes. The more accurately the type and location of the

boundaries can be predicted, the more accurately can the amount of recoverable fluid be calculated. The following schematic chart (Figure 2.5) shows the typical pressure responses for reservoir models with different boundaries.

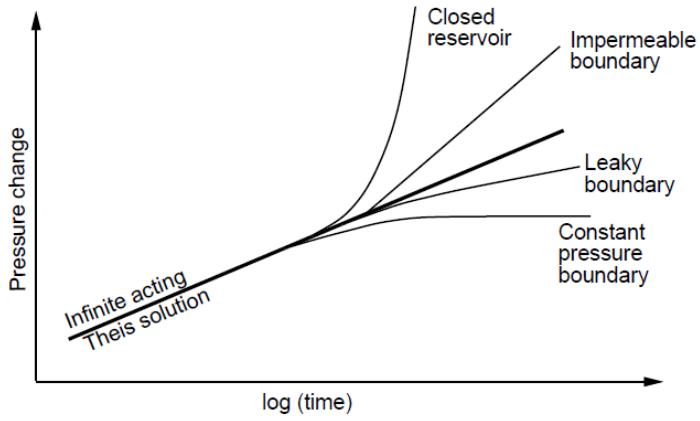

Figure 2.5: Typical pressure responses for different reservoir models (Bödvarsson and Witherspoon, 1989).

2.3.3 Types of well tests

During conventional well tests, fluid is extracted to the surface or injected into the well at controlled rates. A program of flow and shut in periods is used to establish deliverability and completion efficiency of the well. Tests can involve a single well or many wells. Depending on test objectives and operational considerations, a range of well tests can be carried out. The tests usually fall into the following categories (Horne, 1995; Bourdet, 2002):

- *Build-up test*: This test is conducted in a well that has been producing for some time at a constant rate and is then shut in. The build-up downhole pressure is then recorded for a given time.
- *Drawdown test*: This test is conducted when a well is flowed at a constant rate. The flowing downhole pressure and the production rate are measured as functions of time and analysed to estimate the reservoir properties. The major difficulty of the drawdown is the inability to maintain a constant flow rate.
- *Injection test*: This test is identical to a drawdown test, except that the flow is into the well rather than out of it. Fluid is injected into the well at a constant rate and the injection rate and the downhole pressure are measured as functions of time.
- *Falloff test*: This test is analogous to a build-up test and it measures the pressure decline as a function of time subsequent to the shut in of an injection.

The combined response can be interpreted in a number of ways to estimate the permeability-thickness and the skin factor. Tests with more than one well are called *interference tests*. Interference tests investigate the reservoir properties and establish pressure connectivity between wells. Figure 2.6 illustrates the types of well tests defined here.

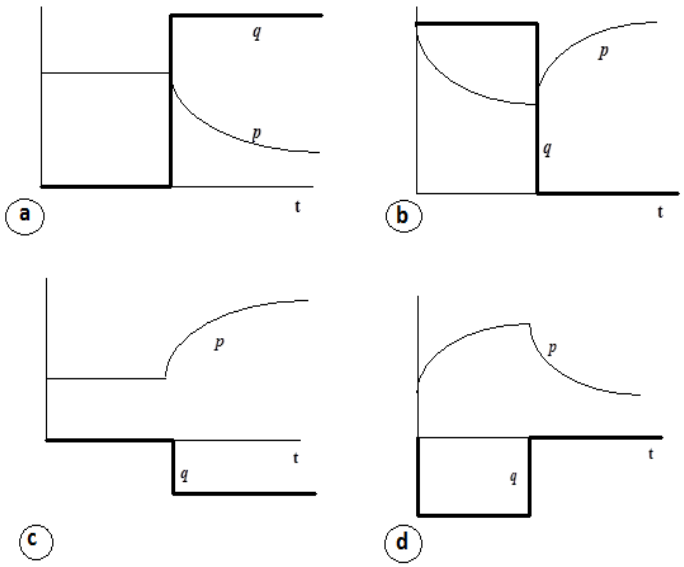

Figure 2.6: Types of well tests: a) Drawdown test, b) Build-up test, c) Injection test and d) Falloff test (Horne, 1995).

2.4 Geothermal well test data

Data from well tests in the Reykjanes geothermal field are used as an example for the application of the methodology used in the thesis. The Reykjanes geothermal system is located in the southwest of the Reykjanes Peninsula in southwest Iceland.

The exploration and development of the Reykjanes field dates back to several decades but the utilization was limited until 2006 when a 100 MW_e power plant was commissioned. The first well was drilled in 1956 to a depth of 162 m with a temperature of 185 ^oC (Gudmundsson et al., 1981). The fluid produced was a brine of seawater origin, different from rainwater commonly found in Icelandic hydrothermal systems (Sigurðsson, 2010). In the 1980's, nine wells were drilled from which two wells were used for a sea chemical plant (salt production) that was operational for only a few years. Today about 30 wells have been drilled in the area. The reservoir temperatures below 1 km depth range from about 275 ^oC to 310 °C and the fluid is hydrothermally modified seawater with some addition of magmatic gases (Arnórsson, 1978). The areal extent of geothermal surface manifestations is of the order of 2 km^2 (Pálmason et al., 1985). A resistivity survey carried out in the Reykjanes area shows a low resistivity anomaly with an aerial extension of 11 km^2 at 800 m to 1000 m depth b.s.l. (Karlsdóttir, 2005). Currently plans are made to expand the electrical power generation by adding a 50 MW_e turbine unit and possibly yet another 30 to 50 MW_e low pressure turbine unit (Sigurdsson, 2010).

Six wells in the Reykjanes geothermal field, RN-12, RN-13b, RN-17b, RN-18, RN-23 and RN-29 were selected for this study (see Table A.1). Figure 2.7 shows the location of the boreholes.

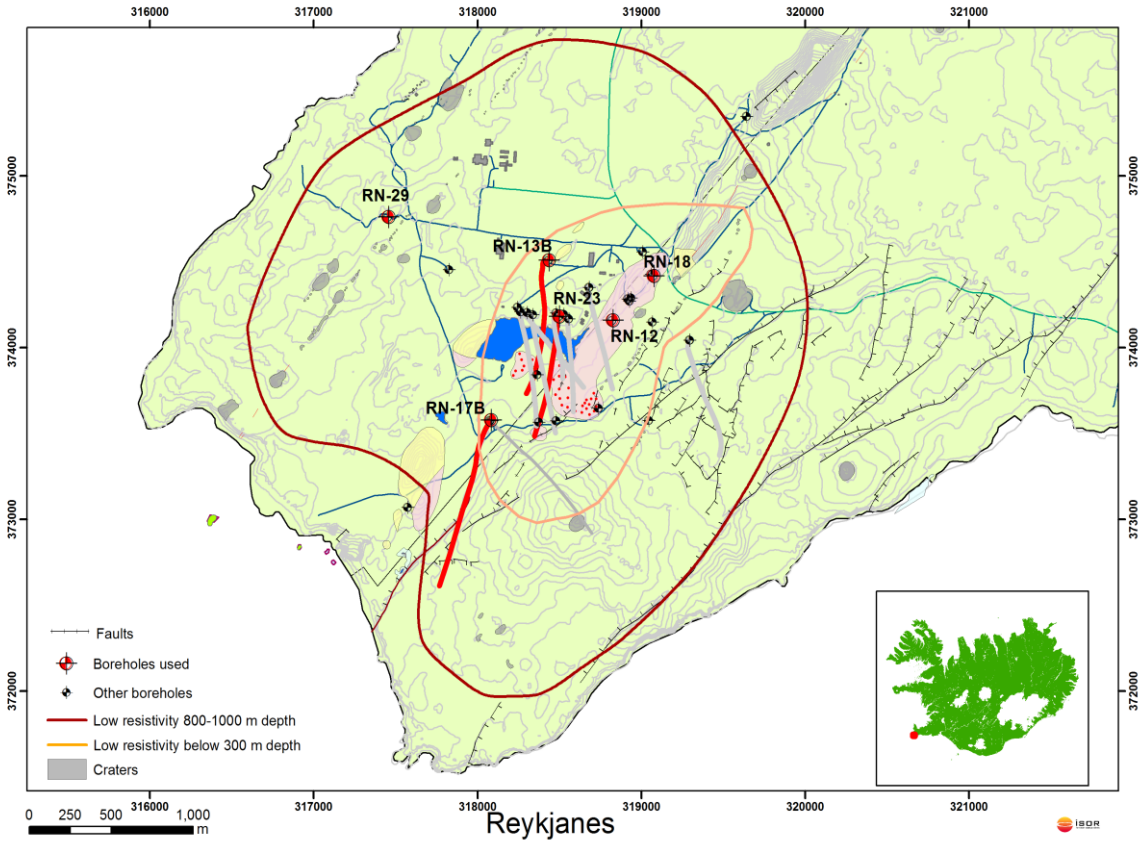

Figure 2.7: Reykjanes geothermal field and location of boreholes used in this study, shown in red. Low resistivity areas are from Karlsdóttir (2005) and craters, faults and alteration from Saemundsson et al. (2010).

3 Well test interpretation methods

The well tests and pressure transient analysis are conducted to evaluate the conditions of the wellbore and the reservoir to determine the parameters that characterize the reservoir. Therefore, a model is needed to interpret the measurements and link them to the reservoir properties. The founding principle of well testing is given by a physical equation, the pressure diffusion equation. The diffusion equation describes the spatial and temporal variations of pressure due to production or injection which is a diffusive process. The solutions of this equation give the expected outcome of the measurements of the well test (Horne, 1995).

Methods to analyse a well test are generally classified into two main groups: conventional methods and methods using type curves. All these methods depend on the type of well and reservoir as well as reservoir boundaries and can provide information on the size and shape of the formation and its ability to produce fluids.

In the following, the derivation of the pressure diffusion equation is discussed in Section 3.1 and some solutions of the diffusion equation are given in Section 3.2. Finally, the well test interpretation methods are reviewed in Sections 3.3 to 3.6.

3.1 Derivation of the pressure diffusion equation

The pressure diffusion equation is used to calculate the pressure, P, in the reservoir at a certain distance, r, from a production well producing fluid at a given volumetric flow rate, q, or mass flow rate Q equivalent to, $\rho \cdot q$ where ρ the fluid density, as a function of time, t (Horne, 1995; Grant and Bixley, 2011). It is important to emphasise here that $q > 0$ when producing from the well and $q < 0$ when injecting into the well.

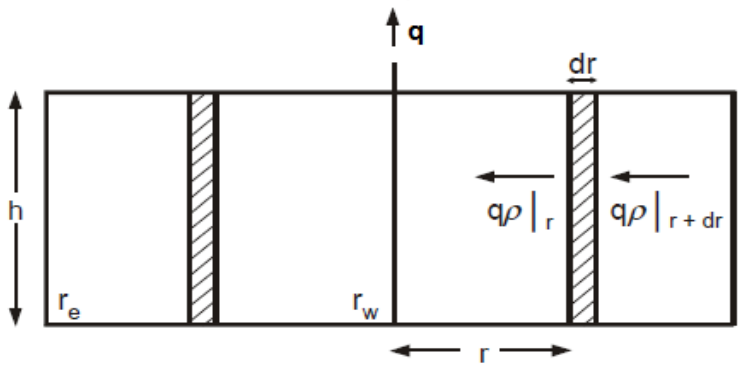

Figure 3.1: Radial flow of a single phase fluid in the vicinity of a producing well (Dake, 1978).

The pressure diffusion equation is derived using a simple model of a single phase fluid flow in a porous medium through a vertical well, circular in cross section that fully penetrates a uniform horizontal aquifer of infinite radial extent that is sealed above and below (Figure 3.1). The reservoir is considered homogeneous in all rock properties. The permeability of the reservoir is considered constant and isotropic (uniform physical

properties in all directions). The fluid is uniform and of constant compressibility. The formation is completely saturated with a single phase fluid (Horne 1995). Two governing laws and one equation of state are used in deriving the pressure diffusion equation (Earlougher, 1977; Dake, 1978; Horne, 1995; Grant and Bixley, 2011).

Considering the flow through a cylindrical shell of an infinitesimal thickness, *dr,* situated at a distance, *r,* from the centre of the radial cell. Then applying the principle of mass conservation (1), the Darcy's law (2), and the basic thermodynamic definition of isothermal compressibility (3) (Dake, 1978), we have:

1. Conservation law of mass inside a cylindrical shell around the well:

Mass flow rate in – Mass flow rate out = mass rate of change

$$(q\rho)_{|r+dr} \quad - \quad (q\rho)_{|r} \qquad = 2\pi rhdr\frac{\partial(\varphi\rho)}{\partial t}$$

where $2\pi rhdr$ is the volume of the cylindrical shell of thickness *dr*. The left hand side of this equation can be expanded as (Dake, 1978):

$$\left((q\rho)_{|r} + \frac{\partial(q\rho)}{\partial r}dr - (q\rho)_{|r}\right) \quad = 2\pi rhdr\frac{\partial(\varphi\rho)}{\partial t}$$

This simplifies to:

$$\frac{\partial(q\rho)}{\partial r} = 2\pi rh\frac{\partial(\varphi\rho)}{\partial t} \tag{3.1}$$

where, q is the production (or injection), φ is the medium's porosity, h is the reservoir thickness, ρ is the fluid density and r is the distance from the centre of the well.

2. Darcy's law:

Darcy's Law is an equation that describes the flow of a fluid through a porous medium. It is the most fundamental law used in well testing. In differential form it relates the flow rate, q, across a surface to the pressure gradient, $\partial p/\partial r$, across its section.

In the radial (axial) form, the flow rate is:

$$q = 2\pi rh\frac{k}{\mu}\frac{\partial p}{\partial r} \tag{3.2}$$

where, k is the reservoir permeability, μ the dynamic viscosity of the fluid and p is the pressure.

By substituting the flow rate (3.2) into equation (3.1), we get:

$$\frac{\partial}{\partial r}\left(2\pi rh\frac{k}{\mu}\frac{\partial p}{\partial r}\rho\right) = 2\pi rh\frac{\partial(\varphi\rho)}{\partial t}$$

This simplifies to:

$$\frac{1}{r}\frac{\partial}{\partial r}\left(r\rho\frac{k}{\mu}\frac{\partial p}{\partial r}\right)=\frac{\partial(\varphi\rho)}{\partial t} \tag{3.3}$$

3. Equation of state for isothermal compressible fluids:

In the diffusion equation, the pressure differences between two locations in the reservoir are essential. These differences would not be there without compressibility. All the information from well testing is obtained because the porous medium and the fluids are compressible (Dake, 1978).

The basic thermodynamic definition of isothermal compressibility is given by:

$$c_w=-\frac{1}{V}\left(\frac{\partial V}{\partial p}\right)$$

where, c_w is the fluid compressibility and V is the fluid volume. Since $\rho=\frac{m}{V}$ where m is the mass of fluid, the isothermal compressibility can be expressed as:

$$c_w=\frac{1}{\rho}\left(\frac{\partial\rho}{\partial p}\right)_T \tag{3.4}$$

The right hand side of equation (3.3) can then be written as:

$$\frac{\partial(\varphi\rho)}{\partial t}=\rho\frac{\partial\varphi}{\partial t}+\varphi\frac{\partial\rho}{\partial t} \tag{3.5}$$

From equation (3.4), it can be shown that (Bear, 1979):

$$\varphi\frac{\partial\rho}{\partial t}=\varphi c_w\rho\frac{\partial p}{\partial t} \tag{3.6}$$

and,

$$\rho\frac{\partial\varphi}{\partial t}=(1-\varphi)c_r\rho\frac{\partial p}{\partial t} \tag{3.7}$$

where, c_r is the compressibility of the rock matrix. Inserting equations (3.6) and (3.7) into (3.5) gives:

$$\frac{\partial(\varphi\rho)}{\partial t}=\rho c_t\frac{\partial p}{\partial t} \tag{3.8}$$

where, c_t is the total compressibility of the system defined as $c_t=\varphi c_w+(1-\varphi)c_r$

By inserting (3.8) into (3.3) and expanding the left hand side of (3.3) assuming that the reservoir is homogeneous and therefore variations in ρ, k and μ are small, we can express the pressure diffusion equation as:

$$\frac{1}{r}\frac{\partial}{\partial r}\left(r\,\frac{\partial p}{\partial r}\right)=\frac{\mu c_t}{k}\frac{\partial p}{\partial t} \tag{3.9}$$

By introducing the parameters:

$$T=\frac{kh}{\mu} \quad \text{and} \quad S=c_t h$$

where T is the transmissivity and S is the storativity, equation (3.9) can be rewritten as:

$$\frac{1}{r}\frac{\partial}{\partial r}\left(r\,\frac{\partial p}{\partial r}\right)=\frac{S}{T}\frac{\partial p}{\partial t} \tag{3.10}$$

Equation (3.9) is the basic equation for well test analysis. In principle, an infinite number of solutions of equation (3.9) can be obtained depending on the initial and boundary conditions imposed (Dake, 1978).

In some liquid dominated reservoirs, the water table is measured instead of the pressure. In such cases, equation (3.9) can be rewritten as follows:

$$\frac{1}{r}\frac{\partial}{\partial r}\left(r\,\frac{\partial W}{\partial r}\right)=\frac{\mu c_t}{k}\frac{\partial W}{\partial t} \tag{3.11}$$

with the water table $W=z+{}^{p}/_{\rho g}$ where, z is the elevation and g is the acceleration of gravity. In this case, the appropriate initial and boundary conditions must be formulated in elevation of the water table (Kjaran and Elíasson, 1983).

3.2 Solutions of the diffusion equation

An infinite number of solutions for the diffusion equation (3.9) can be obtained for different regimes depending on the initial and boundary conditions imposed. These boundary conditions are assumptions based on a prior knowledge of the reservoir. These regimes are the transient, semi steady (pseudo-steady) state and steady state regimes (Dake, 1978; Kjaran and Elíasson, 1983). The transient flow occurs before the pressure response shows the presence of a boundary. The steady state and pseudo-steady state represent two types of boundary effects; constant pressure and closed boundary, respectively.

3.2.1 Transient flowing regime

This condition is only applicable for a relatively short period after some pressure disturbance has been created in the reservoir. For the period that the transient regime is applicable it is assumed that the pressure response of the reservoir at the top of the wellbore is not affected by the presence of a boundary (Figure 3.2). Thus the reservoir radius, r_e appears infinite in extent and the pressure at outer boundary, p_e is equal to the initial pressure, p_i (Dake, 1978).

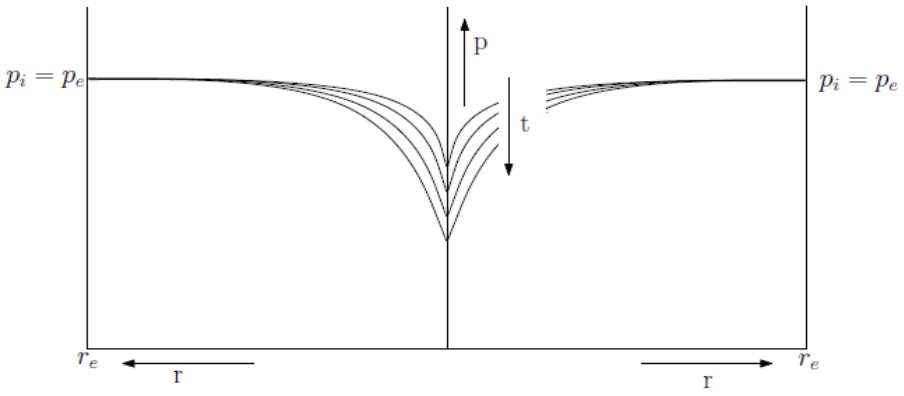

Figure 3.2: Pressure distribution under transient flow regime (modified from Dake, 1978).

The transient regime can be split up in two sub-regimes:

- **Wellbore dominated regime**. The wellbore dominated regime describes the very early part of the well test where the dynamics of the wellbore are dominating the reservoir dynamics in the pressure response. It is assumed that the pressure response in this regime does not contain any information about the reservoir, but only about the wellbore storage and skin.

- **Infinite flowing regime**. The infinite flowing regime describes the pressure response of the reservoir when the dynamics of the reservoir are assumed to be dominating the wellbore dynamics and there is no significant influence of the boundaries in the pressure response.

The most common solution of the diffusion equation for a transient flowing regime is described here. It is assumed that the wellbore is a line meaning that the wellbore radius, r_w is zero and the solution is often called the Theis solution (Theis, 1935) or the line source solution. To solve the pressure diffusion equation, one initial and two boundary conditions are needed. The initial condition describes the pressure state in the reservoir at a certain time while the boundary conditions describe the effect of the environment on the flow process. These conditions involve several assumptions and are therefore only valid for specific time intervals. For the Theis solution, the following initial and boundary conditions are assumed (Earlougher, 1977; Dake, 1978; Horne, 1995):

Initial condition: The pressure, p is the same all over the reservoir at time $t = 0$ and is equal to the initial pressure, p_i

$$p = p_i \quad at\ t = 0,\ for\ all\ r$$

Outer-boundary condition: The pressure is equal to the initial pressure at infinity

$$p = p_i \quad for\ r \rightarrow \infty,\ for\ all\ t$$

Inner-boundary condition: Darcy's law at the wellbore producing at constant rate q (equation 3.2)*:*

$$\lim_{r\to 0}\left(r\frac{\partial p}{\partial r}\right)=\frac{q\mu}{2\pi kh} \quad \text{for } t>0$$

In addition, the assumptions made in deriving the diffusion equation are the same as stated in the previous section. That is, the formation is homogeneous and isotropic, and drained by a fully penetrating well ensuring radial flow. The fluid properties are constant. Under these conditions, the line source solution of the diffusion equation known as the Theis solution (Theis, 1935) is given by:

$$p(r,t)=p_i+\frac{q\mu}{4\pi kh}Ei\left(\frac{-\mu c_t r^2}{4kt}\right) \tag{3.12}$$

where *Ei* represents the exponential integral function defined by:

$$Ei(-x)=-\int_x^{\infty}\frac{e^{-u}}{u}du \tag{3.13}$$

For small values of x (x < 0.01) the exponential integral *Ei* can be approximated by:

$$Ei(-x)\cong\gamma+\ln(x) \tag{3.14}$$

where γ = 0.5772 is the Euler's constant and ln is the natural logarithm. Therefore, for $>100\frac{\mu c_t r^2}{4k}$, the Theis solution or line source solution is simplified and represented as:

$$p(r,t)=p_i+\frac{2.303\,q\mu}{4\pi kh}\left[log\left(\frac{\mu c_t r^2}{4kt}\right)+\frac{\gamma}{2.303}\right] \tag{3.15}$$

where 2.303 ≈ ln10 and log is the logarithm with base 10.

The Theis solution describes the pressure response with time, *t*, at location, *r*, from the wellbore given the inherent assumptions. The limitation of the Theis solution is for drawdown tests at the distance, *r* at time, *t* when producing at a constant rate, *q* and for unbounded boundaries. From this solution, it can be observed that by suitable observation of the pressure change, it may be possible to identify two important parameters: the permeability-thickness and the storativity (Earlougher, 1977; Horne, 1995).

At the active well, the skin factor is introduced as an extra pressure change. At an observation point or a well where the skin does not apply, the pressure drawdown can be defined as:

$$\Delta p_{well}=p_i-p_{no\ skin}(r,t) \tag{3.16}$$

The change in drawdown due to skin is defined by:

$$\Delta p_{skin}=\frac{q\mu}{2\pi kh}s \tag{3.17}$$

Therefore, the total drawdown at the wellbore ($r=r_w$) is then $\Delta p=\Delta p_{well}+\Delta p_{skin}$ and equation (3.15) can be rewritten as:

$$p(r_w, t) = p_i + \frac{2.303\, q\mu}{4\pi kh}\left[log\left(\frac{\mu c_t r_w^2}{4kt}\right) + \frac{\gamma - 2s}{2.303}\right] \quad (3.18)$$

3.2.2 Semi steady state regime

The semi steady state or pseudo-steady state flow is applicable to a reservoir which has been producing for a sufficient period so that the effect of the outer boundary has been noticed. This means that the pressure decline has struck impermeable boundaries all around the producing well. In terms of the radial flow model, the situation is illustrated in Figure 3.3 (Dake, 1978).

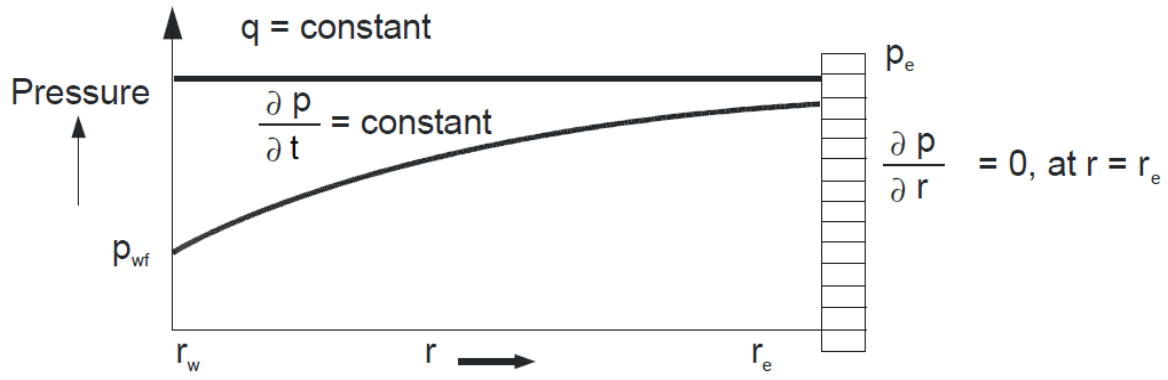

Figure 3.3: Pressure distribution under semi steady state regime, where r_e is the distance from the well to the boundary (Dake, 1978).

The first assumption is that at the outer boundary of the reservoir, in accordance with Darcy's law, the pressure gradient is zero meaning that there is no recharge in the system:

$$\frac{\partial p}{\partial r} = 0 \quad at\ r = r_e$$

The second assumption considers that, if the well is producing at a constant rate, the pressure will decline in such a way that the pressure derivative with respect to time is constant everywhere in the reservoir meaning that the system is closed.

$$\frac{\partial p}{\partial t} = \text{constant} \quad \text{for all r and t}$$

Using the definition of compressibility, the constant of the second assumption can easily be obtained as:

$$\frac{\partial p}{\partial t} = -\frac{q}{Vc_t} \quad (3.19)$$

in which V is the pore volume of the radial cell; q is the constant production rate and t is the total flowing time.

For a radial reservoir with radius r_e , the volume is $V = \pi r_e^2 h$, and the second assumption can be rewritten as:

$$\frac{\partial p}{\partial t} = -\frac{q}{c_t \pi r_e^2 h} \tag{3.20}$$

When substituting the equation (3.20) into (3.9), the diffusion equation becomes:

$$\frac{1}{r}\frac{\partial}{\partial r}\left(r\,\frac{\partial p}{\partial r}\right) = -\frac{q\mu}{kh\pi r_e^2} \tag{3.21}$$

The solution of the diffusion equation (3.21) for the semi steady state regime is then given by (Dake, 1978):

$$p(r,t) - p(r_w,t) = \frac{q\mu}{2\pi kh}\left(ln\frac{r}{r_w} - \frac{r^2}{2r_e^2} + \frac{r_w^2}{2r_e^2}\right) \tag{3.22}$$

Introducing the skin factor, we get:

$$p(r,t) - p(r_w,t) = \frac{q\mu}{2\pi kh}\left(ln\frac{r}{r_w} - \frac{r^2}{2r_e^2} + \frac{r_w^2}{2r_e^2} + s\right) \tag{3.23}$$

where *p (r, t)* is the pressure at a distance *r* from the centre of the wellbore and *p* (r_w, *t)* is the pressure at the wellbore with radius r_w at time *t*. The term $\frac{r_w^2}{2r_2^2}$ can be considered negligible since $r_w << r_e$ (Dake, 1978).

3.2.3 Steady state regime

The steady state regime is used when the pressure response does not drop anymore for example due to some displacing fluid leading to a constant pressure with time at the boundary (Figure 3.4). The steady state condition applies, after the transient period, to a well draining a reservoir which has a completely open outer boundary. It is assumed that, for a constant rate of production, fluid withdrawal from the reservoir will be exactly balanced by fluid entry across the open boundary and therefore (Dake, 1978):

$$p = p_e = constant, at\ r = r_e$$

and

$$\frac{\partial p}{\partial t} = 0\ for\ all\ r\ and\ t$$

The diffusion equation (3.9) then reduces to:

$$\frac{1}{r}\frac{\partial}{\partial r}\left(r\,\frac{\partial p}{\partial r}\right) = 0 \tag{3.24}$$

The solution of the diffusion equation for the steady state regime is known as the Theim solution (Theim, 1906) and is given by:

$$p(r) - p(r_w) = \frac{q\mu}{2\pi kh}\left(ln\frac{r}{r_w}\right) \tag{3.25}$$

With the introduction of the skin factor, this gives:

$$p(r) - p(r_w) = \frac{q\mu}{2\pi kh}\left(ln\frac{r}{r_w} + s\right) \tag{3.26}$$

Equation (3.25) determines a pressure difference as a function of the radius. The solution is independent of time (Dake, 1978).

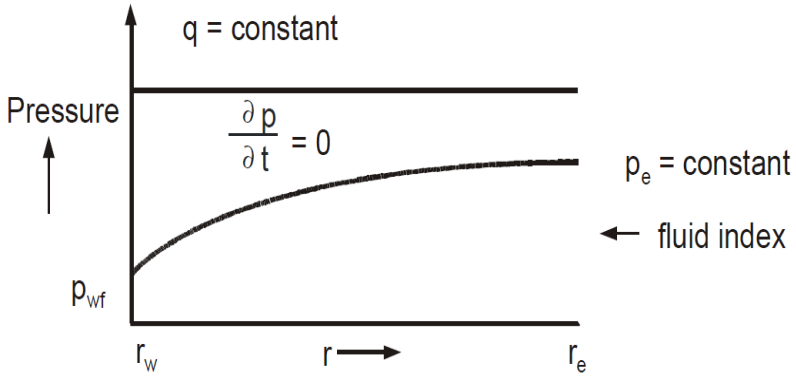

Figure 3.4: Pressure distribution under steady state regime (Dake, 1978).

It should be noted that the semi-steady state or the steady state conditions may never be fully realised in the reservoir during well tests. However, it is the solution of the transient flow regime (3.15) that is often used to interpret the well test data since it is the pressure disturbance for a relatively short period that gives the information on the reservoir (Dake, 1978).

3.3 Semi logarithmic analysis

During radial flow, the pressure change or drawdown is related to the logarithm of time. In other words, if the pressure is plotted against the log of time, infinite-acting radial flow (the intermediate time response between the wellbore storage and the boundary response) will give a straight line (Figure 3.5). The semi-logarithmic approach to well test interpretation is based upon plotting the pressure or the drawdown, p or Δp, versus time t, in a semi-logarithmic graph and identifying a straight line portion of the drawdown or build-up data, from which the permeability-thickness product, the storativity and the skin damage are obtained (Earlougher, 1977; Horne, 1995).

By rearranging (3.15) into the form $\Delta p = A + m \log(t)$, the pressure change or the drawdown, Δp can be plotted versus time on a semi logarithmic graph and a straight line portion of the graph with a slope, m is obtained as the pressure drop for one log-cycle (Horne, 1995):

$$m = \frac{2.303q\mu}{4\pi kh} \tag{3.27}$$

When the slope m is found according to equation (3.27), the permeability-thickness can be evaluated as:

$$kh = \frac{2.303q\mu}{4\pi m} \tag{3.28}$$

The storativity is obtained by using the value of the drawdown $\Delta p = p_i - p(r,t)$ at some particular time *t* and some value of *r* (usually r_w) from equation (3.15):

$$c_t h = 2.25\left(\frac{kh}{\mu}\right)\left(\frac{t}{r^2}\right)10^{-\Delta p/m} \tag{3.29}$$

In order to calculate the skin factor *s*, equation (3.18) can be used, isolating *s* from it. The value of $p\ (r_w,\ t)$ is read from the solid straight line with slope *m*. Often the time *t* equivalent to 1 hour is chosen but any point $(t,\ p\ (r_w,\ t))$ on the straight line can be used. In the later case, the constants in the formulas will change depending on the time value selected:

$$s = 1.151\left[\frac{\Delta p}{m} - log\left[\left(\frac{4kh}{\mu}\right)\left(\frac{1}{c_t h}\right)\frac{t}{r_w^2}\right] + 0.251\right] \tag{3.30}$$

Note that the direct interpretation method is an indirect estimation method, since the step response has to be plotted first (Earlougher, 1977; Horne, 1995).

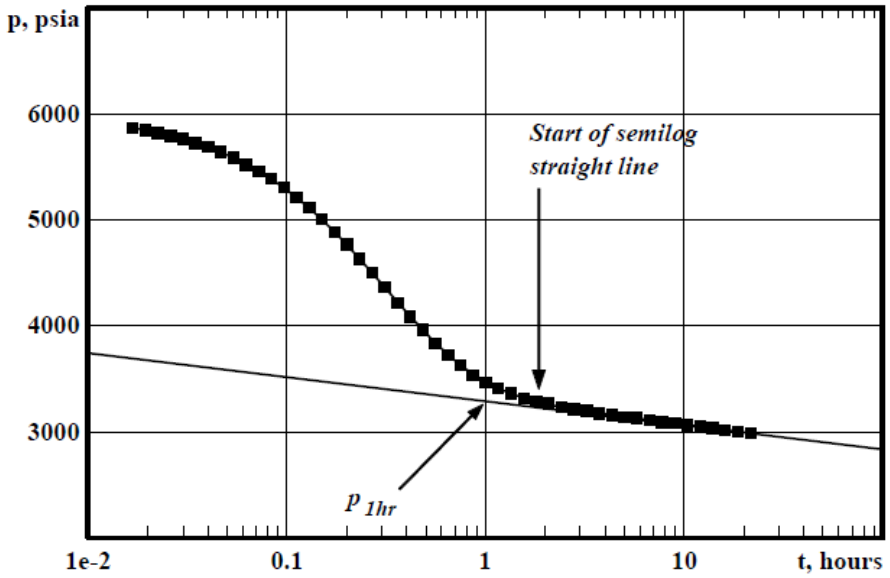

Figure 3.5: Semi log representation (Horne, 1995).

The best known and most commonly used semi-logarithmic analysis techniques or conventional methods are the *Miller-Dyes- Hutchinson or MDH plot* and *the Horner plot*.

The Miller-Dyes-Hutchinson, MDH plot (Miller et al., 1950) is strictly valid only for the first drawdown in a well, but in exceptional circumstances it can be used for the analysis of a later drawdown or a build-up test. It applies to wells that have reached pseudo-steady (semi-steady) state during injection. For the MDH plot, the pressure is plotted versus the logarithm of time, *log (t)*.

It is common to use the Horner plot to estimate the formation temperature (Horner, 1951; Dowdle and Cobb, 1975). The Horner plot is also the most used method and is more convenient for pressure build up tests (Horne, 1995). Pressure build-up tests require shutting in a production well. The effect of these two flow rates can be represented by a well which is produced for a time t_p, at rate q, and then shut in for a running time Δt. The pressure response is plotted versus log $((t_p+\Delta t)/\Delta t)$ on a semi-log plot. The superposition time $((t_p+\Delta t)/\Delta t)$ is known as the Horner time (Earlougher, 1977; Horne, 1995).

3.4 Dimensionless variables and type curve analysis

Another method for estimating the reservoir properties is to compare the plot of the measured pressure response with type curves. The type curve method (log-log method) was introduced in the petroleum literature by Ramey (1970) in an attempt to overcome the limitations of the semi-log straight line based analysis methods (Earlougher, 1977). To generalise the solution of the pressure diffusion equation, it is beneficial to transform the equation into a dimensionless form as it simplifies the reservoir models by representing the reservoir parameters independently of any particular unit system. Any variable can be made dimensionless by multiplying it by a group of constants with the opposite dimensions. These groups of constants depend on the reservoir parameters (Earlougher, 1977; Horne, 1995).

Dimensionless pressure $p_D\,(r_D,\, t_D)$,

$$p_D = \frac{2\pi kh}{q\mu}\Delta p \tag{3.31}$$

where $\Delta p = p_i - p_w$ and p_w is the pressure measured in the well

Dimensionless time t_D

$$t_D = \frac{kt}{c_t \mu r_w^2} \tag{3.32}$$

Dimensionless radius r_D

$$r_D = \frac{r}{r_w} \tag{3.33}$$

By defining dimensionless pressure and dimensionless time in this way, it is possible to create an analytical model of the well and reservoir, or theoretical type-curve log (p_D) versus log (t_D), that provides a description of the pressure response that is independent of the flow rate or of the actual values of the well and reservoir parameters. The data from the well test are plotted and the plot is compared with plots derived from theory. The reservoir properties are estimated by finding the best match (Horne, 1995).

The log-log type curve approach described here above is now somehow out of date in the industry compared to the semi-log approach, or the approach combining the log-log plot of Δp versus Δt with the pressure derivative where it is possible to make the entire analysis with a single plot. The pressure derivative approach is described in the following section.

The procedure for the type curve analysis (Figure 3.6) can be outlined as follows (Earlougher, 1977; Horne, 1995):

- The data are plotted as log Δp versus log (Δt) using the same scale as that of the type curve.
- The curves are then moved one over the other by keeping the vertical and horizontal grid lines parallel until the best match is found.
- The best match is chosen and the pressure and time values are read from some fixed point (match point) on both graphs, Δp_M, p_{DM}, Δt_M and t_{DM}.

For infinite acting system, the permeability-thickness and the storativity are given by the expression:

$$kh = \frac{q\mu}{2\pi}\left(\frac{p_D}{\Delta p}\right)_M \tag{3.34}$$

$$c_t h = \frac{kh}{\mu r_w^2}\left(\frac{\Delta t}{t_D}\right)_M \tag{3.35}$$

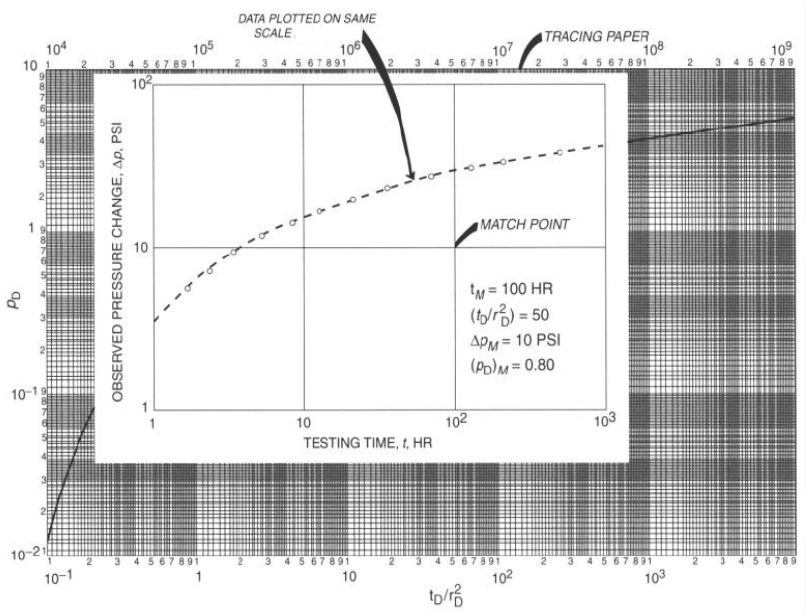

Figure 3.6: Illustration of a type curve matching for an interference test (Earlougher, 1977).

3.5 Pressure derivative plot

The introduction of the pressure derivative in the 80's by Bourdet and others (Bourdet et al., 1983; Bourdet et al., 1989) transformed the science of well test interpretation, which until that time had mostly been based on the semi-logarithmic plot and the type curve analysis. With the derivative approach, the time rate of change of pressure during a test period is considered for the analysis. In order to emphasise the radial flow regime, the partial derivative is taken with respect to the logarithm of time $\frac{\partial p}{\partial(lnt)}$ which equals $t\frac{\partial p}{\partial t}$ (Bourdet et al., 1983). The derivative plot provides a simultaneous presentation of log (Δp)

versus log *(Δt)* and log $(t\frac{\partial p}{\partial t})$ versus log *(Δt)*. The advantage of the derivative plot is that it is possible to display in a single graph many different characteristics that would otherwise require different plots (Horne, 1995).

Reservoir permeability, wellbore storage and skin can be determined directly using the measured curve and its derivative provided that the stabilization of the derivative has been reached. When the flow at early time corresponds to pure wellbore storage, pressure and pressure derivative curves will merge on a unit slope straight line on the log-log plot (Horne, 1995).

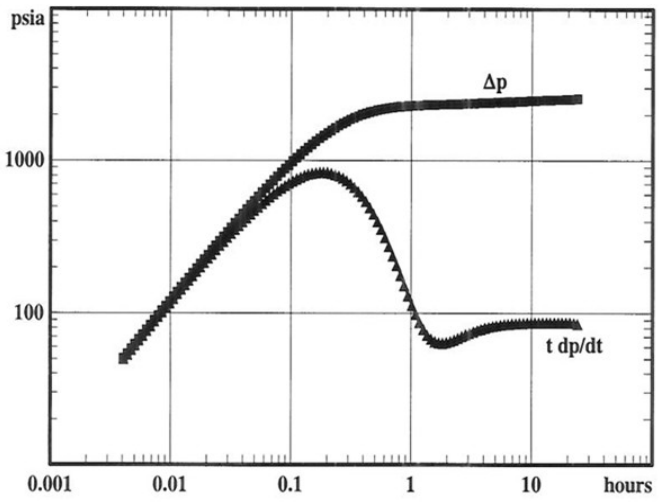

Figure 3.7: Illustration of a derivative plot (Horne, 1995).

Until a few decades ago, the plotted data and the type curves were compared by hand. The use of computers and software developed for well testing, such as Well Tester used in Iceland (introduced in Chapter 4), make the calculation of the derivative much easier, and this has become one of the major tools in well test analysis methods (Bourdarot, 1998; Gringarten, 2008).

3.6 Deconvolution

Deconvolution has received much attention recently (Von Schroeter et al., 2001; Levitan, 2005; Ilk et al., 2005; Levitan et al., 2006). Deconvolution is not a new interpretation but a new tool to process pressure and flow rate data (Gringarten, 2008). According to the general definition, the aim of deconvolution is to calculate the impulse response of the system, based on the pressure response and both constant and varying flow rates.

The data used for deconvolution are better from built up data than drawdown data, because of their good quality compared to drawdown data. The deconvolution does not assume a reservoir model but it assumes a mathematical model. It is a direct method using non-linear regression compared to the conventional methods used for well testing. Changing skin, changing wellbore storage, missing or incorrect initial pressure and gaps in the data can have a significant effect on the shape of the deconvolved type curves (Gringarten, 2008).

The steps for the deconvolution method can be described as follows:

- The partial derivative $t\frac{\partial p}{\partial t}$ is assumed,
- The starting point, P_i on the type curve is assumed,
- The derivative is then integrated to obtain the type curve,
- The type curve is superposed with flow rates,
- The calculated results are compared with the measured data,
- The total error is quantified,
- The derivative is modified and the procedure repeated until the minimum error in a least square sense is found.

The deconvolution method removes the restriction for a shut in, but does not remove the need for type curves. The final result of this identification method is an estimate of a type curve. This type curve can be used in order to estimate the reservoir properties. Different deconvolution methods and mathematical formulas can be found in Von Schroeter et al., 2001; Levitan, 2005; Ilk et al., 2005; Levitan et al., 2006.

4 Injection tests

4.1 Introduction

A common procedure in Iceland and elsewhere is to perform a step-rate injection test soon after the drilling and completion of the borehole. The injection tests consist of injecting cold water into the borehole and simultaneously recording downhole pressure and temperature (pressure and temperature profiles are analysed in Chapter 5). The injection test, opposite to the production test, causes an increase of the pressure in the well.

The twofold purpose of the injection test is to stimulate the well and to obtain data that can be analysed to calculate the transmissivity and storativity of the formation together with the skin (Bödvarsson et al., 1981; Axelsson et al., 2006).

Another characteristic of the borehole that is evaluated during injection test is the injectivity index *(II)*. The injectivity index predicts the performance of an injection well and is believed to reflect the success of the well meaning that the bigger its value, the better the reservoir permeability. It is defined by the ratio of the change of injection flow rate to the change in reservoir pressure measured in the borehole:

$$II = \frac{\Delta q}{\Delta p} \tag{4.1}$$

The numerical software Well Tester V.1.0.0 (Juliusson et al., 2008) is used for modelling and calculation of the reservoir parameters. Well Tester is a computer software that was developed at the Iceland GeoSurvey (ISOR) to handle data manipulation and analysis of well tests (mainly multi-step injection tests) in Icelandic geothermal fields. The process is divided into six simple steps (Juliusson et al., 2008):

- Parameters: The estimation of the reservoir temperature and pressure, the wellbore radius, the viscosity of the fluid, the porosity and the total compressibility are fed into the program in this step;
- Set steps: The number of injection steps are defined;
- Modify: This step is designed to clean, resample and correct the data for temperature variations within the wellbore during the course of the well test;
- Model: In this step, the most appropriate model for the reservoir being investigated is selected. To achieve this, the derivative plot is used, along with the pressure data on a log-log scale graph.
- Model all: This tab is designed to find the model parameters that give the best correspondence between a multi-step model and data set, modeling all the step together.
- Report: The program prepares a report of results at the end of the modeling.

In the following Section 4.2, Well Tester is used to estimate the transmissivity, the storativity and the injectivity indices for wells RN-17b, RN-18 and RN-23. Section 4.3 gives the summary of the results from Well Tester.

4.2 Well Tester modelling

4.2.1 RN-17b injection test

Well RN-17b is a directional well and it was drilled in 2008 to a measured depth, MD of 3077 m (True vertical depth, TVD is 2804 m). The injection test in RN-17b started just after completion of drilling in December 2008. A three-step injection test was performed the same day and the injection rates were from 20.1 L/s to 30.3 L/s; 30.3 L/s to 44.9 L/s and 44.9 L/s to 20.1 L/s, respectively. The total injection test was done in 9 hours with a pressure gauge being lowered to a depth of 2300 m.

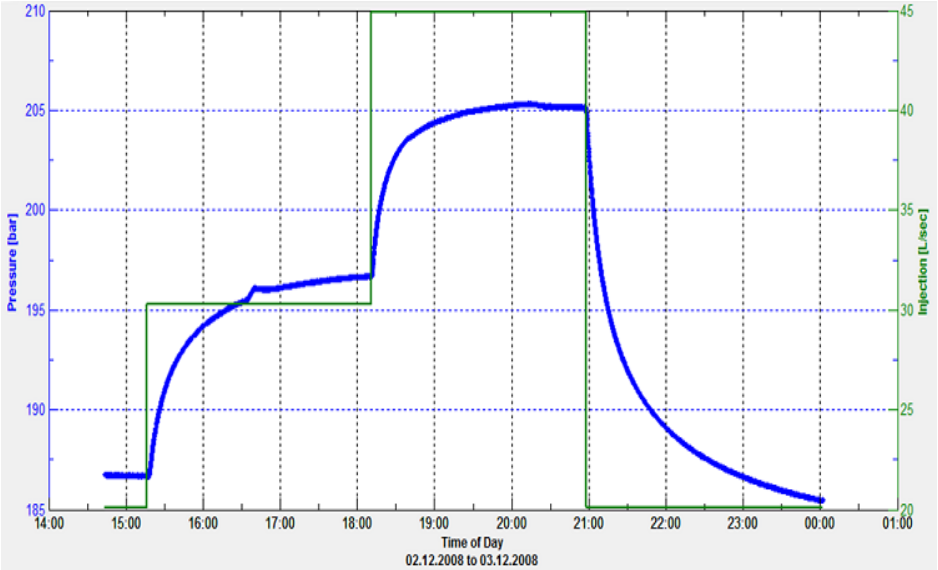

Figure 4.1: Pressure changes during step rate injection test for RN-17b.

Figure 4.1 shows the steps of the injection test and the pressure response for each step. A small hump on the pressure response for step 1 is observed, which could be an indication of an error from the tool during measurement. Step 2 shows a pressure drop towards the end of the step and this could indicate a small opening in the reservoir. The last step, step 3 indicates a falloff test and it can be observed that the pressure did not reach equilibrium at the end of the test. For this reason, it was decided to disregard this step in the modelling.

The well test model selected for RN-17b assumed a homogeneous reservoir, constant pressure boundary, constant skin and a wellbore storage. The pressure gauge depth was an input into the program and the data were cleaned. Using this model, a non-linear regression analysis was performed to find the parameters of the model that best fit the data. The best model was calculated by considering step 1 and 2, respectively and then, both steps together.

The results from the regression analysis for step 1 and step 2 are shown graphically in Figure A.1 and A.2. Figure 4.2 shows the best model calculated for RN-17b. The estimation of the parameters obtained on the basis of the steps and model selected for both step 1 and 2 (Table 4.1) indicate a permeability-thickness of 1 Dm, a storativity of $7 \cdot 10^{-8}$ $m^3/(Pa \cdot m^2)$ and an injectivity index of 1.3 (L/s)/bar. The values of the permeability-

thickness and the injectivity index can be interpreted as a poor permeability in this part of the reservoir although the skin is negative.

Table 4.1: Summary of the results from non-linear regression parameter estimate using injection test data from well RN-17b

Step	Transmissivity ($m^3/(Pa \cdot s)$)	Storativity ($m^3/(Pa \cdot m^2)$)	Permeability thickness (Dm)	Skin	Injectivity index (L/s)/bar
1	$1.08 \cdot 10^{-8}$	$4.5 \cdot 10^{-8}$	0.9	-0.7	1.5
2	$1.4 \cdot 10^{-8}$	$3.03 \cdot 10^{-8}$	1.24	-0.9	1.7
1 and 2	$1.14 \cdot 10^{-8}$	$7.04 \cdot 10^{-8}$	1.02	-0.7	1.31

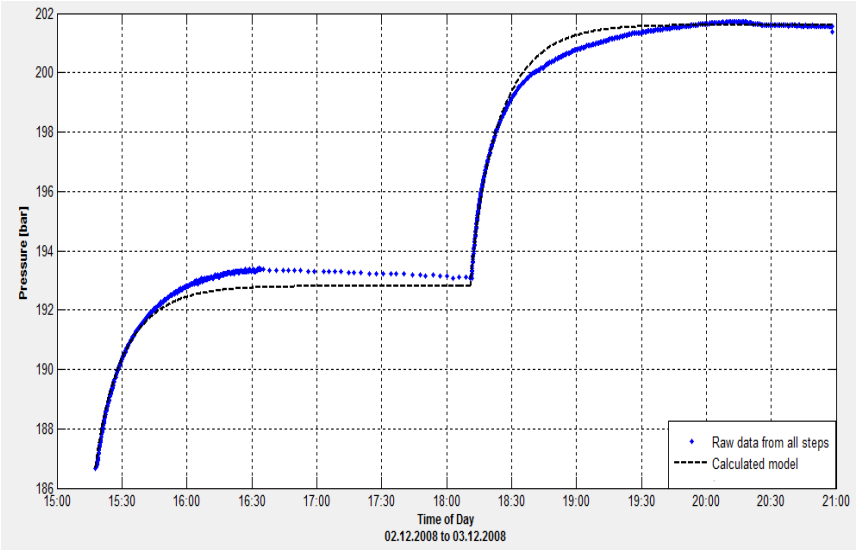

Figure 4.2: Fit between model and measured data for step 1 and 2 for well RN-17b

4.2.2 RN-18 injection test

Borehole RN-18 was drilled vertically to a depth of 1815 m and completed in January 2005. Two injection tests were performed afterwards with a pressure gauge being lowered to a depth of 1740 m. The two step injection rates were from 30.1 L/s to 48.2 L/s and 48.2 L/s to 25 L/s, respectively (Figure 4.3). The well test model selected for RN-18 assumed a dual porosity reservoir, constant pressure boundary, constant skin and a wellbore storage. The dual porosity behaviour is a pressure effect which is common in natural fractured reservoirs; it indicates the heterogeneity of the reservoir. This effect is noticeable in pressure transients in reservoir that have distinct and secondary porosity. The dual porosity effect is shown as a minimum on a derivative plot (Horne, 1995). The pressure gauge depth was an input into the program and the data were cleaned. The best model was calculated by considering step 1 and step 2, respectively and then, both steps together.

Using this reservoir model and after calculations, the best fit indicate a permeability-thickness of 3.5 Dm, a storativity of $5 \cdot 10^{-8}$ $m^3/Pa \cdot m^2$ and an injectivity index of

4.3 (L/s)/bar with a negative skin (Figure 4.4 and Table 4.2). The results from the regression analysis for step 1 and step 2 are shown graphically in Figure A.3 and A.4.

The permeability-thickness and the injectivity index for RN-18 is higher than the one calculated for RN-17b showing a better permeability in this part of the reservoir. This could mean that either RN-18 intersects more permeable features than RN-17b or that it is drilled into a steam cap.

Table 4.2: Summary of the results from non-linear regression parameter estimate using injection test data from well RN-18.

Step	Transmissivity ($m^3/(Pa \cdot s)$)	Storativity ($m^3/(Pa \cdot m^2)$)	Permeability Thickness (Dm)	Skin	Injectivity index (L/s)/bar
1	$2.5 \cdot 10^{-8}$	$4.9 \cdot 10^{-8}$	2.2	-2.6	4.6
2	$1.5 \cdot 10^{-8}$	$2.8 \cdot 10^{-8}$	1.3	-3.7	4.5
1 and 2	$3.4 \cdot 10^{-8}$	$4.7 \cdot 10^{-8}$	3.5	-0.85	4.3

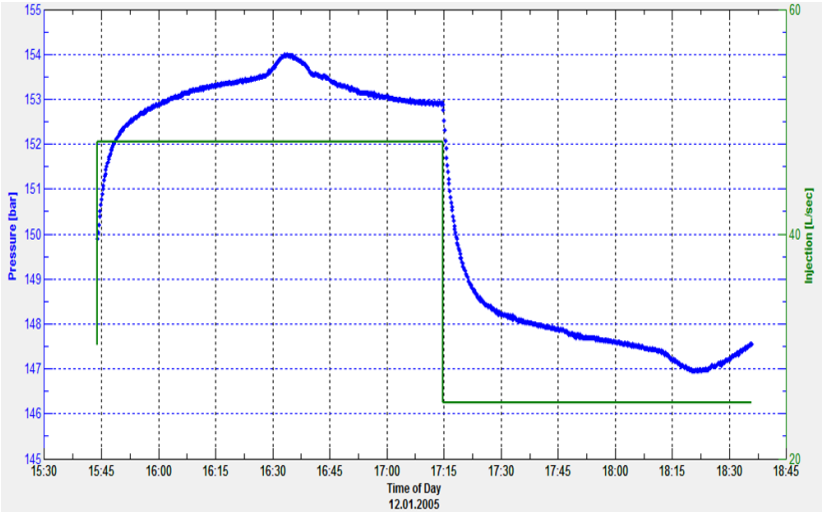

Figure 4.3: Pressure changes during step rate injection test for RN-18.

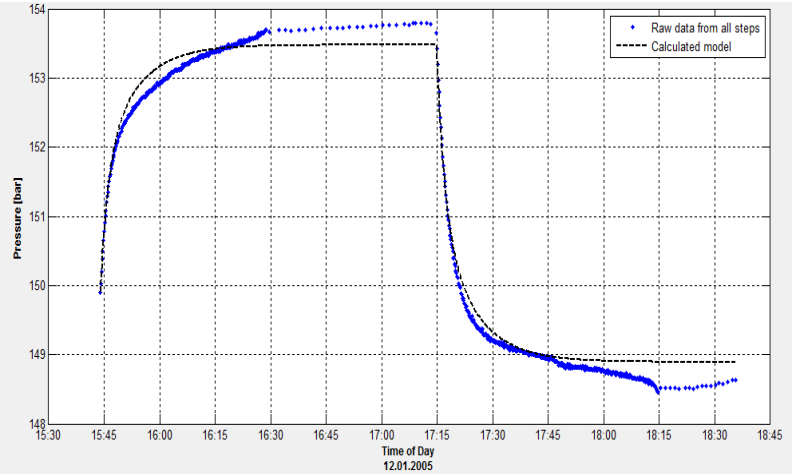

Figure 4.4: Fit between model and measured data for step 1 and 2 for well RN-18.

4.2.3 RN-23 injection test

RN-23 is a directional well that was drilled in early 2006 and completed in late March at a depth of 1924 m. A three step rate injection test was performed after drilling with a pressure gauge being lowered to a depth of 1330 m. The three step injection rates were from 65 L/s to 30 L/s; 30 L/s to 45 L/s and 45 L/s to 60 L/s, respectively The well test model selected for RN-23 assumed a dual porosity reservoir, infinite boundary, constant skin and a wellbore storage.

Figure 4.5 shows the steps of the injection test and the pressure response for each step. It can be observed that data are missing in the pressure response for step 1. For this reason, this step was not considered in the modelling. Therefore, the best model was calculated by considering only pressure build-up for step 2 and 3, respectively and then, both steps together. The pressure gauge depth was an input and the data were cleaned. The results from the regression analysis for the individual steps (step 2 and step 3) are shown graphically in Figure A.5 and A.6.

Figure 4.6 shows the best match calculated for RN-23 for both step 2 and step 3. The results in Table 4.3 show a permeability-thickness of 29 Dm, a storativity of $2 \cdot 10^{-7}$ $m^3/Pa \cdot m^2$ and an injection index of 36 (L/s)/bar.

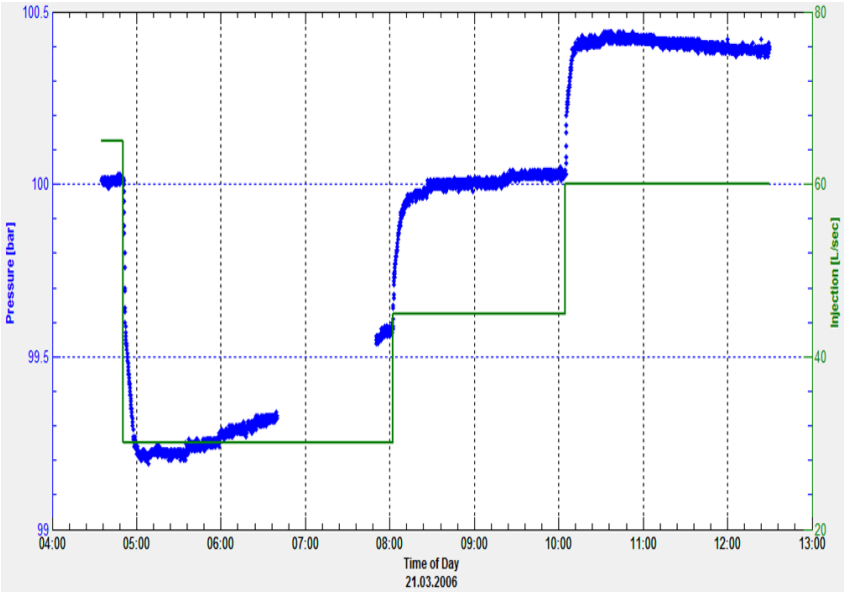

Figure 4.5: Pressure changes for step-rate injection test for RN-23.

Table 4.3: Summary of the results from non-linear regression parameter estimate using injection test data from well RN-23.

Step	Transmissivity ($m^3/(Pa \cdot s)$)	Storativity ($m^3/(Pa \cdot m^2)$)	Permeability Thickness (Dm)	Skin	Injectivity index (L/s)/bar
2	$1.4 \cdot 10^{-7}$	$1.14 \cdot 10^{-7}$	12.4	-4.3	33.2
3	$4.6 \cdot 10^{-7}$	$8.3 \cdot 10^{-7}$	40.6	-1.02	39.9
2 and 3	$3.3 \cdot 10^{-7}$	$1.7 \cdot 10^{-7}$	28.9	-2.5	36.2

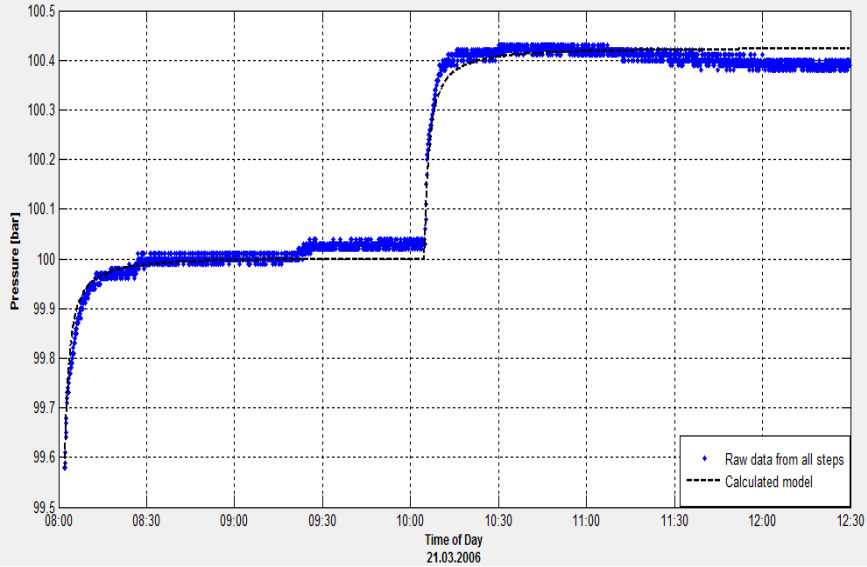

Figure 4.6: Fit between model and measured data for step 2 and 3 for well RN-23.

The permeability-thickness and the injectivity index values for RN-23 are higher than for the other two wells, RN-17b and RN-18. The explanation of the results found here could be that well RN-23 is intersecting more permeable features or that, the well is intersecting a steam cap in this part of the reservoir. The good permeability is also confirmed by the high value of the negative skin. The storativity value is high meaning that RN-23 intersects a steam cap.

4.3 Summary

The results in Table 4.4 give a summary of different transmissivity, storativity and permeability values for RN-17b, RN-18 and RN-23, respectively. To calculate the permeability, a constant reservoir thickness of 2000 m was assumed.

Table 4.4: Summary of the results for wells RN-17b, RN-18 and RN-23.

Well	Transmissivity (m^3/Pa·s)	Storativity (m^3/Pa· m^2)	Permeability Thickness (Dm)	Permeability (mD)	Skin	Injectivity index (L/s)/bar
RN-17b	$1.14 \cdot 10^{-8}$	$4.5 \cdot 10^{-8}$	0.9	0.5	-0.7	1.3
RN-18	$3.4 \cdot 10^{-8}$	$4.7 \cdot 10^{-8}$	4.1	2.1	-0.8	4.3
RN-23	$3.3 \cdot 10^{-7}$	$1.7 \cdot 10^{-7}$	28.9	14.5	-2.5	36.2

The results indicate that RN-23 has the highest transmissivity, while RN-17b has the lowest transmissivity. The transmissivity of RN-23 is one order of magnitude higher than for RN-18 and RN-17b. The permeability values show high permeability in RN-23. Considering that well RN-23 is not far away from well RN-18, the high value of the permeability could be that well RN-23 is drilled into a steam cap (relative permeabilities are considered) and/or that it intersects more permeable fractures than RN-18. The poor permeability of RN-17b in this part of the reservoir could be explained as a thermal expansion of the reservoir rocks due to the high temperature measured in this well (see sub

section 5.2.2) increasing the number of closed voids in the rock matrix (Björnsson and Bödvarsson, 1990). The poor permeability of RN-17b can also simply mean that the well does not intersect as many fractures or that the reservoir is less permeable at the outskirts than in the central part of the geothermal field.

The storativity values for the three wells are of the same order of magnitude for RN-17b and RN-18 and one order of magnitude higher for RN-23. The high storativity value for RN-23 could be as stated above because the well is drilled into a steam cap. The skin factors for the injection test of wells RN-17b, RN-18 and RN-23 are estimated -0.7, -0.8 and -2.5, respectively. This indicates stimulated wells and/or fractured zone in the reservoir.

The injectivity index is used as a rough estimate of the connectivity between the well and the surrounding reservoir. The results show an injectivity index which is one order of magnitude higher for RN-23 as compared to RN-18 and RN-17b. The values of the injectivity indices for RN-23 and RN-18 are compared with the productivity indices for the same wells in Chapter 6.

5 Analyses of pressure and temperature profiles

5.1 Introduction

The downhole profiles of temperature and pressure with depth are a valuable tool in gaining information on the physical conditions of the reservoir and well performance. In geophysics the term "log" indicates continuous measurement of a parameter with time or, in space carried out in boreholes (Stefánsson and Steingrímsson, 1990). The basic measurements made in geothermal wells are pressure and temperature logs or profiles. The logs are normally measured over the full depth of the wellbore. The well may be shut in, flowing or under injection (Grant and Bixley, 2011).

The purpose of analysing downhole data is therefore to deduce from the logging made within the dynamic fluid inside the wellbore the properties of the reservoir around the well. However, caution must be taken when interpreting logs as measurements are not made directly in the reservoir but in the well where internal flows and boiling can cause disturbances and give misleading results even though the well is shut in (Stefánsson and Steingrímsson, 1990).

Analyses of temperature and pressure profiles during warm up leads to an estimation of the formation temperature and the initial reservoir pressure as well as the location of the feed zones. Temperature measurements during fluid injection or production can indicate the feed or loss zones under the test conditions. The feed zones or permeable zones are the regions where hot and cold water flows in and out of a well and usually show up as temperature anomalies, either hot or cold.

In this study, the formation temperature is estimated by using an analytical method, the Horner method (Dowdle and Cobb, 1975) through the BERGHITI program (Helgason, 1993) from the ICEBOX software package (Arason et al., 2004). The Horner method is an analysis method based on the straight line relationship between the wellbore temperature, T and the logarithm of relative time, τ called the Horner time, where $\tau = \frac{t_0+\Delta t}{\Delta t}$ and t_o is the circulation time that is the time that the well has been cooled by the drilling fluid, and Δt is the time since the circulation of drilling fluid was stopped. The measured wellbore temperature at a given depth from several temperature logs is plotted against log (τ). This plot is a straight line that intersects the vertical line $\tau = 1$, corresponding to $\Delta t \rightarrow \infty$, at the formation temperature.

The boiling point curve was considered when estimating the formation temperature to determine if there is boiling in the borehole and at which depth. The boiling point curve for an individual borehole was calculated assuming initial water level and the program BOILCURV from ICEBOX was used for this purpose.

The initial pressure condition of the wells is estimated by feeding the evaluated formation temperature into the program PREDYP (Björnsson, 1993), from the ICEBOX package. The program computes pressure in a static fluid column with known temperature. The water level (or wellhead pressure) is required for the calculation and is adjusted until the calculated profile matches the measured pressure at the pivot point. The pivot point shows

the depth to and pressure at the best feed zone in the borehole and can be considered as the actual pressure value in the reservoir.

In the following sections (5.2 to 5.3), the temperature and pressure profiles are analysed to locate the feed zones, pivot points and estimate the initial reservoir pressure and the formation temperatures for the Reykjanes wells RN-12, RN-17B, RN-18, RN-23 and RN-29. The temperature and pressure measurements in these wells were performed during injection, warm up and flowing of the wells.

5.2 Temperature and pressure analyses

In this section, the temperature and pressure profiles for wells RN-12, RN-17B, RN-18, RN-23 and RN-29 are interpreted to identify the main feed zones and locate the pivot point of each well where possible.

5.2.1 RN-12

Borehole RN-12 was drilled in 2002 to a depth of 2506 m. No liner was put in the hole. The casing design is as follows:

Hole diameter	Hole depth (m)	Casing size	Casing depth (m)
21”	293	18 5/8”	291
17 ½”	845	13 3/8”	842
12 ¼”	2506	no liner	

Figure A.7 shows the temperature and pressure profiles for well RN-12 after drilling with and without injection, during warm up and during flowing of the well. The injection temperature profiles show three main feed zones. One located around 1000 m and the second at 1300 m showing fluid inflow identified as steps in the profile. Another feed zone is observed around 2200 m representing an outflow which is indicated by a change in the temperature gradient. Temperature profiles during warm up show the same pattern and indicate feed zones at 1000 m, 1300 m and around 2200–2300 m. Below 1000 m depth, cross flow between the two feed zones from 1300 m to 2200 m is observed characterized by a fairly constant temperature and consequently vertical connection between these levels. From September 2003 to October 2004, the temperature was 279 ^{o}C from 1300 m to 2200 m depth and it increased in the last logs to 298–299 ^{o}C from 1500 m to 2200 m depth. At the feed zone at around 2200–2300 m, a small temperature inversion was observed, lowering the temperature to 279 ^{o}C and after complete recovering this temperature increased to 290 ^{o}C. The well has a maximum recorded temperature of 310 ^{o}C at the well bottom. The temperatures from 2007 to 2011 indicate a constant profile indicating that the well has reached the formation temperature.

Pressure profiles during warm up show a pivot point at around 1300 m with a pressure of 106 bar-g. The pivot point indicates the pressure control point and is represented as a single point at which the pressure in the well is the same as the reservoir pressure because of the connection of the well to the reservoir. It should be emphasised that for a single feed zone well, the feed zone and the pivot point should be at the same depth. However, for multiple feed zones, the pivot point will be between the top and bottom feed zone and its exact location will depend on the permeability of the feed zones (Stefánsson and Steingrímsson, 1990; Grant and Bixley, 2011). A drawdown, meaning a decrease of pressure, at the well bottom of about 8 bar is observed from 2007 to 2008 but from 2008 to 2011, the drawdown has been almost constant varying between 1 bar and 2 bar per year. Pressure profiles during discharge indicate a flashing level (boiling in the well) at about 1000 m depth.

5.2.2 RN-17b

This well is a directional well and it was drilled in 2008 to a measured depth of 3077 m. The casing design for well RN-17b is as follows:

Hole diameter	Hole depth (m)	Casing size	Casing depth (m)
21”	352	18 5/8”	340
17 ½”	901	13 3/8”	892
12 ¼”	3077	9 5/8” liner	3075

Figure A.8 shows the temperature and pressure profiles for well RN-17b during injection, warm up and discharge testing. The profiles were plotted versus MD. The temperature profiles during injection show two main feed zones at around 1250-1300 m and around 1750-1800 m. Temperature profiles during warm up indicate similar feed zones at 1250 m and around 1750-1800 m. In 2009, the bottomhole temperature recovered in two months from 299 ^{o}C to 330 ^{o}C. The highest temperature measured in RN-17b is 348 ^{o}C at the bottom. The temperature profiles suggest a heat transfer by conduction from the reservoir to the well.

Pressure profiles show pressure instability in the well. In 2009, the wellhead pressure rose from 5.5 bar-g to 43 bar-g in five months and suddenly dropped again to 5.8 bar-g when the well was opened to flow in the same month. The last flowing test in November 2010 indicates a wellhead pressure of 45 bar-g and a bottomhole pressure of 182 bar-g. The previous test in March the same year indicates a wellhead pressure of 6 bar-g and bottomhole pressure of 152 bar-g. The pressure profiles indicate no pivot point indicating that there is a bad connection between the well and the reservoir. The pressure instability in RN-17b and the difficulty to determine a pivot point indicate the poor permeability of the reservoir in the area of drilling. Pressure profiles during warm up indicate a water level in the well at around 350 m depth.

5.2.3 RN-18

This borehole was drilled vertically and completed in January 2005 at a depth of 1815 m. The casing design is described as follows:

Hole diameter	Hole depth (m)	Casing size	Casing depth (m)
21”	351	18 5/8”	349
17 ½”	750	13 3/8”	749
12 ¼”	1815	9 5/8” liner	1799

Figure A.9 shows the temperature and pressure profiles for well RN-18 during injection, warm up and discharge testing. The temperature profiles during injection show a feed zone just under the production casing shoe at around 800 m depth. The temperature profiles from 2006 indicate similarly a feed zone at 800 m and small feed zones at 1100 m and 1300 m depth, respectively. From 1100 m to 1300 m depth, the temperature is isothermal varying from 278 ^{o}C to 280 ^{o}C, respectively, suggesting down flowing fluids indicating vertical movement of fluid. In 2008, the temperature profiles show a slight increase in temperature to 285 ^{o}C at 1400 m depth. The temperatures from 2007 to 2011 indicate a constant profile from 1500 m down to the bottom showing that the well has reached the formation temperature.

There were not enough warm up pressure profiles to determine the pivot point. A drawdown of 6 bars is observed for the years 2007 to 2008 and of 4 bars for the years 2008 to 2011 indicating a progressive stabilisation of the well bottom pressure. The last pressure profiles during discharge indicate a flashing level close to 950 m depth.

5.2.4 RN-23

RN-23 is a directional well and was drilled in early 2006 to a measured depth of 1924 m. The true vertical depth (TVD) is 1742 m. The casing design for well RN-23 is as follows:

Hole diameter	Hole depth (m)	Casing size	Casing depth (m)
21”	296	18 5/8”	295
17 ½”	702	13 3/8”	701
12 ¼”	1924	9 5/8” liner	1923

Figure A.10 shows the temperature and pressure profiles of well RN-23 during injection, warm up and discharge testing. The temperature and pressure profiles were plotted versus the measured depth. Feed zones at around 950 to 1000 m, 1100 m and 1350 to 1400 m can be identified from the temperature profiles. The profile shows boiling during flowing of the well at around 1150 m depth. Cross flow characterized by a fairly constant temperature of 310 ^{o}C between the two feed zones at 1100 m and 1350 m is evident suggesting a vertical fluid flow between those two feed zones. The temperature profiles from 2007 to 2011 indicate a stable profile meaning that the well has probably reached the formation temperature.

There were not enough warm up pressure profiles to determine the pivot point. The pressure profiles show a drawdown of about 10 bar from 2006 to 2008 and 5 bar from 2008 to 2011 indicating a progressive stabilisation of the well bottom pressure. The pressure profiles indicate a flashing level at around 1150 m depth.

5.2.5 RN-29

The casing design for well RN-29 is as follows:

Hole diameter	Hole depth (m)	Casing size	Casing depth (m)
21”	306	18 5/8”	305
17 ½”	902	13 3/8”	901
12 ¼”	2837	9 5/8” liner	2500

This borehole is vertical and was drilled in 2010 to a depth of 2837 m. Figure A.11 shows the temperature and pressure profiles of well RN-29 during injection, warm up and discharge testing. The temperature profiles during injection show the main feed zone at 2150 m depth. Small feed zones can be observed at 1100 m, 1750 m and 2500 m depth. Temperature profiles during warm up indicate a water level at around 300 m depth and reveal a temperature inversion to a minimum of 230 ^{o}C from 1800 m to 2500 m depth which could be an indication that the outer boundary of the system has been reached. Feed zones are observed during warm up at around 1200 m, 1600 m, 1850 m and 2500 m depth. RN-29 has a maximum recorded temperature of about 320 ^{o}C at the well bottom.

Pressure profiles show a pivot point between 1750 m and 1800 m with 131 bar-g pressure. The last logs performed in January 2011 were done down to a depth of 1200 m and could not be interpreted. The pressure profile from November 2010 during discharge, indicate a flashing level at a depth of about 2200 m.

5.3 Reservoir temperature and pressure

In this section the formation temperature and the initial reservoir pressure for the Reykjanes wells RN-12, RN-17b, RN-18, RN-23 and RN-29 are estimated (Figure A.7 to

A.11) from the analyses of Section 5.2. The reservoir temperature and initial pressure for each well are represented in Figure 5.1 and 5.2, respectively. The temperature profiles during warm up and flowing were considered for individual wells to estimate their formation temperature.

The formation temperature for well RN-12 (Figure A.7) suggests pure gradient in the top 400 m. The formation temperature profile follows the boiling point curve in the zone from 500 m to 1000 m depth indicating supersaturated or steam dominated conditions in the well and reservoir at this level. Below 1000 m depth, the formation temperature profile is below the boiling point curve indicating a liquid dominated reservoir at this depth. A slight temperature inversion is observed at around 2000-2200 m depth. The reservoir temperature for RN-12 is estimated around 300 ^{o}C with a maximum of 310 ^{o}C at the bottom.

The formation temperature for RN-17b in Figure A.8 suggests that there is no boiling in the well. The reservoir temperature is estimated to be around 340 ^{o}C at the bottom of the well.

The formation temperature for RN-18 in Figure A.9 suggests a temperature corresponding to the boiling point curve of water at around 400-900 m depth. Below 900 m depth, the formation temperature profile is below the boiling point curve indicating a liquid dominated reservoir from this depth and downwards. The profile is vertical to the bottom of the well indicating a vertical flow. The reservoir temperature is estimated to be around 284 ^{o}C.

The formation temperature for RN-23 in Figure A.10 suggests a temperature corresponding to the boiling point curve of water from 500 m down to 1100 m depth. The reservoir temperature is estimated to be around 302 ^{o}C. Below 1100 m depth, the formation temperature profile is below the boiling point curve and constant indicating a vertical flow.

The formation temperature for RN-29 in Figure A.11 shows conduction in the casing and a possible temperature inversion at 1800-2500 m depth. The formation temperature at the bottom is estimated to be around 320 ^{o}C.

The initial reservoir pressure down to 1000 m depth is high for RN-12 and low for RN-17b. Below 1000 m depth, the initial reservoir pressure is high for RN-23 and low for RN-17b. Between 1400 and 1550 m depth, the pressure for RN-12 and RN-23 are the same.

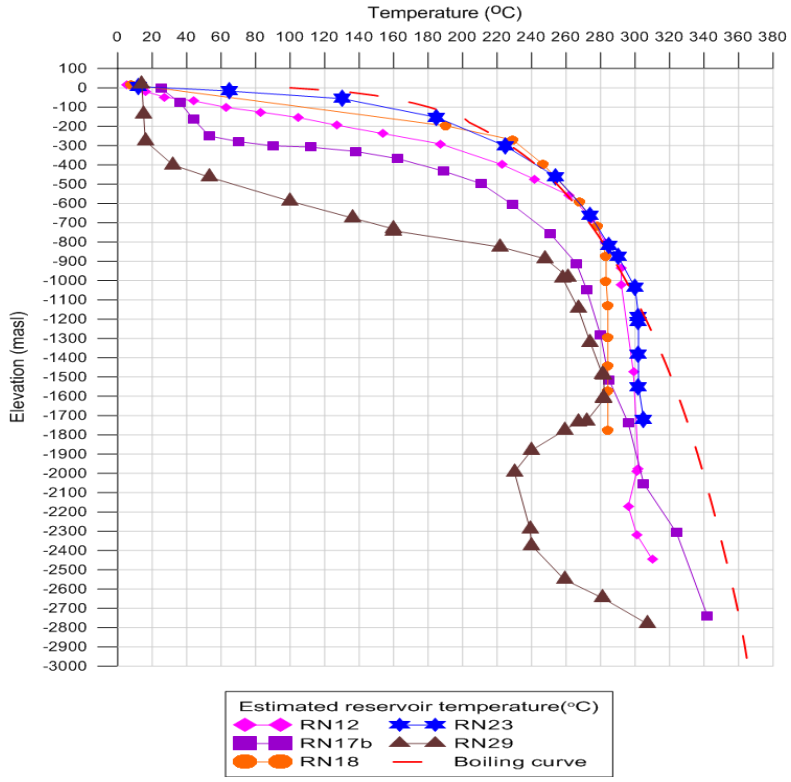

Figure 5.1: Estimation of the formation temperature for wells RN-12, RN-17b, RN-18 and RN-29.

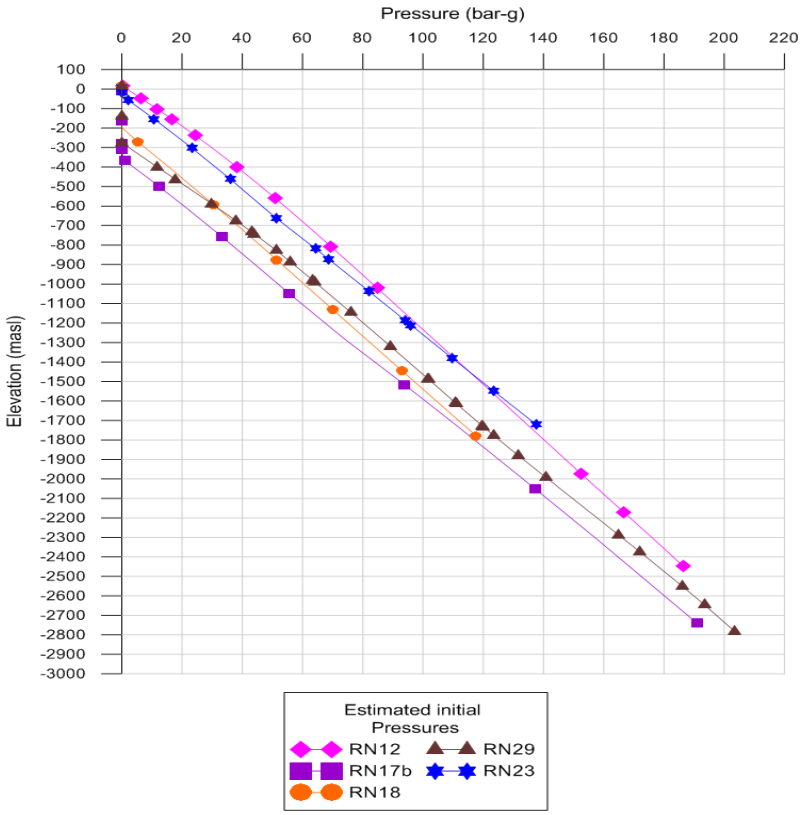

Figure 5.2: Estimation of the initial pressures for wells RN-12, RN-17b, RN-18 and RN-29.

6 Discharge tests

6.1 Introduction

After a long warm up period (often for several months), the fluid temperature in the well increases. Eventually there is a build up of a wellhead pressure above the atmospheric pressure if the well is artesian, meaning that pressurised fluid naturally rises to the surface when the well is open to flow. The well can then be discharged through an orifice to estimate the production capacity of the well. In case the well does not spontaneously discharge, different methods are used to start off the discharge. More information about these methods can be found in Grant and Bixley (2011).

During the production test, the fluid flow (total flow rate), its energy content (enthalpy) and chemical characteristics are measured. The pressure (and temperature) logger are usually placed at the bottom of the hole for pressure (and temperature) measurements. The lip pressure method (James, 1966) or the separator method can be used to determine the flow characteristics with a simple weir being used to measure the liquid flow. Where environmental conditions permit, a brief vertical discharge directly to the atmosphere can be used with the lip pressure method to get the first estimate of the longer-term production potential. In this case the fluid enthalpy can be estimated by observation of the discharge plume and downhole conditions at the feed zone prior to discharge (Grant and Bixley, 2011). The well productivity as a function of wellhead pressure can be determined by repeating the flow test with different size orifices or by a step-rate test. The pressure and temperature logs together with information from the discharge tests can also be simulated to estimate the productivity indices of the wells. The wellbore simulator HOLA (Björnsson et al., 1993) is used for this purpose as discussed in Section 6.4.

The lip pressure method, the separator method and the HOLA wellbore simulator are described in the following Sections (6.2 to 6.4) and used to calculate the flow characteristics and productivity indices for three wells; RN-13b, RN-18 and RN-23. Injectivity and productivity indices are then compared in Section 6.5.

6.2 Lip pressure testing

This method is based on an empirical formula developed by James (1966). The James lip pressure method is the most flexible and economical method for flow testing. This method consists of discharging the steam-water mixture produced by a test well through an appropriately sized pipe into a silencer or some other device for separating the steam and water phase at atmospheric pressure (Figure 6.1). Sometimes the orifice pipe simply opens to the atmosphere. The lip pressure or critical pressure, which is the pressure at which the flow changes from subcritical to supercritical flow. This pressure is measured at the extreme end of the discharge pipeline as it enters the separator. The separated water flow rate exiting from the separator is measured using a sharp-edged weir near the silencer outlet while the steam is discharged to the atmosphere (Grant and Bixley, 2011).

The James formula is represented as follows:

$$\frac{Q_t H_t^{1.102}}{A P_c^{0.96}} = 184 \tag{6.1}$$

Where Q_t is the total mass flow rate in kg/s, H_t is the total enthalpy in kJ/kg, A is the cross-sectional area of the lip pipe in cm^2, and P_c is the lip pressure in bar-a (absolute).

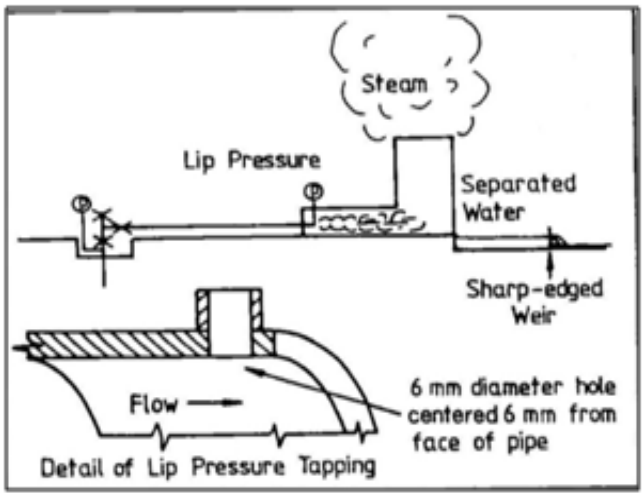

Figure 6.1: Flow measurement using the lip pressure method (Grant et al., 1982)

For the discharged fluid that is separated at atmospheric pressure, the enthalpies of the two phases, steam and water, H_s (kJ/kg) and H_w (kJ/kg), are used in the formula together with the total enthalpy of the well fluid. Knowing the separated water flow rate Q_w (kg/s), the total flow rate is given by:

$$Q_t = Q_w \frac{H_s - H_w}{H_s - H_t} \tag{6.2}$$

Since the well is discharged at atmospheric pressure, the specific enthalpies of steam and water at atmospheric pressure should be used and equation (6.2) can be rewritten as follows:

$$Q_t = Q_w \frac{2256}{2676 - H_t} \tag{6.3}$$

The enthalpy H_t can then be determined by combining equation (6.1) and (6.3)

$$184\, A \frac{P_c^{0.96}}{H_t^{1.102}} = Q_w \frac{2256}{2676 - H_t} \tag{6.4}$$

By measuring the lip pressure, the water flow rate and knowing the cross sectional area of the orifice, the total enthalpy can be calculated numerically.

RN-13b, a directional well that was drilled down to a measured depth of 2530 m and a true vertical depth of 2200 m. RN-13b and RN-18 were discharged on October 11, 2007 and August 11, 2005, respectively, through a lip pressure pipe of 16 cm in diameter into a silencer that also acts as a steam/water separator at atmospheric pressure. The flow of the liquid phase was measured using a V-notch weir box. RN-23 was discharged on May 23, 2006 directly to the atmosphere through a vertical discharge pipe of 21.2 cm in diameter. There was no measurement of the water flow rate and no separator. The measurements for the wells were done in five steps, four steps and six steps for RN-13b, RN-18 and RN-23, respectively. Table 6.1 shows the average of the measurements and the calculated values for the parameters during the flow test of well RN-13b, RN-18 and RN-23. Enthalpy and mass flow rate parameters for RN-13b and RN-18 were calculated using the LIP program from ICEBOX. The LIP program requires the input of the pipe diameter, the lip pressure and the water height in the weir to calculate the flowing mass and enthalpy. The same parameters for RN-23 were calculated directly from equation 6.1 using an estimated total enthalpy from the temperature and pressure profiles. The enthalpy at the wellhead for RN-23 was considered to be the same as the enthalpy at the bottom of the well and could be estimated knowing the downhole pressure and temperature.

The productivity index was calculated by dividing the change in flow rate by the change in pressure at each step for individual wells. The average productivity indices for well RN-13b, RN-18 and RN-23, respectively are given in Table 6.1.

Table 6.1: Calculated flow characteristics for RN-13b, RN-18 and RN-23 using the lip pressure method

Well	WHP (bar-g)	Lip Press (bar-g)	Enthalpy H (kJ/kg)	Q_t (kg/s)	Q_w (kg/s)	Q_s (kg/s)	PI (kg/s)/bar
RN-13b	41	2.5	1570	33	16	17	3.4
RN-18	32	3	1420	41	23	18	1.4
RN-23	46	2.7	1406	56			66

6.3 Steam-water separator testing

The separator method (Figure 6.2) is the most accurate method for measuring two-phase flow from geothermal wells (Bangma, 1961). The water flow rate is measured using a sharp–edged weir after flashing to atmospheric pressure and the steam flow rate is measured at separator pressure (Grant and Bixley, 2011).

The general equation for the separated steam flow rate is given by:

$$Q_s = C \cdot \varepsilon \cdot \sqrt{\frac{\Delta P}{v_{fluid}}} \tag{6.5}$$

where C is an orifice constant, which depends on the pipe and orifice geometry and pressure tapping geometry; ε is the expansibility factor for compressible gases; ΔP the differential pressure across the orifice in millibar (mbar) and v_{fluid} is the specific volume of the fluid passing through the orifice in cm^3/gm (Grant and Bixley, 2011).

The water flow rate, Q_w can also be calculated from the water height W in the weir box by the following formula:

$$Q_w = C \cdot (W - W_o)^b \tag{6.6}$$

where, C, W_o and b are constants (Linford, 1961). C depends on the geometry of the weir and the friction between the fluid and the weir sides. W_o is the water level at which the water flow rate is zero. The constant, b describes the geometry of the weir.

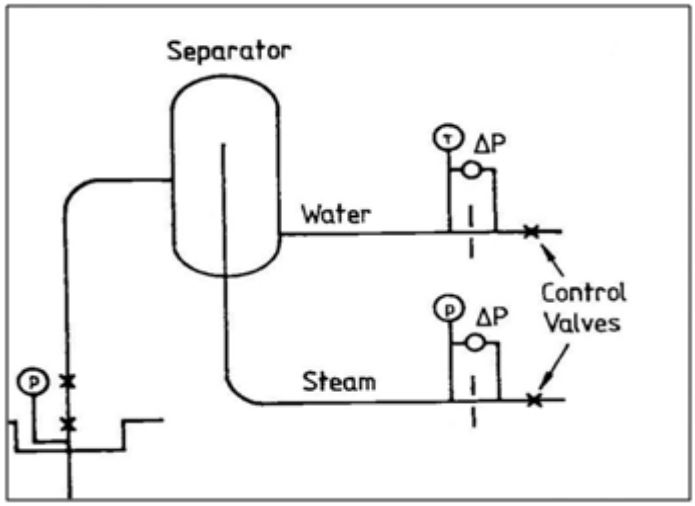

Figure 6.2: Separator used in well testing (Grant et al., 1982)

For the Reykjanes geothermal field, the separator is calibrated and the following equations are used for the calculations:

$$Q_s = 2.733 \cdot \sqrt{\Delta P} \tag{6.7}$$

$$Q_w = 0.0146 W^{2.47} \tag{6.8}$$

Where, the flow rates Q_s and Q_w are measured in kg/s, ΔP in mbar and W in cm.

The steam and water flow rate parameters for RN-13b and RN-18 were calculated using equations (6.7) and (6.8) and the enthalpy was calculated, using the following equation:

$$H = XH_s + (1 - X)H_w \tag{6.9}$$

where X is the mass ratio of steam, Q_s/Q_t, and H_s and H_w are the specific enthalpies of steam and water, respectively, at atmospheric pressure. Table 6.2 shows the measured and calculated parameters during the flow tests of wells RN-13b and RN-18.

The steam and water flow rates for RN-23 could not be estimated since the well was discharged directly to the atmosphere.

Table 6.2: Calculated flow characteristics for RN-13b and RN-18 using the separator method

Well	WHP (bar-g)	Lip Press (bar-g)	Enthalpy H (kJ/kg)	Q_t (kg/s)	Q_w (kg/s)	Q_s (kg/s)
RN-13b	41	3	1580	33	16	17
RN-18	32	3	1338	39	23	16

The calculated parameters from the two methods show some similarities. By assuming that the conversion rate is 2 kg/s of steam per Megawatt electric, MW_e (Grant et al., 1982), the power generation for wells RN-13b and RN-18 is about 8.5 MW_e and between 8 MW_e and 9 MW_e, respectively.

6.4 Simulation of wellbore flow

6.4.1 Theory

The wellbore simulator HOLA (the Icelandic word for "well") reproduces the measured pressure and temperature profiles in a flowing well and determines the thermodynamic properties of the water, relative flow rates at each feed zone for a given discharge condition at the wellhead. The simulator can handle both single and two-phases flow in vertical pipes (Björnsson et al., 1993).

HOLA has two approaches (mode 1 and mode 2) for wellbore flow simulation that are mostly used out of the six modes offered by the simulator. For the first approach (mode 1), one needs to know the discharge condition at the wellhead (pressure, temperature and enthalpy), in addition to flow rates and enthalpies of all but the last feed zone. The simulator proceeds from the wellhead to the bottom of the hole, calculating the flowing temperature and pressure profiles down the well. In mode 2, the user specifies the required flowing wellhead pressure and the bottomhole pressure. For each feed zone, the productivity index, the thermodynamic properties of the reservoir fluid and the wellbore geometry must be known. The simulator then proceeds from bottomhole to wellhead to calculate the expected wellhead output (wellhead enthalpy, flow rate, temperature and phase composition) for the required wellhead pressure.

The simulator solves numerically the differential equations that describe the steady state mass, momentum and energy flow in a vertical pipeline as follows (Björnsson, 1987; Björnsson et al, 1993):

Mass balance

$$\frac{dQ_t}{dz} = 0 \tag{6.10}$$

Momentum balance

$$\frac{dP}{dz} - \left[\left(\frac{dP}{dz}\right)_{fri} + \left(\frac{dP}{dz}\right)_{acc} + \left(\frac{dP}{dz}\right)_{pot}\right] = 0 \tag{6.11}$$

Energy balance

$$\frac{dE_t}{dz} \pm Q = 0 \tag{6.12}$$

Where Q_t is the total mass flow rate in kg/s, P the pressure in Pascal (Pa), E_t the total energy flux in the well in J/s and z is the depth coordinate in m. Q denotes the ambient heat loss over a unit distance in W/m. The plus and minus sign indicates downflow and upflow, respectively. The pressure gradient $\frac{dP}{dz}$ is composed of three terms: wall friction, acceleration of fluid and change in gravitational load over the depth interval, *dz*.

The governing equation of mass flow rate between the well and the reservoir, through a given feed-zone is given by:

$$Q_{feed} = PI\left[\frac{k_{rw}\rho_w}{\mu_w} + \frac{k_{rs}\rho_s}{\mu_s}\right](P_r - P_w) \tag{6.13}$$

where Q_{feed} is the feed zone flow rate in kg/s , PI is the productivity index of the feed zone in m^3, k_r is the relative permeability for water and steam, μ is the viscosity in Pa·s, ρ is the density in kg/m^3, P_r is the reservoir pressure and P_w is the pressure in the well in bar-a. The subscripts, *s* and *w* refer to steam and water, respectively.

The program calculates the productivity index at one feed zone by the following equation:

$$PI = \left(\frac{q_\beta}{P_\beta - P_{wb}}\right)\left(\frac{\mu_\beta}{k_{r\beta}\rho_\beta}\right) \tag{6.14}$$

where the subscript β indicates the feed zone phase, liquid or steam.

The relative permeabilities are calculated by a linear relationship: $k_{rs} = S$ and $k_{rw} = 1\text{-}S$, where S is the volumetric steam saturation of the reservoir. μ and ρ are calculated knowing the temperature at feed zone β (Björnsson, 1987).

In general, wellbore simulators are very sensitive to the phase velocity relations used. They can only be obtained through empirical correlations. The formula for two-phase flow calculations are based on the empirical relations given by Chisholm (1973). Choices are provided to the user, to calculate these velocities, namely Armand (1959) correlation and Orkiszewski (1967) correlation. The reader is referred to Björnsson (1987) and Aunzo et al. (1991) for further details on input-output format of HOLA and the various correlations.

In this sub section, measured pressure and temperature profiles in the flowing wells RN-13b, RN-18 and RN-23 are analysed and feed zone productivity that matches the measured results are calculated for each well using the simulator, HOLA. The wellhead pressure and the bottomhole pressure together with the wellbore geometry are specified

and the calculation proceeds from bottom of the well to the wellhead. It has to be pointed out that RN-13b and RN-23 are directional wells and the temperature and pressure profiles were plotted versus the true vertical depth and not the measured depth (see Table A.1).

6.4.2 RN-13b

The flowing temperature and pressure data measured on October 11, 2007 were selected for the HOLA simulation and plotted versus the true vertical depth. Figure 6.3 shows the calculated and measured temperature and pressure profiles for well RN-13b.

RN-13b was considered down to a depth of 2000 m with three feed zones at 1120 m, 1590 m and at the bottom (2000 m). A wellhead pressure of 41 bar-g was considered since it was the pressure measured during discharge with a bottomhole pressure of 127 bar-g. The production casing and liner diameters are 13 ⅜" and 9 ⅝", respectively. Enthalpy of 1800 kJ/kg, 1260 kJ/kg and 1280 kJ/kg were assumed for the feed zones at 1120 m, 1590 m and 2000 m, respectively.

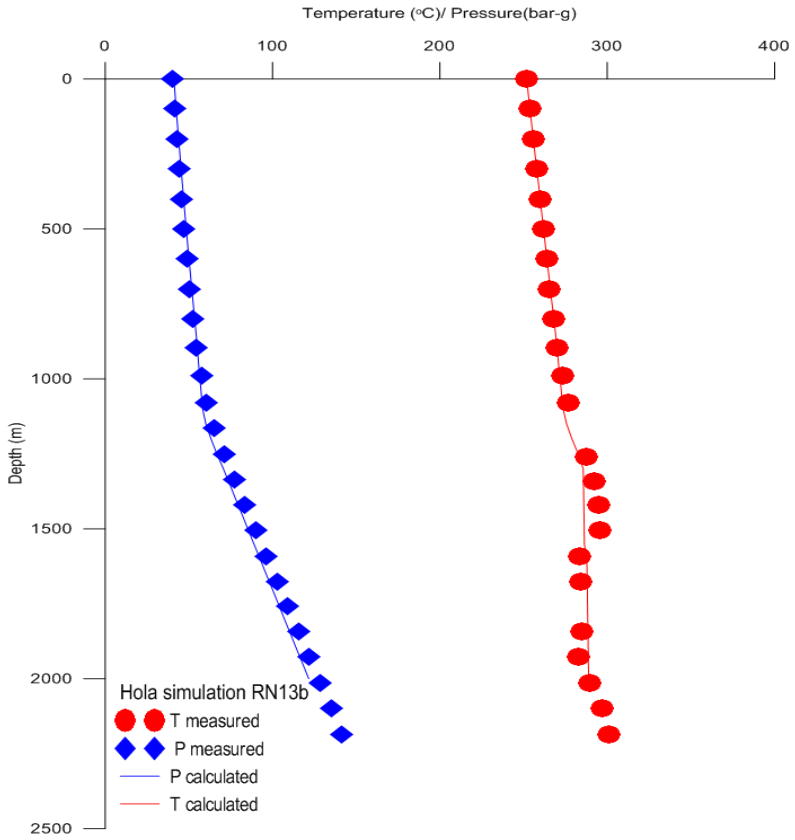

Figure 6.3: Calculated and measured temperature and pressure profiles for well RN-13b

A productivity index of $8 \cdot 10^{-12}$ m^3, $1.5 \cdot 10^{-12}$ m^3 and $2 \cdot 10^{-12}$ m^3 for the feed zones at 1120 m, 1590 m and 2000 m depth, respectively, matched reasonably well with the measured downhole profiles (Figure 6.3). The total productivity was calculated by adding all the productivity indices for the feed zones and was estimated at $11.5 \cdot 10^{-12}$ m^3 or about 5.8 (kg/s)/bar. The productivity index calculated from the simulator is in m^3 units and it is converted to (kg/s)/bar units by using equation (6.13).

The calculated wellhead enthalpy is 1780 kJ/kg which is higher than the one calculated during the discharge test. It could be due to the fact that the well had not fully recovered after the discharge test.

The wellhead total flow is 25 kg/s compared to 33 kg/s from the discharge test. The steam flow rate is 10 kg/s corresponding to about 5 MW_e. The slight difference between the enthalpy and flow rate results from HOLA and the discharge tests, respectively, could be due to the fact that the feed zone at the well bottom was not considered in the HOLA simulation or that the well had not fully recovered after the discharge test. The specified and calculated parameters for the simulation are presented in Appendix A.5.

6.4.3 RN-18

Figure 6.4 shows the measured and simulated flow profiles for the discharge test on August 11, 2005 for borehole RN-18. Two major feed zones are present in the well, one at around 750-800 m, just below the production casing, and the other at the well bottom at 1800 m depth. The calculated pressure and temperature profiles in Figure 6.4 are obtained by assuming a wellhead pressure of 32 bar-g and a bottomhole pressure of 117 bar-g. Enthalpy of 1520 kJ/kg and 1220 kJ/kg were assumed for the feed zones at 800 m and 1800 m depth, respectively.

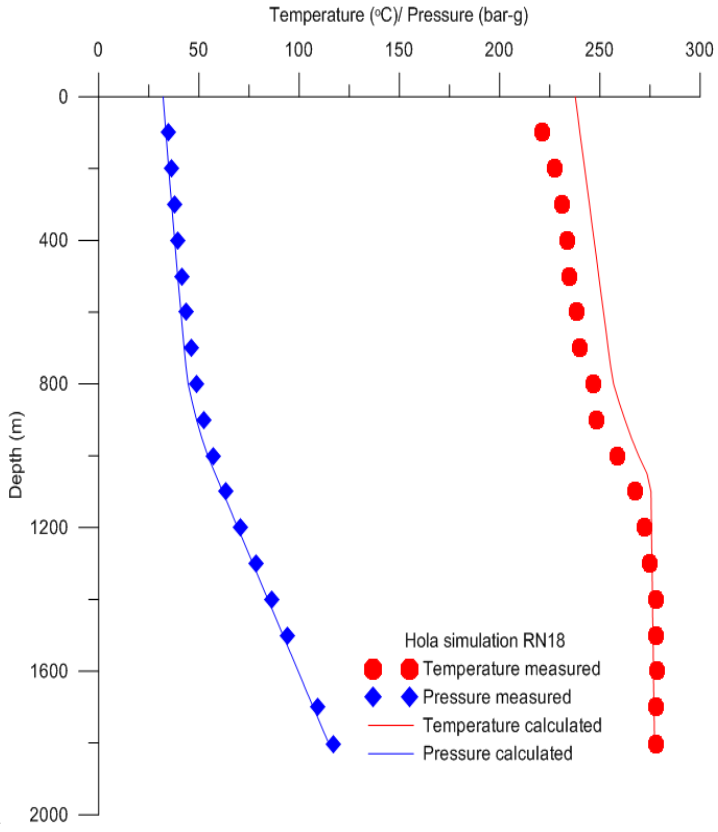

Figure 6.4: Calculated and measured temperature and pressure profiles for well RN-18

The simulation shows a good match for the pressure profile. For the temperature profile the match is close and the shift in the calculated temperature profile could be due to bad calibration of the instrument because there is boiling in the well. The simulation gives a

total flow rate of 51 kg/s at the wellhead which is similar to the flow calculated during the discharge test (47 kg/s). The productivity index at 800 m depth and at the bottom is $1 \cdot 10^{-12}$ m^3 and $1.3 \cdot 10^{-11}$ m^3, respectively, giving a total productivity index of $1.31 \cdot 10^{-11}$ m^3 or about 7.34 (kg/s)/bar. This value is much higher than the one calculated during the discharge test. It could be due to the fact that the well had not fully recovered after the discharge test.

The calculated wellhead enthalpy is 1490 kJ/kg which is similar to the one calculated during discharge (1420 kJ/kg). The steam flow rate is 13 kg/s corresponding to about 7 MW_e. The specified and calculated parameters for the simulation are presented in Appendix A.5.

6.4.4 RN-23

Figure 6.5 shows measured and calculated temperature and pressure profiles for RN-23. Three feed zones are present in the well, at 750 m, 1200 m and 1730 m depth (true vertical depth). The bottom depth was considered at 1730 m instead of 1742 m. A pressure of 46 bar-g was required at the wellhead and a bottomhole pressure of 128.4 bar-g. Enthalpies of 1470 kJ/kg, 1280 kJ/kg and 1370 kJ/kg were assumed for the feed zones at 750 m, 1200 m and 1730 m depth, respectively.

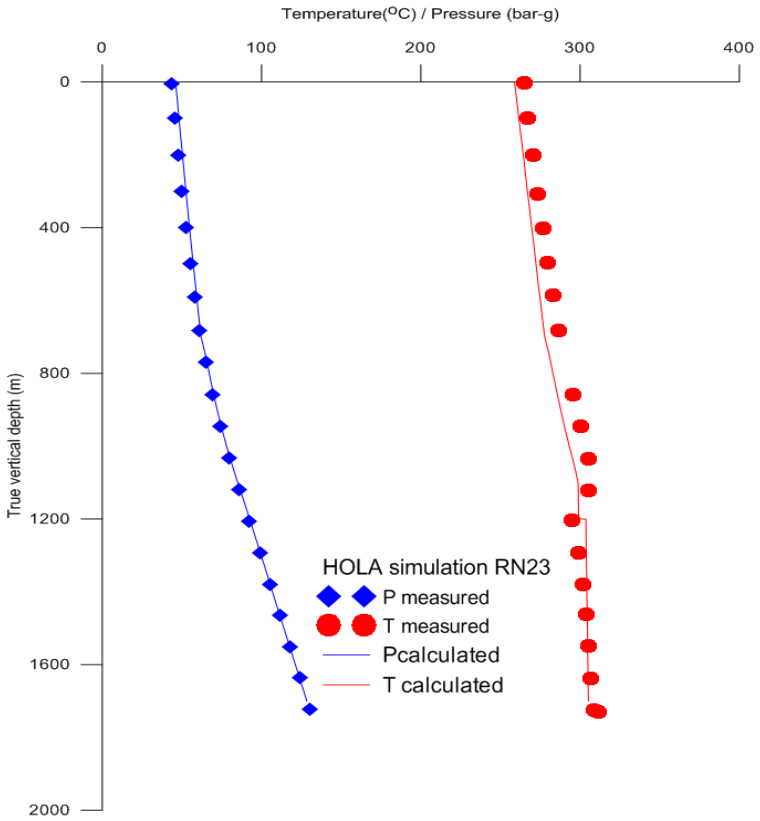

Figure 6.5: Calculated and measured temperature and pressure profiles for well RN-23

The results of the simulation indicate a total flow rate of 155 kg/s at the wellhead which is three times higher than the value calculated during vertical discharge of the well. This difference could be interpreted as the instability of the flow during vertical discharge. The productivity index at 750 m depth and at the bottom of the well is similar, $3 \cdot 10^{-11}$ m^3 but it

is about 10^{-11} m^3 at 1200 m depth. Therefore, the total productivity for RN-23 is about $7 \cdot 10^{-12}$ m^3 or around 45.3 (kg/s)/bar.

The calculated wellhead enthalpy is 1452 kJ/kg which is in the same range as the 1410 kJ/kg calculated during discharge. The steam flow rate is 30 kg/s corresponding to about 15 MW_e. The calculated parameters for the simulation are presented in Appendix A.5.

6.5 Comparison between productivity and injectivity indices

Usually, well test data for both injection tests and production tests are evaluated and interpreted to determine the injectivity and productivity indices for a well. The productivity index, *PI* is the ability of the well to produce fluid while the injectivity index, *II* can be defined as the ease with which a fluid can be pumped into a borehole. The productivity and injectivity indices are key element in well analysis (Craft and Hawkins, 1959). They are defined as the absolute value of the ratio between the flow rate, Q and the difference between the static pressure, P_s and the flowing downhole pressure, P_f (Combs and Garg, 2000):

$$II, PI = \left| \frac{Q}{(P_s - P_f)} \right| \tag{6.14}$$

The productivity and injectivity indices are, therefore, usually considered to be the same in liquid fed wells but it is not always the case for two-phase feed zones due to the variations in the enthalpy and the viscosity of the flowing steam and water phase mixture (Grant and Bixley, 2011). However, knowing the injectivity and productivity indices of a wellbore, it may be possible to devise rules to relate the two.

In this section, injectivity indices from injection tests and productivity indices from discharge tests for several high temperature geothermal fields worldwide are considered (Garg and Combs, 1997; Axelsson et al., 2006; Grant, 2008; Houssein & Axelsson, 2010). The data can be found in Table A.2 in Appendix A.4.

The injectivity index for each well is plotted versus its productivity index in Figure 6.6. The injectivity and productivity indices for RN-18 and RN-23 are both plotted in Figure 6.6. Two relationships from the literature (Garg and Combs, 1997; Grant and Bixley, 2011) were considered. Garg and Combs (1997) suggested that PI=II and Grant and Bixley suggested that PI=II/3 or PI= II/5.

To compare the productivity and injectivity correlations for these high temperature geothermal fields, two lines representing the selected PI versus II relationship are plotted to see where RN-18 and RN-23 fit the best. Figure 6.6 shows a considerable scatter of the data. It can be seen that RN-18 falls into the relationship PI=II/3 while RN-23 shows a higher productivity index compared to its injectivity index. The low value of the productivity index for RN-18 could be explained by a bad calibration of the pressure gauges leading to errors on pressure measurements at the downhole. However, this is not the case for RN-23 which shows a higher productivity index. This could be due to the fact that RN-23 is drilled into a steam cap as pointed out in previous chapters.

From the Figure, it appears also that the productivity indices for the Reykjanes boreholes fall more or less into the same relationship PI=II/3 with a considerable scatter.

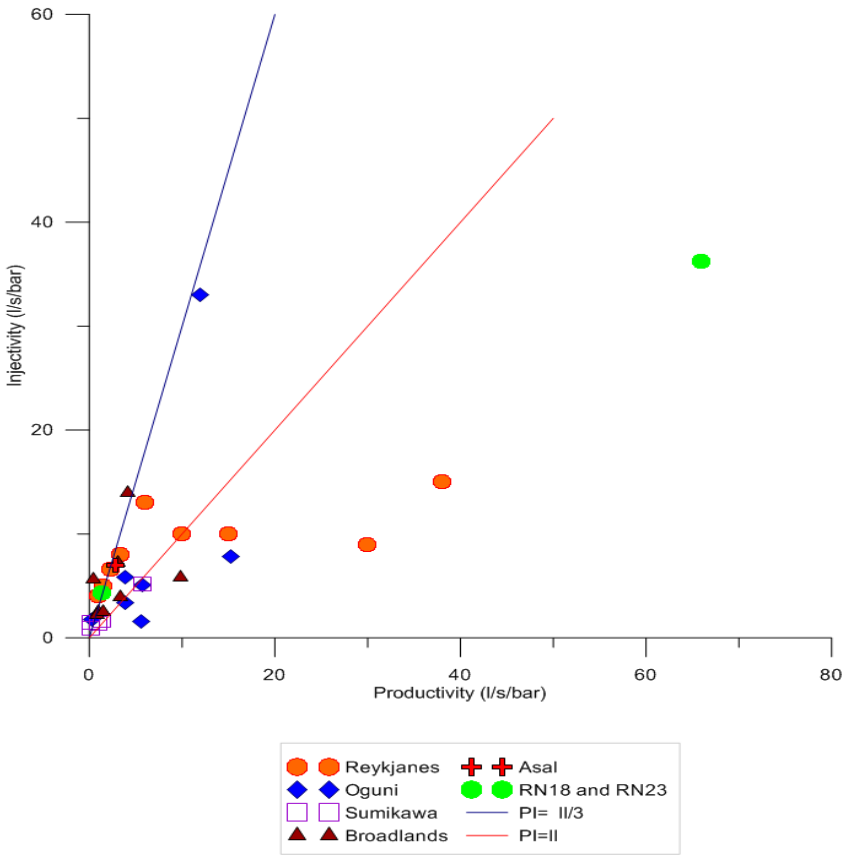

Figure 6.6: Comparison of productivity and injectivity index for several high temperature geothermal fields worldwide

7 Resource estimate

7.1 Volumetric assessment

The most simple and preliminary assessment of a reservoir is the volumetric method. It is used to estimate the stored heat and recoverable power reserves in the early life of geothermal reservoirs. It can only be considered as the first modeling method since it neglects the response of the reservoir to production. This method involves estimating the energy production potential of a geothermal system, based on the available data and present technology.

The volumetric method assumes that the reservoir rocks are porous and permeable and that the water mass extracted from the reservoir extracts the heat from the overall volume of the reservoir. No recharge of reservoir fluids or flux of thermal energy to the reservoir volume is assumed. The following equation is used to calculate the power potential of a homogeneous reservoir by estimating the amount of energy that can be extracted and converted to electricity (Muffler and Cataldi, 1978)

$$E_t = E_r + E_w = (1-\varphi)\rho_r C_r V(T_r - T_0) + \varphi\rho_w C_w V(T_r - T_0) \quad (7.1)$$

Where T_r is the average reservoir temperature (^{o}C) and T_o the reference temperature (^{o}C) that is the endpoint of the thermodynamic process utilizing the fluid. V=Ah is the reservoir volume in m^3, A is the surface area in m^2 and h is the thickness of the reservoir in m. E is the heat energy (J); φ is the porosity of the rock (%), C is the specific heat (J/(°C kg)) and ρ is the density (kg/m^3). The subscripts, r and w refer to rock and water, respectively.

E_t defined by equation (7.1) is usually referred to as the accessible resource base and it can be converted to recoverable power in MW$_e$ by the following equation:

$$P = \frac{E_t\, R_f\, \eta}{L\, t} \quad (7.2)$$

where, P = Power plant capacity (MW$_e$)
R_f = Recovery factor
η = Conversion efficiency (%)
L = Power plant capacity factor (%); and
t = Power plant life (years).

Here, t is the power plant life, represents the fraction of the total time in which the power generation is in operation and gives an average output capacity, P in MW$_e$; η is the conversion efficiency to convert the recovered heat to electricity, R_f is the recovery factor used to determine the amount of heat that can be extracted and L is the power plant capacity factor that combines the plant availability and capacity.

The volumetric method was applied to the Reykjanes field. The purpose was to estimate the electricity capacity assuming 30 year and 50 years power plant life, respectively. Since the reservoir parameters are uncertain, the Monte Carlo simulation was used.

7.2 Monte Carlo simulation

The Monte Carlo calculation is based on a generation of multiple trials to determine the expected value of a random variable. This method relies on a specified probability distribution of each of the input variables and generates an estimate of the overall uncertainty in the prediction due to all uncertainties in the variables (Kalos and Whitlock, 2008). The common distribution functions of poorly known parameters are the rectangular distribution, the triangular distribution, the uniform distribution and the normal distribution. Normal and triangular distributions are suitable when actual data are limited and it is known that they fall near the centre of the limits. In the absence of any other information, rectangular distribution is a reasonable default model. By choosing one random value for each variable out of their probability distributions one possible outcome of the volumetric method can be calculated. To estimate the electric production capacity of the reservoir, two different cases, case I and case II, described below, were considered.

7.2.1 Surface area of the geothermal system

The size of the area considered in this study is the prospect area of the Reykjanes geothermal field. The size of the Reykjanes geothermal system is not yet fully known. Therefore, defining the base of the reservoir can be difficult, even when many wells have been drilled (Grant and Bixley, 2011). Literature from different authors (Björnsson et al., 1970; Pálmason et al., 1985 and Sigurdsson, 2010) assumes different size of the system that can vary between 1 km^2 and 11 km^2. From the INSAR results for the Reykjanes peninsula, a subsidence in an area of more than 16 km^2 is measured (Jónsson, 2009). This indicates that the size of the geothermal system may be larger than what earlier studies indicated (Sigurdsson, 2010).

Information on the extent of a geothermal prospect is usually assumed from the resistivity measurements. For this study, two approaches to define the reservoir area are considered: The area around successful wells which correspond to the low resistivity sheet at 300 m depth b.s.l., an area of 2 km^2 and the area corresponding to the low resistivity sheet at 800 m to 1000 m depth b.s.l., an area of about 11 km^2. The two areas are referred to as case I and case II, respectively. Figure 7.1 shows the low resistivity sheets in Reykjanes.

The wells used in this study are within the two surface areas (Figure 7.2). RN-12, RN-13b, RN-18 and RN-23 are drilled in the small area of geothermal surface manifestations while, RN-17b and RN-29 are drilled outside the alteration area but within the low resistivity sheet at 800 m to 1000 m depth b.s.l.

The area considered for the Monte Carlo simulation is therefore based on these two cases. For case I, it is assumed that the minimum area is 1 km^2 (Björnsson, 1970) and the maximum area is 2 km^2 (Pálmason et al., 1985); and for case II, it is assumed that the minimum area is 1 km^2 and the maximum area is 11 km^2 (Karlsdóttir, 2005). For both cases, the most probable value is taken as 2 km^2.

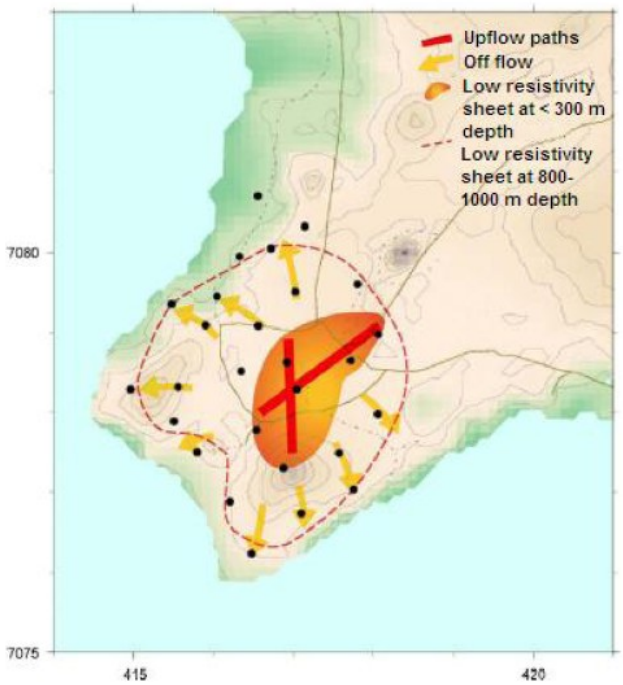

Figure 7.1: TEM resistivity measurements in the Reykjanes geothermal area (Karlsdóttir, 2005). The orange area shows the geothermal surface manifestation referred to as case I and the red dash contour area shows the low resistivity area referred to as case II.

7.2.2 Temperature

The temperature parameter represents the reservoir temperature that was estimated from the temperature profiles for RN-12, RN-17b, RN-18, RN-23 and RN-29 (Figure 5.1). From the temperature profiles, a minimum temperature of 280 °C, a most likely temperature of 300 °C and a maximum temperature of 340 °C were considered for both case I and case II.

7.2.3 Reservoir thickness

The thickness parameter was estimated from the temperature profiles. The minimum depth was considered at the level of the production casing and the maximum level was considered at the well bottom. For case I, the most likely value is assumed to be at 2000 m depth with a minimum of 800 m and a maximum of 2500 m. For case II, the most likely value is assumed to be at 2500 m depth with a minimum of 1000 m and a maximum of 3000 m.

7.2.4 Recovery factor

The thermal recovery factor determines the fraction of the energy that can be extracted from the reservoir rock. Historically, a constant recovery factor of 0.25 has been used for uniformly porous and permeable geothermal reservoirs. More recent analysis of data from fractured reservoirs indicates that the recovery factor is closer to 0.1, with a range of approximately 0.05 to 0.2. In general, this apparent discrepancy in the recovery factor reflects the contrast in thermal energy recovery from complex, fracture-dominated reservoirs compared to uniform, high-porosity reservoirs (Williams, 2007).

For case I, a most likely recovery factor of 0.2 was assumed with a minimum of 0.1 and a maximum of 0.25. This is because for case I which corresponds to a surface area of 2 km^2, the resource is fairly well known with similar reservoir characteristics (RN-12, RN-13b, RN-18 and RN-23).

For case II, which corresponds to the low resistivity area of 11 km^2, the recovery factor was assumed to be as low as 0.1 with a minimum of 0.05 and a maximum of 0.2. A low recovery factor was considered here because wells RN-17b and RN-29, drilled outside the surface alteration area, did not show good permeability despite the high temperature at depth.

7.2.5 Conversion efficiency

Figure 7.2 was used to estimate the conversion efficiency value knowing the reservoir temperature range considered in sub section 7.2.2. Therefore, the most likely conversion efficiency value was estimated to be 14% varying from a minimum value of 13% and a maximum value of 15%.

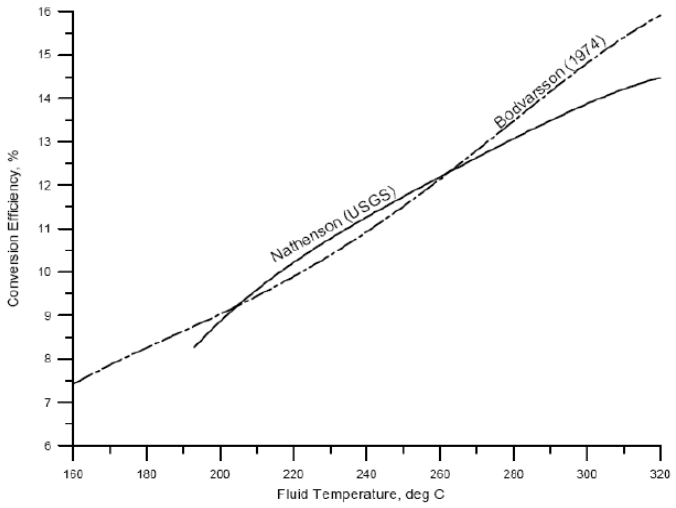

Figure 7.2: Correlation between thermal conversion efficiency and reservoir temperatures (Nathenson, 1975; Bödvarsson, 1974)

7.2.6 Results

In the calculation, a rejection temperature of 40 ^oC was considered. The porosity of basalt was assumed to be 10% for both case I and case II. The fluid density was calculated by considering the reservoir temperatures and the salinity of the Reykjanes fluid. The parameters used to calculate the power potential and the probability distribution functions used to calculate them are summarized in Table A.3.

In this study, two life time scenarios of 30 years and 50 years, respectively, were run using the Monte Carlo simulation @RISK spreadsheet-based software (Palisade Corp., 2004). An estimate of the electrical power, which could be produced from the Reykjanes geothermal field is calculated according to equation (7.1) and (7.2) by using the

parameters in Table A.3. The simulation runs were 10,000. Table 7.1 shows the statistical distribution for the two production periods for case I and case II, respectively.

Table 7.1: Estimation of the power generation capacity for the Reykjanes geothermal field based on Monte Carlo simulation

Size of the geothermal area	Estimated capacity MW_e			
	30 years		50 years	
	A = 2 km^2	A = 11 km^2	A = 2 km^2	A = 11 km^2
Median	64	110	39	68
Mean	65	132	39	79
Maximum	138	640	85	320
90% confidence interval	34-102	38-290	20-61	23-174

The calculated parameters (Figure A.12 and Figure A.13) for case I indicate that the power production for the Reykjanes geothermal field lies with 90% confidence interval between 34 MW_e and 102 MW_e for a recoverable heat used with a most likely value of 65 MW_e and between 20 MW_e and 61 MW_e with a most likely value of 39 MW_e for 30 years and 50 years, respectively.

For case II, the model predicts with 90% confidence interval, a power production of 38 MW_e to 290 MW_e with a most likely value of 132 MW_e and between 23 MW_e and 174 MW_e with a most likely value of 79 MW_e for 30 years and 50 years, respectively (Figure A.14 and Figure A.15).

8 Conclusions

The purpose of this study was to demonstrate the importance of well testing in the evaluation of geothermal resources with a particular emphasis on the methodology and the interpretation of temperature and pressure profiles at well completion and during discharge tests. Various methods were selected to estimate the well and reservoir properties as well as the characteristics of the Reykjanes geothermal field in southwest Iceland. The Reykjanes geothermal field was used as an example for the application of the methodology presented in the thesis.

Step-rate injection tests reveal a permeability distribution of the Reykjanes reservoir. Temperature and pressure logs interpretation contributed to the estimation of the formation temperature and the initial reservoir pressure as well as the location of the feed zones or zones of permeability. The flow characteristics of selected wells are estimated from discharge tests and also simulated to evaluate the generating capacity of individual wells. Finally, a volumetric assessment based on well-test data is used to predict the electrical generation capacity of the Reykjanes geothermal system. It important to point out that the results presented in the thesis do not fully describe the Reykjanes geothermal reservoir since all wells were not considered.

The summary of the results from this study is given in Section 8.1, the results are discussed in Section 8.2 and the recommendations based on this are made in Section 8.3.

8.1 Summary of results

The step-rate injection tests were performed for wells RN-17b, RN-18 and RN-23. The estimated value of the permeability-thickness ranges from 1 Dm to 30 Dm for the Reykjanes reservoir. The storativity for the system varies between $5 \cdot 10^{-8}$ m/Pa and $2 \cdot 10^{-7}$ m/Pa. The skin factor is negative varying between -0.7 and -2.5 indicating stimulated wells and presumably fractured reservoir. Injectivity indices are different for each well, ranging from 1 (L/s)/bar to 36 (L/s)/bar indicating heterogeneity in the permeability of the reservoir.

Temperature and pressure profiles were analysed for RN-12, RN-17b, RN-18, RN-23 and RN-29 and the initial reservoir pressure and the formation temperature estimated. The formation temperatures vary between 280 ^{o}C and 320 ^{o}C with the highest value of 340 ^{o}C for RN-17b indicating a high temperature geothermal field. Boiling is observed at a depth of 500 m to 1000 m for RN-12, RN-18 and RN-23 indicating a steam cap or two phase reservoir. Below 1000 m depth, a single-phase liquid is dominating. This corresponds well with the literature (Arnórsson, 1995). RN-29 indicates a possible temperature inversion or slow temperature recovery below 1750 m depth which could indicate that the outer boundary of the system has been reached. RN-17b and RN-29 indicate a hot reservoir zone but rather impermeable rock.

For Reykjanes, the initial reservoir pressures are quite different suggesting heterogeneity in the reservoir. The pressure in RN-17b was low as compared to the other wells while the pressure in RN-23 was the highest one.

Discharge tests were performed for RN-13b, RN-18 and RN-23 and the results for RN-13b, and RN-18 indicate a power generating capacity of approximately 10 MW_e per well for the productive part of the Reykjanes reservoir. The capacity of RN-23 could not be estimated during the discharge tests since the well was discharged directly to the atmosphere without steam and water separation.

Temperature and pressure logs for wells RN-13b, RN-18 and RN-23 measured during discharge tests were simulated using the HOLA wellbore simulator to estimate the capacity of the wells during discharge as well as their productivity indices. The simulation results compared reasonably well with the flow characteristics calculated from the discharge tests. The capacity of the wells varies between 5 MW_e and 15 MW_e. RN-23 shows a high capacity of 15 MW_e. However, the comparison of the productivity indices with the ones calculated during discharge shows some variations. This can be due to the fact that the well had not fully recovered after the discharge test and/or bad calibration of the instrument (pressure gauges). Another reason could be that more feed zones are affecting the behaviour of the wells.

Different relationships between injectivity and productivity indices for different high temperature geothermal fields worldwide were considered in order to estimate the II/PI correlation for the two wells RN-18 and RN-23 in the Reykjanes geothermal field. The relationships seem to indicate that PI=II/3 for RN-18 but RN-23 shows a higher productivity index than the injectivity index. Other wells from the Reykjanes field indicate a relation of PI=II/3 with a considerable scatter.

The Monte Carlo simulation for case I, discussed in Chapter 7, predicts with 90% confidence interval a generating capacity between 34 MW_e and 102 MW_e , with a most likely value of 65 MW_e and between 20 MW_e and 61 MW_e , with a most likely value of 39 MW_e for 30 years and 50 years, respectively. For case II, also discussed in Chapter 7, the model predicts with 90% confidence interval a generating capacity of 38 MW_e and 290 MW_e , with a most likely value of 132 MW_e and between 23 MW_e and 174 MW_e , with a most likely value of 79 MW_e for 30 years and 50 years, respectively.

Considering a generating capacity of 290 MW_e , the maximum number of wells to be drilled in the area could be estimated at about 30 wells.

8.2 Discussion

The questions that were posed in the introduction of the thesis can be answered here. What are the current approaches and methods used in well testing? What kind of information is expected at different stages and well testing and how can this information contribute to the development of a new geothermal field? How can the results of well testing be used to estimate the production capacity of a geothermal field? How can the results be used in guiding decision making for the development of a field?

The pressure is the most important parameter and it is its response to perturbation that gives information on the well and the reservoir properties through well testing. The reservoir pressure is an indication of how much the potential energy the reservoir contains.

From the results of this study, it can be said that the permeability of a geothermal reservoir is not uniform; it varies for different parts of the reservoir. A well can be drilled into a

high temperature part of a reservoir but if the permeability is low, the well is not productive like in the case of wells RN-17b and RN-29. Therefore, the permeability is a direct indication of the well productivity and it is a parameter that is telling if a well is good or bad depending on the utilisation of the fluid. The permeability-thickness is telling how easily the reservoir fluid can flow to a well and help designing well spacing and deciding the number of wells to be drilled.

The permeability can be estimated during the injection test since it depends on the injectivity index. When the injectivity index is low or high, the permeability is assumed to be low or high. However, the injectivity index of a well is not always the same as the productivity index as usually suggested, particularly for high temperature geothermal fields as indicated in the thesis. The productivity index can be as low as one third the injectivity index for the same well as seen for RN-18. This shows that a well with high injectivity index cannot always be considered to have a high productivity index especially for high temperature geothermal fields. However, exceptions can be found where the productivity index is higher than its injectivity index like for well RN-23. The injectivity and productivity indices must therefore, always be measured when testing a well. A conservative estimate assuming that PI=II/3 can be considered for the Reykjanes field.

The simulation of the discharge data shows that the productivity index can be estimated from the results and that the results from the simulator represents better the productivity of the wells. For RN-18, the discharge test shows a small productivity index 1.4 (kg/s)/bar while the HOLA simulator shows a productivity index of 7 (kg/s)/bar. The productivity index value from HOLA is a better indication since for HOLA, the pressure at the bottom of the well is a fixed input in the simulation, allowing accurate calculations. However, the simulation process is long and this method cannot be used when information is needed fast.

To know the storativity is important because it is an indication of the fluid reserves in the reservoir. If the storativity is small, the resource development will not sustain a long production period. Also, a high value of storativity can tell if a well is drilled into a steam cap or not.

The temperature of the fluid or the corresponding enthalpy can assist in deciding how to utilise the resource (electricity production or some other utilisation), and/or if the power plant should use steam turbine or binary units. The reservoir fluid in the Reykjanes geothermal field has high temperature. Therefore, it is used for electricity production. Analyses of the formation temperature and information on the initial reservoir pressure can assist in determining the fluid flow directions in the reservoir.

The output curves give an indication about the ability of a well to produce and about the well capacity in MW_e. This can lead to decisions on the number of wells required to develop a field. But before a decision is made, the reservoir must be delineated by drilling wells to confirm the productive size of the reservoir. It was shown here that RN-17b and RN-29, drilled recently at the outskirts of the surface alteration zone are not productive and RN-29 indicates that the outer boundary has been reached. This shows that additional wells are needed to delineate the reservoir. A concentration of wells in the same area can lead to a pressure drawdown in the system as indicated in the Reykjanes field from the pressure profiles.

The results of well testing, both at completion of the well and during discharge test, can be used to develop a conceptual model of the field by integrating geological, geochemical and geophysical data. Furthermore, those results can be used to monitor the energy output and the reservoir response during production.

At the beginning of a field exploration, the power production capacity is roughly estimated by the volumetric method knowing a range of parameters for the reservoir. This estimate can be used for commercial purposes to interest private companies in developing a field. The volumetric method does not consider the recharge of the reservoir fluid. The Monte Carlo simulation involves an uncertainty in the results. However, the 90% confidence interval can give an indication of the lower limit of the capacity of the field. The results found for the two different cases indicate that possibly the Reykjanes field is larger. However, it might also be the other way around. Other simple modelling like the lumped parameter modeling can give a better estimate based on available data during production.

8.3 Recommendations

Recommendations can be made from the results and discussion above:

- Additional tests have to be carried out, such as interference tests to understand the connection between the wells, and tracer tests to understand the pathways of the fluid flow in the reservoir.
- Long term discharge tests are recommended for better analysis of the reservoir properties.
- The volumetric assessment gives a rough estimate of the field capacity and does not reveal a clear overall capacity of the area. The results indicate that the extent of the reservoir must be defined more clearly. It has been observed that the wells considered outside the surface alteration area do not seem to be productive (RN-17b and RN-29). It is recommended that before expanding the Reykjanes power plant as planned, more wells should be drilled and tested to define the outer boundary of the reservoir.
- If continuous well flow is limited because of time and other constraints, the wellbore simulation is a good tool to compute the performance of the well when reliable production data together with pressure and temperature profiles are available.
- It is recommended to include wellbore direction to the wellbore geometry option in HOLA to better simulate directional wells.
- Finally, it would be interesting to analyse the well test data using the new deconvolution analysis method and use it as a diagnostic tool to confirm the results from the conventional methods.

References

Agarwal, R., Al-Hussainy, R., & Ramey H.J. (1970). An investigation of wellbore storage and skin effect in unsteady liquid flow. I. Analytical treatment. *Soc. Pet. Eng. J., 5*, 279-290.

Arason, Th., Björnsson, G., Axelsson, G., Bjarnason, J.Ö., & Helgason, P. (2004). ICEBOX – geothermal reservoir engineering software for Windows. A user's manual. ISOR, Reykjavík, *report 2004/014*, pp. 80.

Armand, A.A. (1959): Investigation of the Resistance during movement of the steam-water mixtures in a heated boiler pipe at high pressures. *Atomic Energy Research Establishments*, Hartwell, Berkshire.

Arnórsson, S. (1978). Major element geochemistry of the geothermal seawater at Reykjanes and Svartsengi. *Mineral Mag., 42*, 209-220.

Arnórsson, S. (1995). Geothermal systems in Iceland; structures and conceptual models; I, high-temperature areas. *Geothermics, 24,* 561-602.

Aunzo, Z.P., Björnsson, G., & Bödvarsson, G.S. (1991). Wellbore models GWELL, GWNACL and HOLA. *Lawrence Berkeley Laboratory report LBL-31428*. Berkeley, CA, USA, pp.102.

Axelsson, G. (1989). Simulation of pressure response data from geothermal reservoirs by lumped parameters. *XIV Workshop on Geothermal Reservoir Engineering*. Stanford, CA: Stanford University, 1-7.

Axelsson, G. (2010). The physics of geothermal resources and their managements during utilisation. *UNUGTP lecture notes.*

Axelsson, G., & Gunnlaugsson, E. (2000). Geothermal utilization, management and monitoring. *In: Long-term monitoring of high- and low-enthalpy fields under exploitation. World Geothermal Congress 2000 Short Courses,* Kyushu – Tohoku, Japan, 3-10.

Axelsson, G., Thórhallsson, S., & Björnsson, G. (2006). Simulation of geothermal wells in basaltic rock in Iceland. *Enhanced geothermal innovative network for Europe Workshop 3*, Switzerland.

Bangma, P. (1961). The development and performance of a steam water separator for use on geothermal bores. *Proc. UN conference on New Sources of Energy.v3*.

Bear, J. (1979). *Hydraulics of groundwater*. Dover publications, New York, pp.569.

Björnsson, G. (1987). A multi-feedzone geothermal wellbore simulator. *Lawrence Berkeley Laboratory, report LBL-23546*, 8-19.

Björnsson, G. (1993). Program PREDYP. *In: Arason, Th., Björnsson, G., Axelsson, G., Bjarnason, J.Ö., and Helgason, P., 2004: ICEBOX – Geothermal reservoir engineering software for Windows, a user's manual. ÍSOR, Reykjavík, report ISOR-2004/014,* pp. 80.

Björnsson, G., & Bödvarsson, G.S. (1990). A survey of geothermal reservoir properties. *Geothermics, 19-1,* 17-27.

Björnsson, G., Arason, P., & Bödvarsson, G.S. (1993). The wellbore simulator HOLA. Version 3.1. User's guide. *Orkustofnun, Reykjavík*, pp. 36.

Björnsson, S., Arnorsson, S., & Tomasson, J. (1970). Exploration of the Reykjanes thermal brine area. *Geothermics 56*, 2380-2391.

Bödvarsson G.S. (1964). Physical characteristics of natural heat sources in Iceland. *Proc. UN confererence on New sources of Energy, volume 2*: geothermal Energy, Rome, August 1961. United Nations, New York, 82-89.

Bödvarsson G.S. (1974). Geothermal resources energetics. *Geothermics, V.3.*

Bödvarsson, G.S., Benson, S.M., Sigurdsson, Ó., Halldorsson, G.K., & Stefánsson, V. (1981). Analysis of well test data from the Krafla geothermal field, Iceland. *Proceedings of Seventh Workshop in Geothermal Reservoir Engineering*, Stanford, California.

Bödvarsson, G.S., & Witherspoon, P.A. (1989). Geothermal reservoir engineering, part 1. *Geotherm. Science & Tech, 2-1,* 1-68.

Bourdarot, G. (1998). *Well Testing: Interpretation Methods*. Editions Technip, Institut Français du Petrole, Paris.

Bourdet, D. (2002). *Well test analysis: the use of advanced interpretation models.* Handbook of Petroleum Exploration and Production. Elsevier, Amsterdam.

Bourdet, D., Whittle, T., Douglas, A., & Pirard, Y. (1983). A new set of type curves simplifies well test analysis. *World Oil*, 95–106.

Bourdet, D., Ayoub, J.A., & Pirard, Y.M. (1989). Use of Pressure Derivative in Well-Test Interpretation, *SPEFE*, June 1989, 293-302.

Chisholm, D. (1973). Pressure Gradients Due to Friction during the Flow of Evaporating Two-Phase Mixtures in Smooth Tubes and Channels. *International Journal Heat Mass Transfer*, 16, 347- 358.

Combs, J., & Garg, S.K. (2000). Discharge capability and geothermal reservoir assessment using data from slim holes. *Proceedings World Geothermal Congress 2000*, 1065-1070. Kyushu, Japan, May 28-June 10, 2000.

Craft, B.C., & Hawkins, M.F. (1959). *Applied Petroleum Reservoir Engineering*. Englewood Cliffs: Prentice-Hall.

Dake, L. P. (1978). *Fundamentals of Reservoir Engineering*. Elsevier Science, B.V, pp. 436.

Dowdle, W.L., & Cobb, W.M. (1975): Static formation temperature from well logs-an empirical method. *J.Petrol. Techn*., 27, 1326-1330

Earlougher, R.C. (1977). *Advances in well test analysis*. Soc. Petr. Eng., Monograph 5, pp. 264.

Garg, S.K., & Combs, J. (1997). Use of slim holes with liquid feedzones for geothermal reservoir assessment. *Geothermics, 26-2*, 153-178.

Goldemberg, J., Baker, J.W., Ba-N'Daw, S., Khatib, H., Popescu, A., & Viray, F.L. (eds). (2000). World energy assessment. *UN Development Program, New York, Bureau for Development Policy*, 135-171.

Grant, M.A. (2008). Decision tree analysis of possible drilling outcomes to optimize drilling decisions. *Proceedings of Geothermal Reservoir Engineering Thirty-Third Workshop*, Stanford, California, January 28-30, 2008. SGP-TR-185.

Grant, M.A., Donaldson, I.G., & Bixley, P.F. (1982). *Geothermal reservoir engineering*. Academic Press, New York, pp. 369.

Grant, M.A., & Bixley, P.F. (2011). *Geothermal reservoir engineering*, II Edition. Academic Press, New York.

Gringarten, A. C. (2008). From straight lines to deconvolution: The evolution of the state of the art in well test analysis. *SPE Reservoir Evaluation and Engineering*, 11(1), 41–62.

Gudmundsson, J.S. (1986). Composite model of geothermal reservoirs. *Geothermal Resources Council bulletin*. January 3-10.

Gudmundsson, J.S., Hauksson, T., & Tomasson J. (1981). The Reykjanes geothermal field in Iceland: Subsurface exploration and well discharge characteristics. *Proceedings seventh Workshop Geothermal Reservoir engineering,* Stanford.

Helgason, P. (1993). Step by step guide to BERGHITI. User's guide. *In: Arason, Th., Björnsson, G., Axelsson, G., Bjarnason, J.Ö., and Helgason, P., 2004: ICEBOX – Geothermal reservoir engineering software for Windows, a user's manual*. ÍSOR, Reykjavík, report ISOR-2004/014, pp. 80.

Horne, R.N. (1995). *Modern well test analysis, a computer aided approach.* 2nd edition, Petroway Inc., USA, pp. 257.

Horner, D.R. (1951). Pressure build-up in wells. *Third World Petroleum Congress*, 503–523.

Houssein, D.E., & Axelsson, G. (2010). Geothermal resources in the Asal region, Republic of Djibouti: An update with emphasis on reservoir engineering studies. *Geothermics, volume 39, Issue 3*, September 2010, 220-227.

Ilk, D., Valko, P.P., & Blasingame, T.A. (2005). *Deconvolution of variable –rate reservoir performance data using B-Splines*. SPEREE 9 (4): 582-595. SPE-95571-PA. DOI: 10.2118/95571-PA.

James C.R. (1966). Measurement of steam and water mixtures discharging at the speed of sound to the atmosphere. *New Zealand engineering 21* (10).

Jonsson, S. (2009). Subsidence around the Reykjanes ans Svartsengi power plants during 1992-1999 and 2003-2008 obsreved by INSAR. *Report t*o HS, pp. 42.

Juliusson, E., Gretarsson, G.J., & Jonsson P. (2008). *Well Tester 1.0b, User's guide*. ISOR, pp. 26.

Kalos, M.V., & Whitlock, P.A. (1998). *Monte Carlo Methods.* John Wiley & Sons, Inc., NY, pp. 183.

Karlsdóttir, R. (2005). *TEM measurements at Reykjanes 2004* (in Icelandic). Report ISOR-2005/002, pp 23.

Kjaran, S.P., & Elíasson, J. (1983). Geothermal reservoir engineering lecture notes. *UNU G.T.P., report 2*, Iceland, pp 250.

Levitan, M.M. (2005). Practical Application of Pressure/Rate Deconvolution to Analysis of Real Well Tests. *SPE Reservoir Evaluation and Engineering* (April) 113.

Levitan, M.M., Crawford, G.E., & Hardwick, A. (2006). Practical Considerations for Pressure-Rate Deconvolution of Well-Test Data, *SPE Journal (March)* 35.

Linford, A. (1961). *Flow Measurement and Meters*, 2nd ed., E. & F. N. SPON Ltd., London.

Miller, C.C., Dyes, A.B., & Hutchinson, G.A. (1950). The Estimation of Permeability and Reservoir Pressure from Bottomhole Pressure Buildup Characteristics, *Trans.* AIME, 189, 91.

Muffler, P.L.J., & Cataldi, R. (1978). Methods for regional assessment of geothermal resources. *Geothermics, 7*, 53-89.

Nathenson, M.(1975). *Physical factors determining the fraction of stored heat recoverable from hydrothermal convection systems and conduction dominated areas*. USGS open file report 38.

Orkiszewski, J. (1967). Predicting Two-Phase Pressure Drops in Vertical Pipe, *J. Pet. Tech.*, pp. 829-838.

Palisade Corp. (2004). *@RISK program, ver. 4.5.5*. Palisade Corporation, NY, USA.

Pálmason, G., Johnsen, G.V., Torfason, H., Saemundsson, K., Ragnars, K., Haraldsson, G.I., & Halldorsson G.K. (1985). Assessment of geothermal energy in Iceland. *National Energy Authority Report OS-85076/JHD-10* (in Icelandic).

Ramey, H.J. Jr. (1970). Short time well test data interpretation in the presence of skin effect and wellbore storage. *JPT 22(1):97-104*. SPE-223-PA. DOI: 10.2118/2336-PA.

Saemundsson, K., Jóhannesson, H., Hjartarson, Á., Kristinsson, S.G. and Sigurgeirsson, M.Á., 2010: Geological map of Southwest Iceland, 1:100.000. *Iceland GeoSurvey*, Reykjavík, Iceland.

Sigurdsson O. (2010). Reykjanes seawater geothermal system-its exploitation under regulatory constraints. *World geothermal Congress 2010,* Bali, Indonesia.

Singhal B.B.S., & Gupta R. P. (2010). *Applied Hydrogeology of Fractured Rocks* . 2nd edition. Springer.DOI:10.1007/978-90-481-8799-7.

Stefánsson, V., & Steingrímsson, B.S. (1990). Geothermal logging I, an introduction to techniques and interpretation, 3rd edition. *Orkustofnun report OS-80017/JHD-09,* pp. 117.

Theis, C. V. (1935). The relation between the lowering of the piezometric surface and the rate and duration of discharge of a well using ground-water storage. *Transactions, American Geophysical Union 16*: 519–524.

Theim, G. (1906) (in German). *Hydrological methods*. Leipzig: J. M. Gebhardt. pp. 56.

Von Schroeter, T., Hollaender, F., & Gringarten, A. (2001). Deconvolution of well test data as a nonlinear total least squares problem. *Society for Petroleum Engineers annual technical conference and Exhibition,* New Orleand.

Williams, C.F. (2007). Updated methods for estimating recovery factors for gethernmal resources. *Proceedings Thirty-Second Workshop on Geothermal Reservoir Engineering*. Stanford University, Stanford, CA.

A. Appendix

A.1 Wellbore characteristics

Table A.1: Characteristics of Reykjanes wells.

Well	Measured depth (m)	True vertical depth (m)	East (m)	North (m)	Elevation (m.a.s.l.)	Production casing depth (m)	Remarks
RN-12	2506		318815	374154	18.1	842	Vertical well
RN-13B	2530	2200	318424	374503	18.2	818	Directional well
RN-17B	3077	2804	318072	373573	12.7	892	Directional well
RN-18	1815		319066	374412	23.1	750	Vertical well
RN-23	1924	1742	318488	374177	16.8	701	Directional well
RN-29	2837		317446	374756	20.0	901	Vertical well

A.2 Injection test

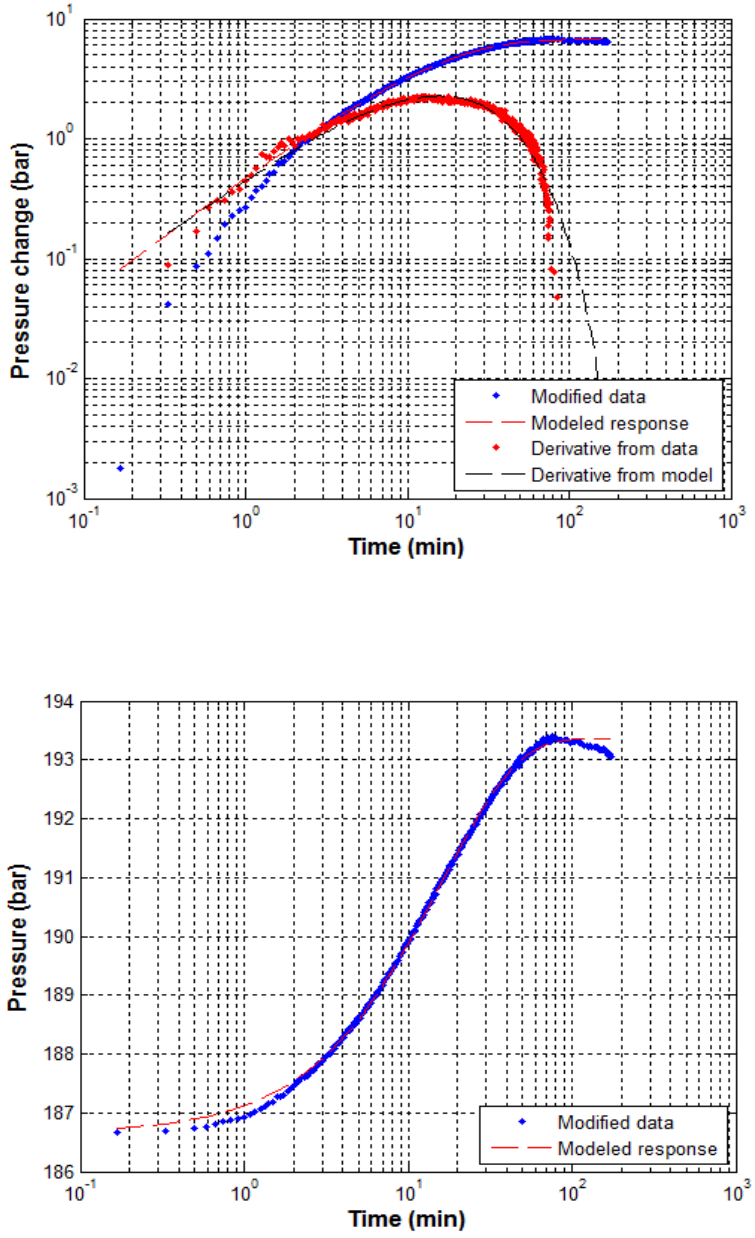

Figure A.1: Fit between model and selected data on log -log scale and log-linear scale for step 1 for well RN-17b.

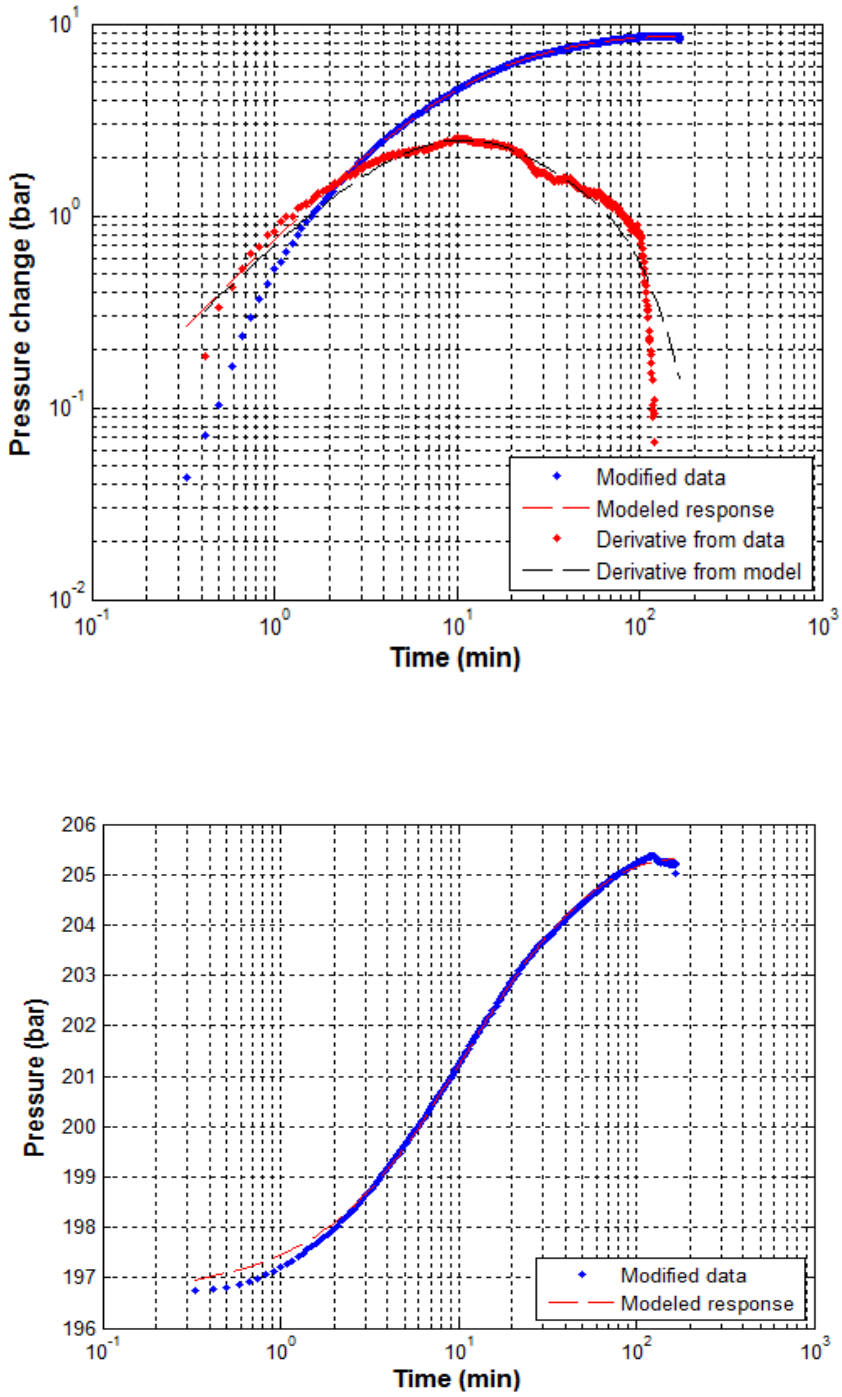

Figure A.2: Fit between model and data on log -log scale and log-linear scale for step 2 for well RN-17b.

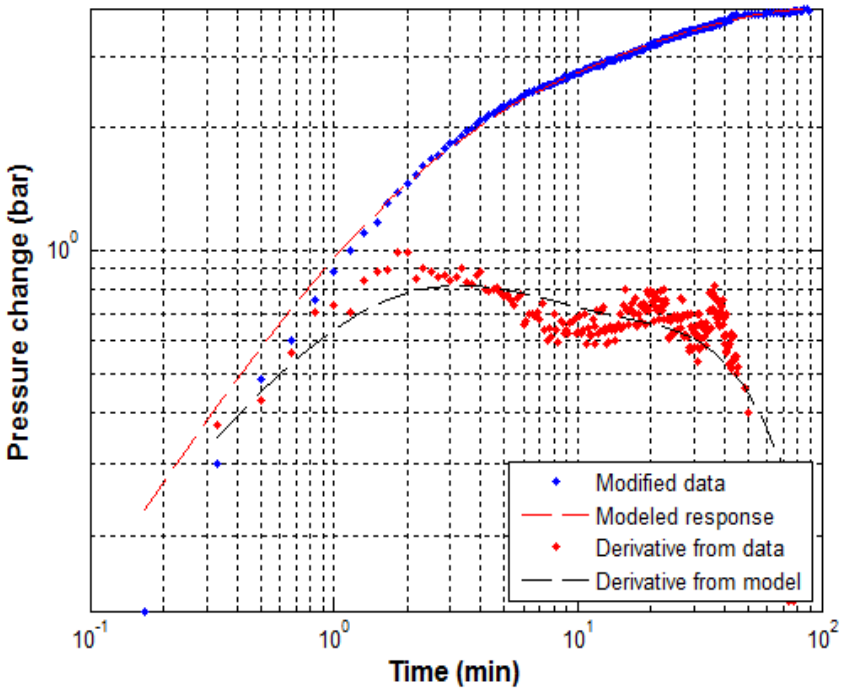

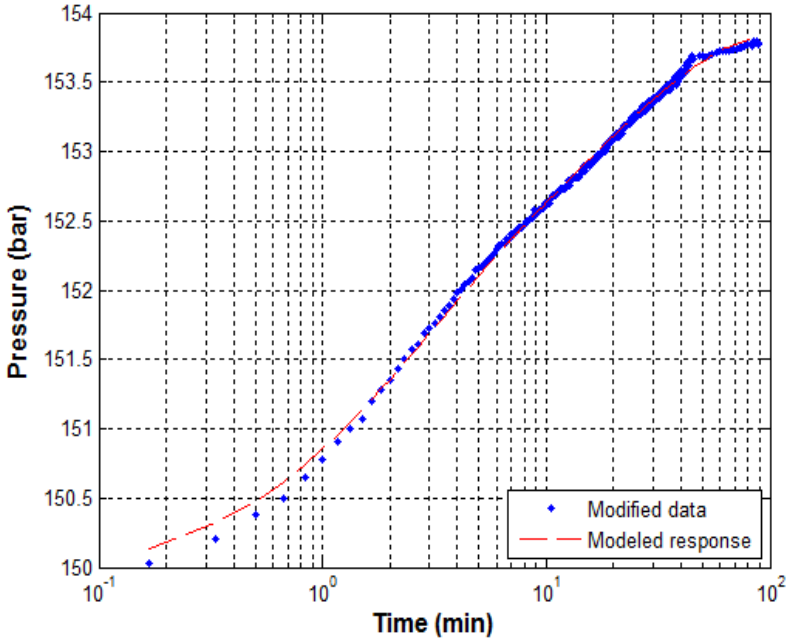

Figure A.3: Fit between model and data on a log- log scale and log-linear scale for step 1 for well RN-18.

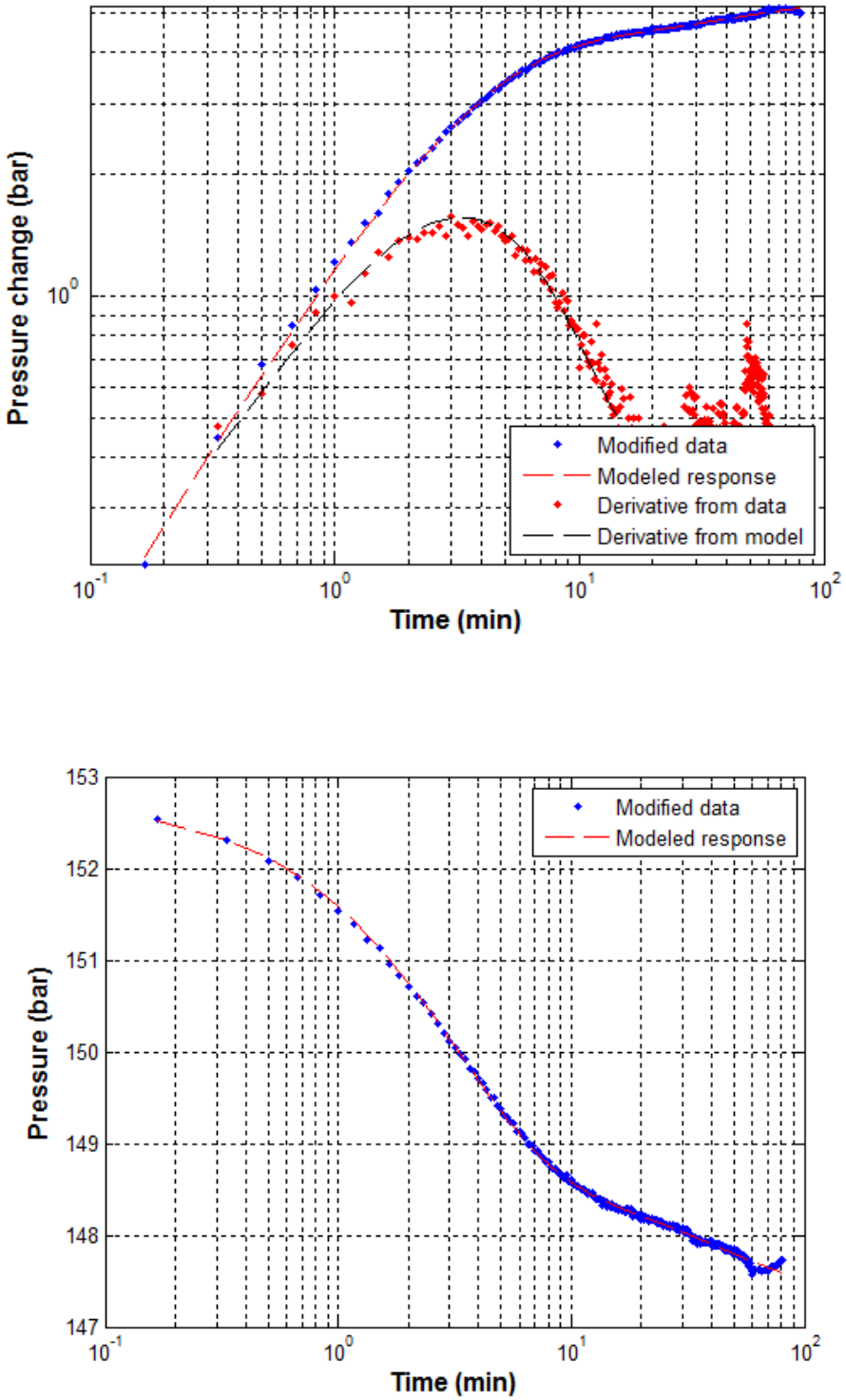

Figure A.4: Fit between model and data on a log- log scale and log-linear scale for step 2 for well RN-18.

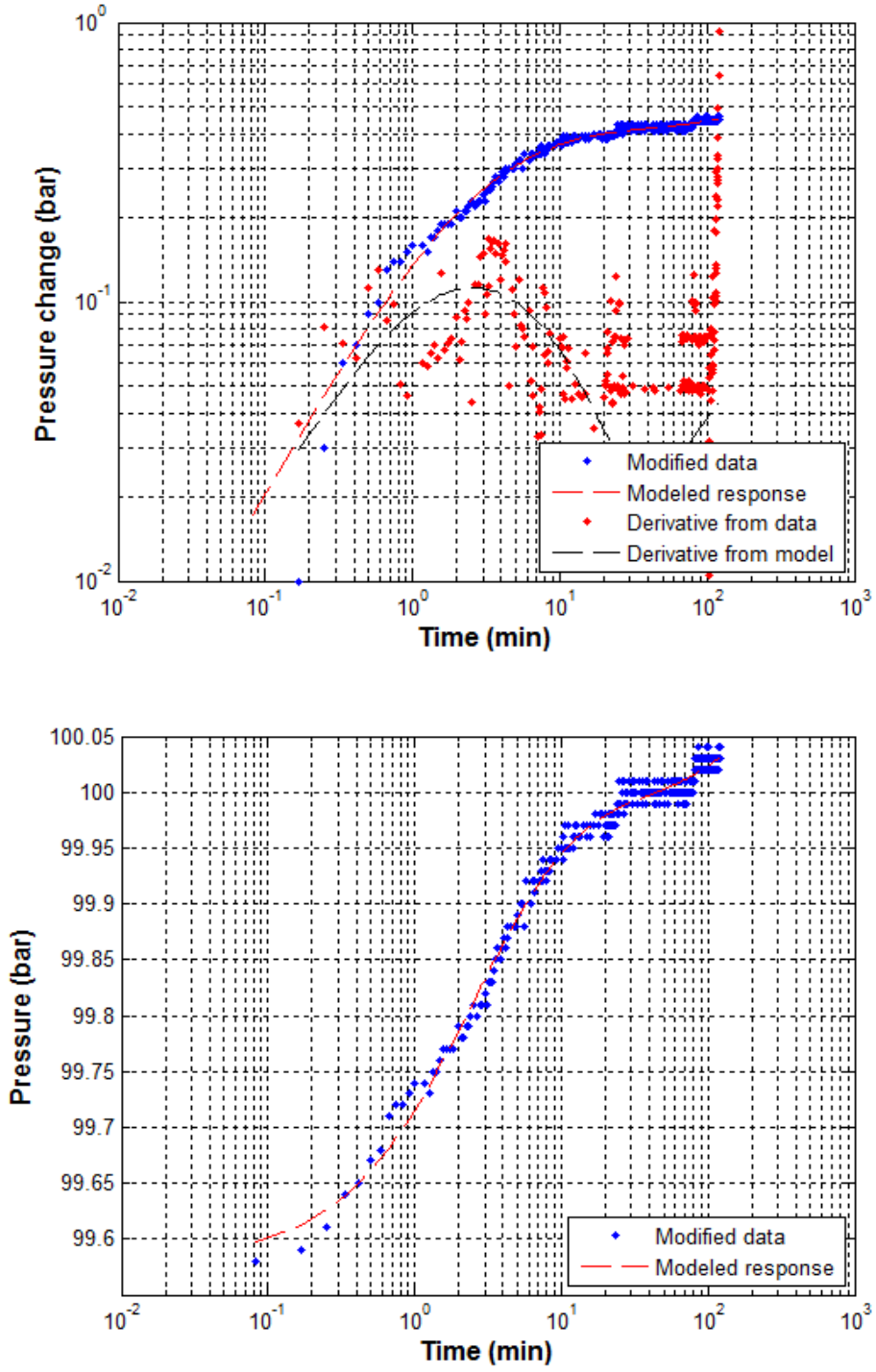

Figure A.5: Fit between model and data on log-log scale and log-linear scale for step 2 for well RN-23.

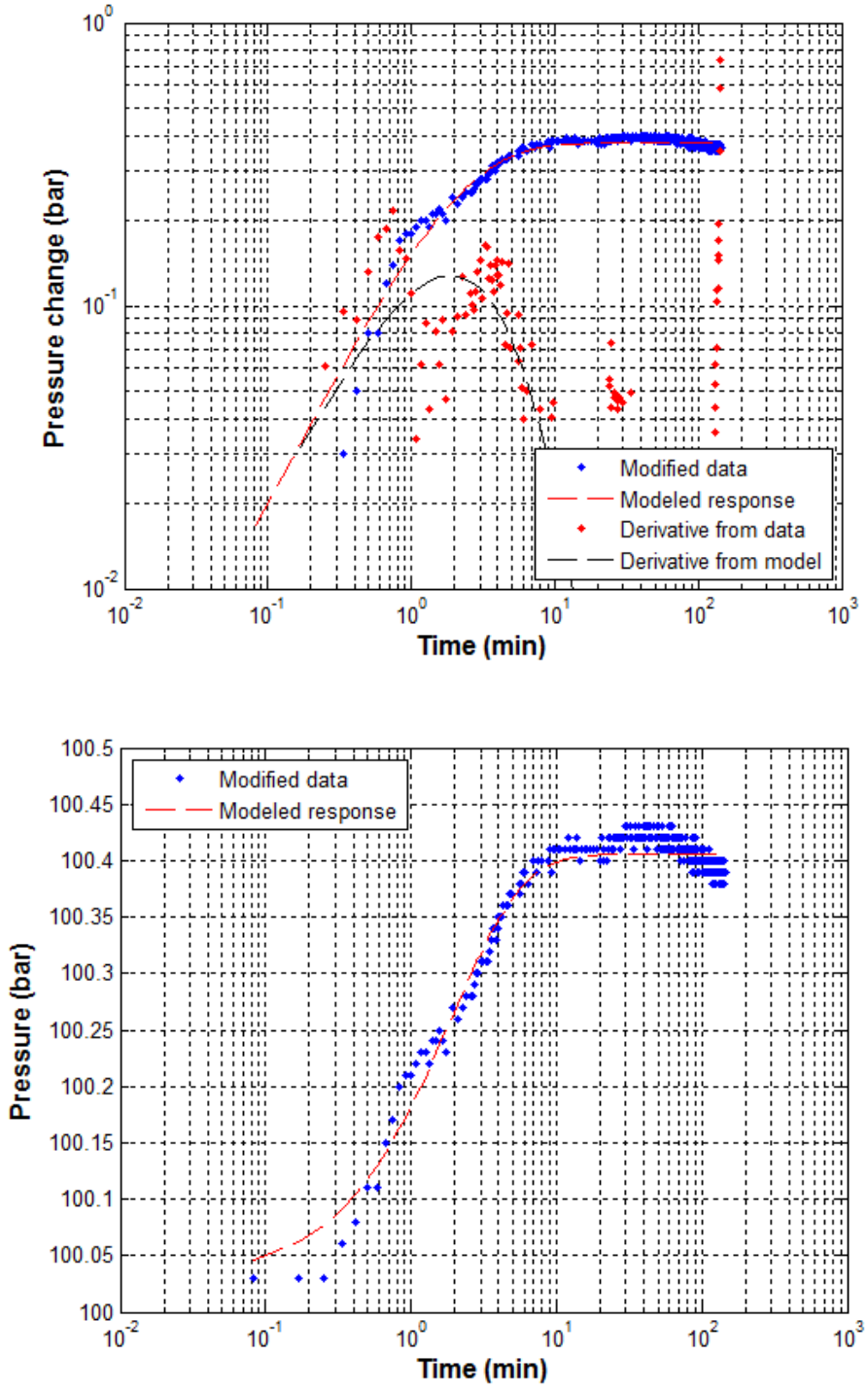

Figure A.6: Fit between model and data on log -log scale and log-linear scale for step 3 for well RN-23.

A.3 Temperatures and pressures profiles

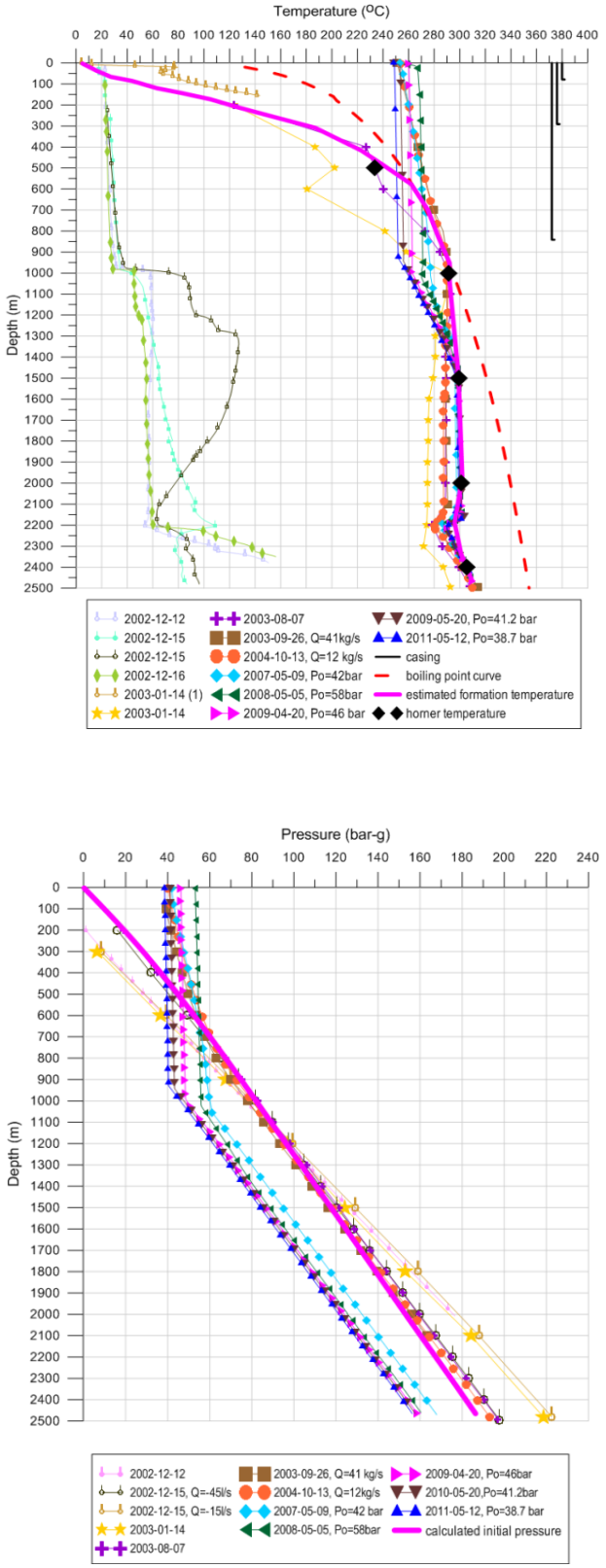

Figure A.7: Estimation of the reservoir temperature and pressure for well RN-12.

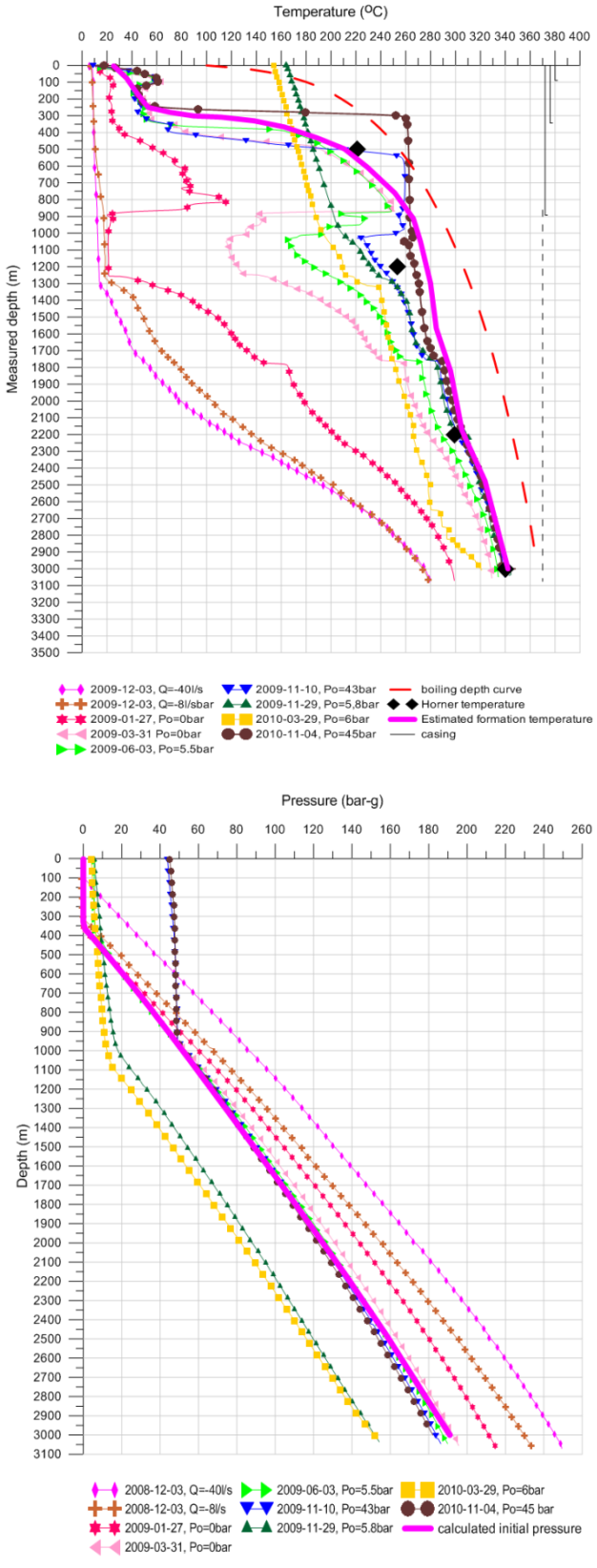

Figure A.8: Estimation of the reservoir temperature and pressure for well RN-17b.

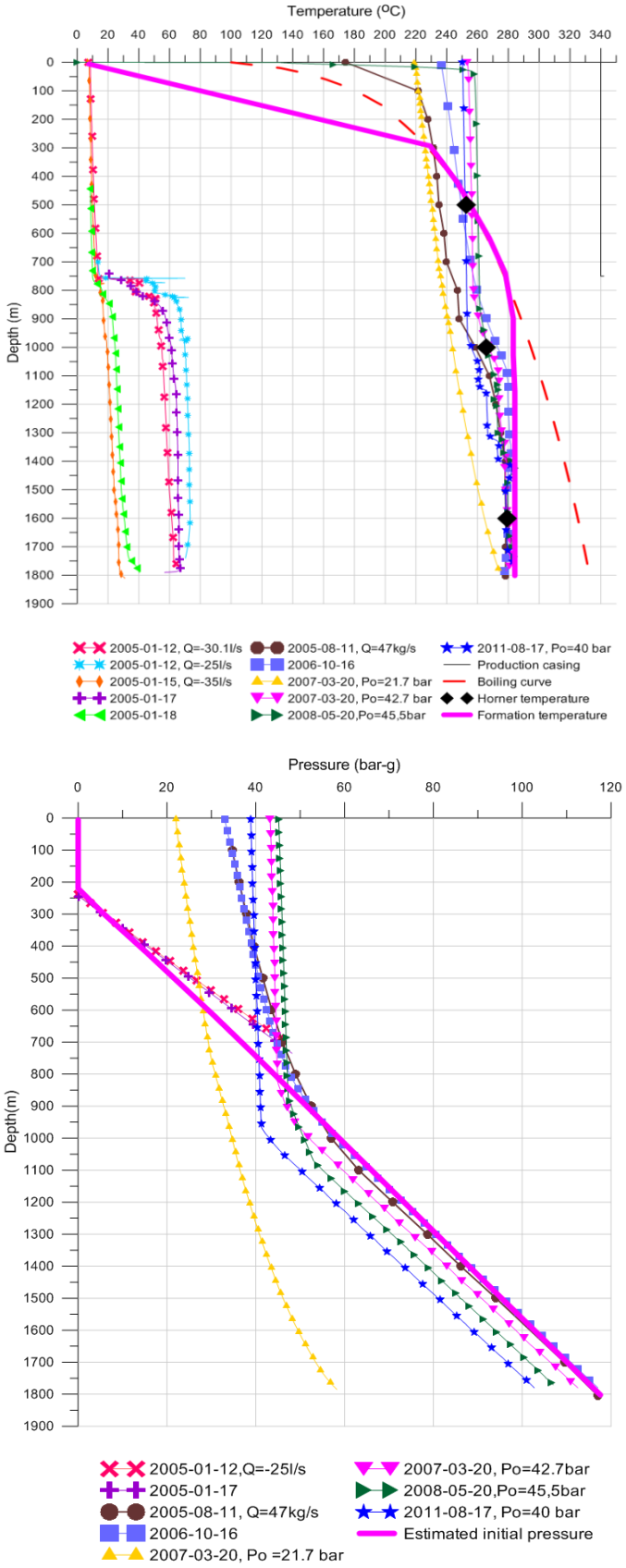

Figure A.9: Estimation of the reservoir temperature and pressure for well RN-18.

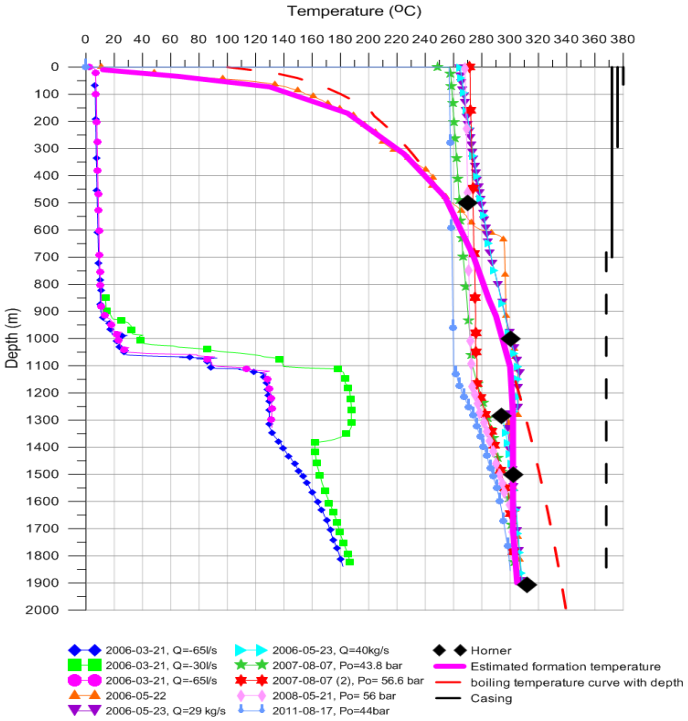

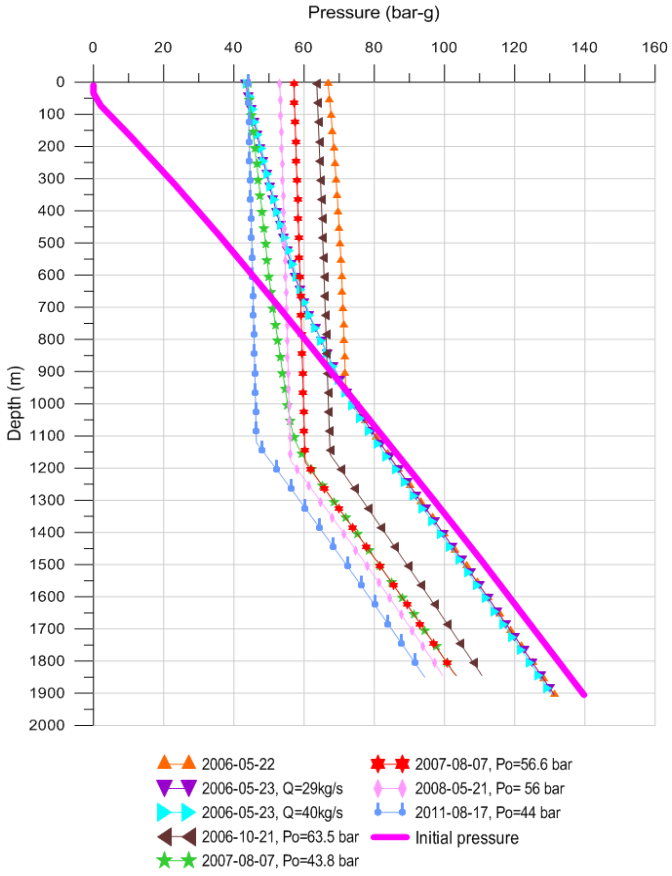

Figure A.10: Estimation of the reservoir temperature and pressure for well RN-23.

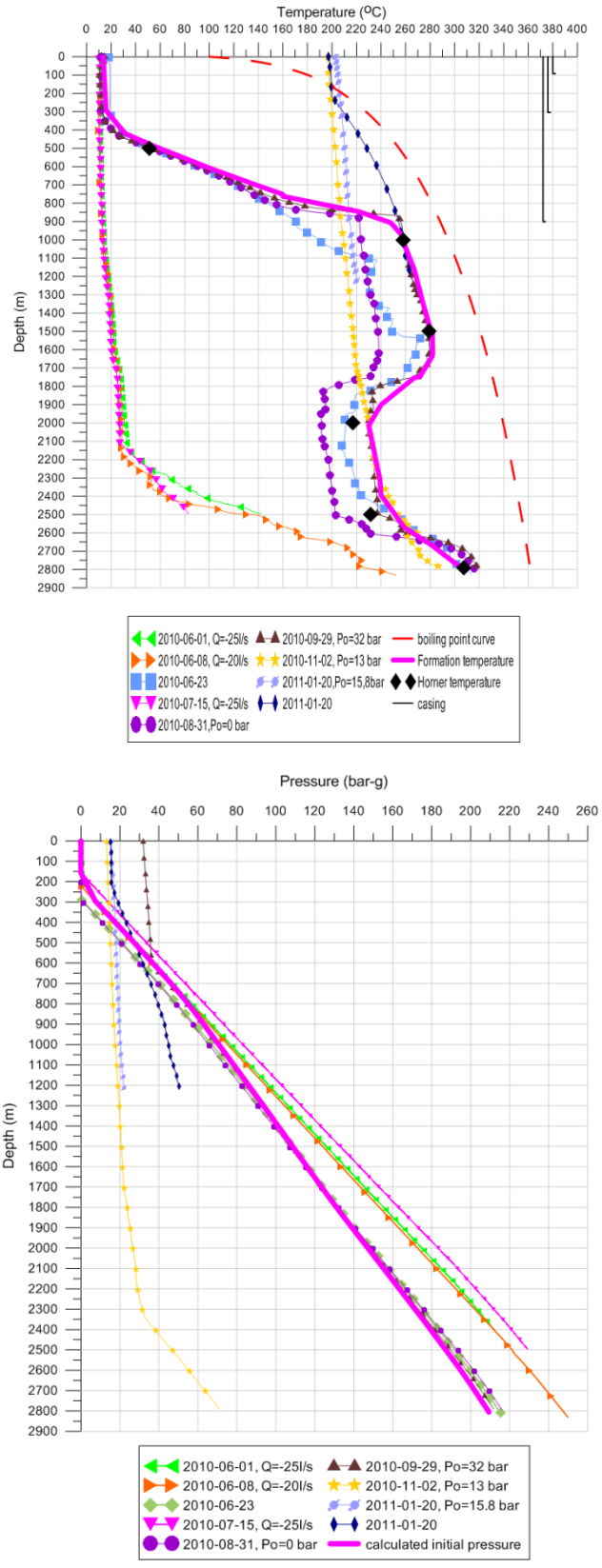

Figure A.11: Estimation of the reservoir temperature and pressure for well RN-29.

A.4 Injectivity and productivity indices

Table A.2: Productivity and injectivity indices for high temperature geothermal fields.

Name	Well	Temperature (^{o}C)	II(L/s/bar)	PI (kg/s/bar)
Reykjanes, Iceland (Axelsson et al., 2006)	RN-10 RN-11 RN-12 RN-13 RN-13B RN-14 RN-15 RN-16 RN-17B RN-18 RN-19 RN-21 RN-22 RN-23 RN-24	310 295 290 290 285 290 280 220 342 283 250-260 275 305 305 >275	6.6 10 9 5 8 7 4 2 1.3 4.3 5 13 10 36 15	2.3 10 30 1.5 3.4 - 1 - - 1.5 - 6 15 68 38
Broadlands, New Zealand (Grant, 2008)	BR-9 BR-13 BR-18 BR-22 BR-23 BR-25 BR-27 BR-28	245-300^{o}C	5.6 2.52 2.24 3.92 7.28 5.88 2.52 14	0.42 0.924 0.896 3.36 3.08 9.8 1.54 4.2
Asal, Djibouti (Houssein and Axelsson, 2010)	A-3	260^{o}C	7	2.8
Oguni, Japan (Garg and Combs, 1997)	GH-10 GH-11 GH-12 GH-20 IH-2 N2-KW-3	Average 225^{o}C	3.39 1.53 5.12 7.82 33 5.85	3.88 5.65 5.77 15.2 11.9 3.85
Sumikawa, Japan (Garg and Combs, 1997)	S-2 SC-1	Average 250^{o}C with a maximum 320^{o}C	1.7 5.2	1.3 5.7

A.5 Hola results

Well RN-13b

Wellhead pressure (bar-a) : 41.04
Wellhead temperature (°C) : 251.85
Wellhead dryness (%) : 40.15
Wellhead enthalpy (kJ/kg) : 1779.38
Wellhead total flow (kg/s) : 25.05

Feedzone	Depth (m)	Flow (kg/s)	Enthalpy (kJ/kg)	Resv.Press (bar-a)	Saturation (m3/m3)	Prod.Index (kg/s/m3)
1	1120.0	7.60	1800.00	62.90	.00	.800E-11
2	1590.0	7.42	1260.00	97.90	.00	.150E-11
3	2000.0	10.03	1280.40	127.80	.00	.200E-11

Depth (m)	Press (bar-a)	Temp (°C)	Dryness (%)	Hw ----(kJ/kg)---	Hs	Ht	Vw ----(m/s)----	Vs	Dw --(kg/m3)--	Ds	Rad (mm)	Reg
0	41.0	251.9	40.1	1095	2800	1779	1.91	6.91	796.4	20.6	160	Sl
50	41.7	252.8	40.0	1100	2800	1780	1.88	6.78	794.9	21.0	160	Sl
100	42.4	253.8	39.9	1105	2799	1780	1.86	6.67	793.4	21.4	160	Sl
150	43.1	254.8	39.7	1109	2799	1781	1.83	6.55	791.9	21.7	160	Sl
200	43.8	255.8	39.6	1114	2798	1781	1.80	6.43	790.4	22.1	160	Sl
250	44.6	256.8	39.5	1119	2798	1782	1.78	6.32	788.8	22.5	160	Sl
300	45.3	257.8	39.3	1124	2797	1782	1.75	6.21	787.3	22.9	160	Sl
350	46.1	258.9	39.2	1129	2797	1783	1.72	6.10	785.7	23.3	160	Sl
400	46.8	259.9	39.0	1134	2796	1783	1.70	5.99	784.1	23.7	160	Sl
450	47.6	260.9	38.9	1139	2796	1784	1.68	5.88	782.5	24.1	160	Sl
500	48.4	261.9	38.8	1144	2795	1784	1.65	5.78	780.9	24.5	160	Sl
550	49.2	262.9	38.6	1149	2795	1785	1.63	5.68	779.3	24.9	160	Sl
600	50.0	263.9	38.5	1155	2794	1785	1.61	5.58	777.7	25.4	160	Sl
650	50.9	265.0	38.3	1160	2793	1786	1.58	5.48	776.0	25.8	160	Sl
700	51.7	266.0	38.2	1165	2793	1786	1.56	5.38	774.3	26.3	160	Sl
750	52.6	267.0	38.0	1170	2792	1787	1.54	5.29	772.6	26.7	160	Sl
800	53.4	268.1	37.9	1176	2791	1787	1.52	5.19	770.9	27.2	160	Sl
850	54.3	269.1	37.7	1181	2791	1788	5.15	10.02	769.2	27.7	110	Sl
900	55.1	270.0	37.6	1185	2790	1788	5.07	9.85	767.7	28.1	110	Sl
950	55.8	270.9	37.4	1190	2789	1789	5.00	9.69	766.2	28.5	110	Sl
1000	56.6	271.8	37.3	1194	2788	1789	4.93	9.54	764.7	29.0	110	Sl
1050	57.4	272.7	37.2	1199	2788	1790	4.86	9.39	763.2	29.4	110	Sl
1100	58.2	273.6	37.1	1203	2787	1790	4.80	9.24	761.7	29.8	110	Sl
1150	60.1	275.7	3.2	1214	2785	1265	.95	1.26	758.1	30.9	110	Bu
1200	63.2	278.9	2.2	1231	2782	1266	.83	1.10	752.5	32.6	110	Bu
1250	66.7	282.6	1.0	1250	2777	1266	.71	.93	745.9	34.6	110	Bu
1300	70.6	285.6	0	1267	0	1267	.62	.00	740.4	.0	110	lp
1350	74.3	285.8	0	1267	0	1267	.62	.00	740.8	.0	110	lp

1400	77.9	285.9	.0	1268	0	1268	.62	.00	741.2	.0	110	1p
1450	81.6	286.1	.0	1268	0	1268	.62	.00	741.6	.0	110	1p
1500	85.2	286.2	.0	1269	0	1269	.62	.00	741.9	.0	110	1p
1550	88.8	286.3	.0	1269	0	1269	.62	.00	742.3	.0	110	1p
1600	92.5	287.8	.0	1276	0	1276	.36	.00	740.1	.0	110	1p
1650	96.1	287.9	.0	1277	0	1277	.36	.00	740.4	.0	110	1p
1700	99.8	288.1	.0	1277	0	1277	.36	.00	740.8	.0	110	1p
1750	103.4	288.2	.0	1278	0	1278	.36	.00	741.2	.0	110	1p
1800	107.0	288.3	.0	1278	0	1278	.36	.00	741.6	.0	110	1p
1850	110.7	288.5	.0	1279	0	1279	.36	.00	741.9	.0	110	1p
1900	114.3	288.6	.0	1279	0	1279	.36	.00	742.3	.0	110	1p
1950	118.0	288.7	.0	1280	0	1280	.36	.00	742.7	.0	110	1p
2000	121.6	288.9	.0	1280	0	1280	.36	.00	743.0	.0	110	1p

Well RN-18

Wellhead pressure (bar-a) : 31.58
Wellhead temperature (°C) : 236.70
Wellhead dryness (%) : 26.29
Wellhead enthalpy (kJ/kg) : 1489.96
Wellhead total flow (kg/s) : 51.03

Feedzone	Depth (m)	Flow (kg/s)	Enthalpy (kJ/kg)	Resv.Press (bar-a)	Saturation (m3/m3)	Prod.Index (kg/s/m3)
1	800.0	.09	1520.00	48.90	.00	.100E-12
2	1800.0	50.94	1220.00	119.00	.00	.130E-10

Depth (m)	Press (bar-a)	Temp (°C)	Dryness (%)	Hw	Hs	Ht	Vw	Vs	Dw	Ds	Rad	Reg
				----(kJ/kg)---			----(m/s)----		--(kg/m3)--		(mm)	
0	31.6	236.7	26.3	1022	2802	1490	5.66	11.74	818.2	15.8	160	Sl
50	32.3	237.9	26.1	1028	2802	1490	5.52	11.43	816.5	16.2	160	Sl
100	33.0	239.2	25.9	1034	2802	1491	5.39	11.13	814.8	16.5	160	Sl
150	33.7	240.4	25.6	1039	2802	1491	5.26	10.83	813.1	16.9	160	Sl
200	34.4	241.6	25.4	1045	2802	1492	5.14	10.55	811.3	17.2	160	Sl
250	35.2	242.8	25.2	1051	2802	1492	5.02	10.27	809.6	17.6	160	Sl
300	35.9	244.0	25.0	1057	2802	1493	4.90	10.01	807.9	18.0	160	Sl
350	36.7	245.3	24.8	1063	2802	1493	4.79	9.75	806.1	18.4	160	Sl
400	37.5	246.5	24.5	1069	2801	1494	4.68	9.50	804.4	18.8	160	Sl
450	38.2	247.7	24.3	1075	2801	1494	4.57	9.25	802.6	19.2	160	Sl
500	39.0	248.9	24.1	1080	2801	1495	4.46	9.01	800.8	19.6	160	Sl
550	39.8	250.1	23.9	1086	2800	1495	4.36	8.78	799.0	20.0	160	Sl
600	40.7	251.3	23.6	1092	2800	1496	4.26	8.55	797.2	20.4	160	Sl
650	41.5	252.5	23.4	1098	2800	1496	4.16	8.33	795.4	20.9	160	Sl
700	42.4	253.8	23.2	1104	2799	1497	4.07	8.12	793.5	21.3	160	Sl
750	43.2	255.0	22.9	1110	2799	1497	3.97	7.91	791.7	21.8	160	Sl
800	44.4	256.6	22.6	1118	2798	1498	11.11	15.38	789.3	22.4	110	Sl
800	44.4	256.6	5.5	1118	2798	1210	4.10	5.40	789.3	22.4	110	Bu
850	46.4	259.2	4.8	1131	2797	1211	3.71	4.87	785.1	23.4	110	Sl
900	48.5	262.1	4.0	1145	2795	1211	3.31	4.33	780.6	24.6	110	Sl
950	51.0	265.2	3.1	1161	2793	1212	2.91	3.79	775.6	25.9	110	Sl
1000	54.0	268.7	2.1	1179	2791	1212	2.49	3.22	769.9	27.5	110	Sl
1050	57.5	272.8	.8	1200	2788	1213	2.03	2.62	763.0	29.5	110	Sl
1100	61.3	275.5	.0	1213	0	1213	1.77	.00	758.7	.0	110	1p
1150	65.0	275.6	.0	1214	0	1214	1.77	.00	759.1	.0	110	1p
1200	68.8	275.7	.0	1214	0	1214	1.76	.00	759.4	.0	110	1p
1250	72.5	275.8	.0	1215	0	1215	1.76	.00	759.8	.0	110	1p
1300	76.3	276.0	.0	1215	0	1215	1.76	.00	760.1	.0	110	1p
1350	80.1	276.1	.0	1216	0	1216	1.76	.00	760.5	.0	110	1p
1400	83.8	276.2	.0	1216	0	1216	1.76	.00	760.8	.0	110	1p
1450	87.6	276.3	.0	1217	0	1217	1.76	.00	761.2	.0	110	1p

1500	91.4	276.5	.0	1217	0	1217	1.76	.00	761.5	.0	110	1p
1550	95.2	276.6	.0	1218	0	1218	1.76	.00	761.9	.0	110	1p
1600	98.9	276.7	.0	1218	0	1218	1.76	.00	762.2	.0	110	1p
1650	102.7	276.8	.0	1219	0	1219	1.76	.00	762.6	.0	110	1p
1700	106.5	277.0	.0	1219	0	1219	1.76	.00	762.9	.0	110	1p
1750	110.3	277.1	.0	1220	0	1220	1.76	.00	763.3	.0	110	1p
1800	114.1	277.2	.0	1220	0	1220	1.75	.00	763.6	.0	110	1p

Well RN-23

Wellhead pressure (bar-a) : 46.04
Wellhead temperature (°C) : 258.81
Wellhead dryness (%) : 19.34
Wellhead enthalpy (kJ/kg) : 1451.64
Wellhead total flow (kg/s) : 154.84

Feedzone	Depth (m)	Flow (kg/s)	Enthalpy (kJ/kg)	Resv.Press (bar-a)	Saturation (m3/m3)	Prod.Index (kg/s/m3)
1	750.0	30.76	1470.00	67.90	.00	.300E-10
2	1200.0	38.07	1280.00	97.20	.00	.100E-10
3	1730.0	86.01	1370.00	134.00	.00	.300E-10

Depth (m)	Press (bar-a)	Temp (°C)	Dryness (%)	Hw	Hs	Ht	Vw	Vs	Dw	Ds	Rad	Reg
				----(kJ/kg)---			----(m/s)----		--(kg/m3)--		(mm)	
0	46.0	258.8	19.3	1129	2797	1452	14.21	18.60	785.8	23.3	160	Sl
50	47.1	260.2	19.0	1136	2796	1452	13.77	18.00	783.6	23.8	160	Sl
100	48.1	261.5	18.8	1143	2796	1453	13.35	17.43	781.5	24.4	160	Sl
150	49.2	262.9	18.5	1149	2795	1453	12.95	16.88	779.3	24.9	160	Sl
200	50.3	264.3	18.2	1156	2794	1454	12.56	16.34	777.2	25.5	160	Sl
250	51.4	265.6	17.9	1163	2793	1454	12.19	15.83	775.0	26.1	160	Sl
300	52.5	266.9	17.6	1170	2792	1455	11.82	15.33	772.8	26.7	160	Sl
350	53.6	268.3	17.3	1177	2791	1455	11.47	14.85	770.6	27.3	160	Sl
400	54.7	269.6	16.9	1183	2790	1456	11.12	14.38	768.4	27.9	160	Sl
450	55.9	271.0	16.6	1190	2789	1456	10.79	13.92	766.2	28.6	160	Sl
500	57.1	272.3	16.3	1197	2788	1457	10.46	13.48	763.9	29.2	160	Sl
550	58.3	273.6	16.0	1204	2787	1457	10.14	13.05	761.6	29.9	160	Sl
600	59.5	275.0	15.7	1211	2786	1458	9.83	12.63	759.3	30.5	160	Sl
650	60.7	276.3	15.3	1218	2784	1458	9.53	12.22	757.0	31.2	160	Sl
700	62.0	277.7	15.0	1225	2783	1459	9.24	11.82	754.6	31.9	160	Sl
750	64.8	280.6	14.2	1240	2780	1459	20.27	22.46	749.5	33.5	110	Sl
750	64.8	280.6	6.1	1240	2780	1334	9.41	10.57	749.5	33.5	110	Bu
800	67.1	282.9	5.4	1252	2777	1335	8.68	9.73	745.3	34.8	110	Sl
850	69.5	285.3	4.7	1265	2774	1335	7.96	8.92	740.9	36.2	110	Sl
900	72.1	287.8	3.9	1278	2771	1336	7.26	8.11	736.3	37.8	110	Sl
950	74.9	290.4	3.0	1292	2767	1336	6.55	7.31	731.3	39.4	110	Sl
1000	78.0	293.2	2.0	1307	2763	1337	5.85	6.51	725.9	41.3	110	Sl
1050	81.4	296.2	1.0	1324	2758	1337	5.21	5.21	720.0	43.4	110	Bu
1100	85.0	298.7	.0	1338	0	1338	4.57	.00	715.0	.0	110	1p
1150	88.8	298.9	.0	1338	0	1338	4.56	.00	715.4	.0	110	1p
1200	92.5	299.0	.0	1339	0	1339	4.56	.00	715.9	.0	110	1p
1200	92.5	303.6	.0	1365	0	1365	3.21	.00	705.3	.0	110	1p
1250	96.1	303.7	.0	1365	0	1365	3.21	.00	705.7	.0	110	1p
1300	99.7	303.9	.0	1366	0	1366	3.20	.00	706.2	.0	110	1p
1350	103.3	304.1	.0	1366	0	1366	3.20	.00	706.7	.0	110	1p

1400	106.8	304.2	.0	1367	0	1367	3.20	.00	707.1	.0	110	1p
1450	110.4	304.4	.0	1367	0	1367	3.20	.00	707.6	.0	110	1p
1500	114.0	304.6	.0	1368	0	1368	3.20	.00	708.0	.0	110	1p
1550	117.6	304.7	.0	1368	0	1368	3.19	.00	708.5	.0	110	1p
1600	121.2	304.9	.0	1369	0	1369	3.19	.00	708.9	.0	110	1p
1650	124.8	305.0	.0	1369	0	1369	3.19	.00	709.3	.0	110	1p
1700	128.4	305.2	.0	1370	0	1370	3.19	.00	709.8	.0	110	1p

A.6 Monte Carlo simulation

Table A.3: Monte Carlo input data for Reykjanes geothermal field in Iceland.

Parameters	Units	Most likely	Probability distribution		
			Type of distribution	Minimum	Maximum
Area for case I	km^2	2	Triangular	1	2
Area for case II	km^2	2	Triangular	1	11
Thickness for case I	m	2000	Triangular	800	2500
Thickness for case II	m	2500	Triangular	1000	3000
Rock density	kg/m^3	3000	Constant		
Rock specific heat	kJ/(kg°C)	0.84	Constant		
Porosity	%	10	Constant		
Temperature for case I & II	°C	300	Triangular	280	340
Rejection temperature	°C	40	Constant		
Fluid density for case I	kg/m^3	740	f (temp., salinity)		
Fluid density for case II	kg/m^3	724	f (temp., salinity)		
Fluid specific heat for case I	kJ/(kg °C)	5.5	f (temp.)		
Fluid specific heat for case II	kJ/(kg °C)	5.75	f(temp.)		
Recovery factor for case I	%	20	Triangular	10	25
Recovery factor for case II	%	10	Triangular	5	20
Conversion efficiency	%	14	Triangular	13	15
Plant life	Years	30,50	Constant		
Load factor	%	95	Constant		

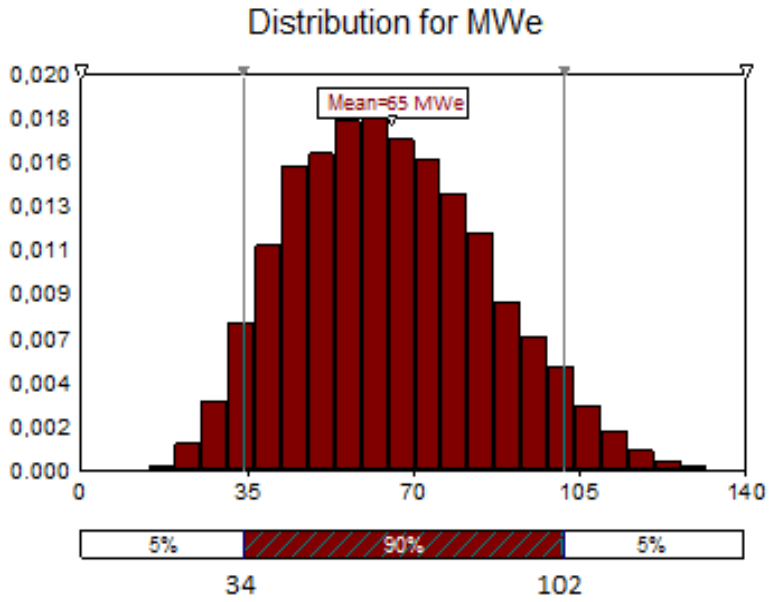

Figure A.12: Frequency distribution for electric power generation for Reykjanes geothermal field case I, 30 years.

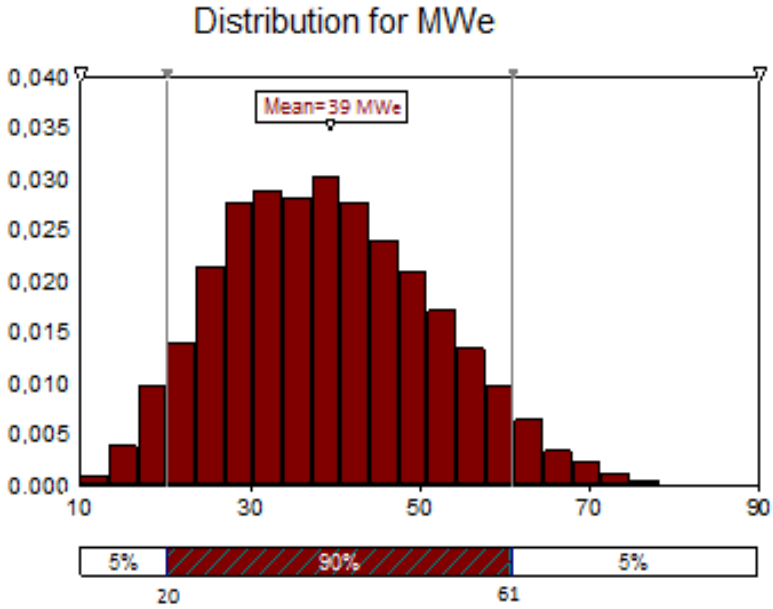

Figure A.13: Frequency distribution for electric power generation for Reykjanes geothermal field case I, 50 years.

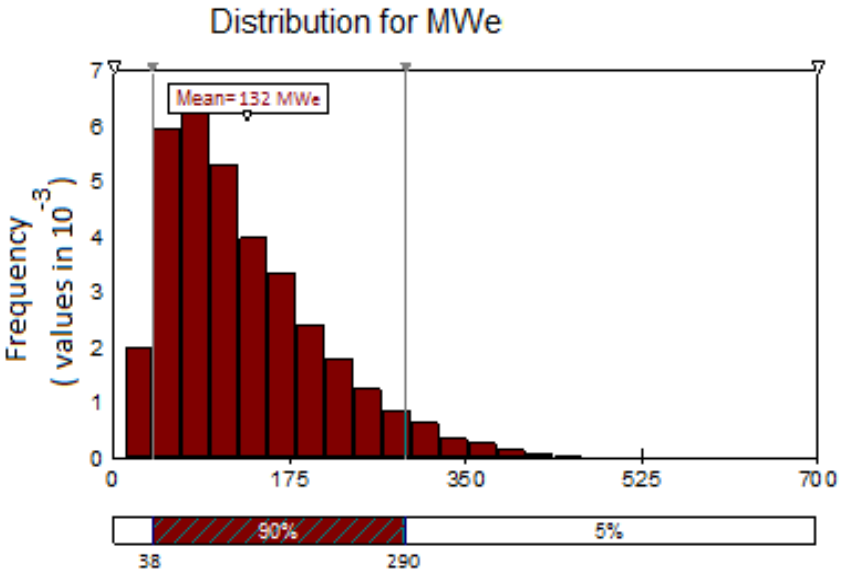

Figure A.14: Frequency distribution for electric power generation for Reykjanes geothermal field case II, 30 years.

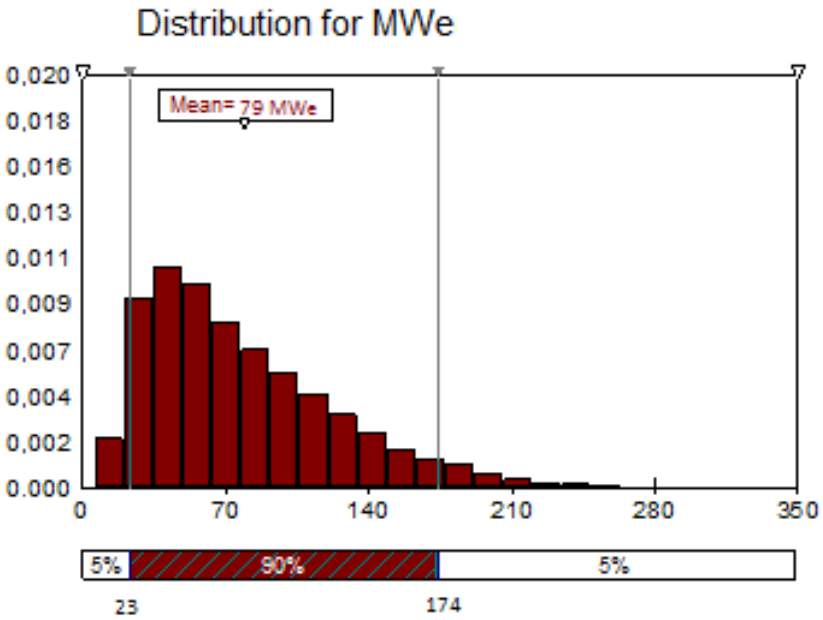

Figure A.15: Frequency distribution for electric power generation for Reykjanes geothermal field case II, 50 years.